Study of Beta Decay of ^{48}Ca

(^{48}Caのベータ崩壊の研究)

Wei WANG

Dissertation in Physics

Graduate School of Science

Osaka University

For Aimee and Zi'ang

Contents

Abstract

It is well known that lepton number non-conservation can be verified in neutrino-less double decay (0νββ). CANDLES (CAlcium fluoride for studies of Neutrino and Dark matters by Low Energy Spectrometer) collaborators are carrying out an experiment to search for the 0νββ of ^{48}Ca (Q value of 4.27MeV) by CaF_2 scintillating crystals. Two-neutrino double beta decay (2νββ), however, is the intrinsic background for 0νββ research. Thus we also need to know 2νββ lifetime to estimate the background contribution to 0νββ.

It is even special for ^{48}Ca that it also has β decay which is energetically forbidden for most of other double beta nucleus. For CANDLES, the β decay could give substantial contribution to 2νββ spectrum since it uses $(10cm)^3$ CaF_2 crystals. Therefore, precise studies about lifetime of the β decay are necessary.

However, it is almost impossible to direct measure the β decay of ^{48}Ca because of the extremely low Q value (278keV). Thus the principle of this experiment was based on coincidence measurement of 3 gamma rays from concentrated ^{48}Sc that is the β decay product of ^{48}Ca with half-life time 43.7 hours. We used 30 CsI(Tl) scintillators to cover (4π solid angle) the sample space with 13^3 cm^3. In order to increase the amount of ^{48}Ca, we enriched the ^{48}Sc from $CaCl_2$ solution using the chelate resin called NOBIAS-CHELATE-PA1 that could capture the Sc ion with efficiency over 94%. We made 634.7L $CaCl_2$ solution with 255.1kg $CaCl_2$ powder (^{48}Ca natural abundance). The $CaCl_2$ solution passed though 138.5g chelate resin with circulation rate of 2.0L/min. The total detection efficiency for this experiment was 8.4% for triple coincidence measurement.

We measured the concentrated ^{48}Sc sample for live-time of 70.7 days. The half-life time of β decay of ^{48}Ca we got was $T_{1/2(\beta)} = (2.2 \pm 0.8_{[statistic]} \pm 0.4_{[systematics]}) \times 10^{21}$ y with 68% C. L. The half-life time we measured is the longest for all known β^- transition. Corresponding to the new measured half lifetime is the log*ft* = 26.7(3) which is greater than that for any observed β^- decay.

For CANDLES experiment, the background contribution from β decay for 2νββ above 3MeV spectrum is about (3±1)% and has no contribution for 0νββ research.

Chapter I: Beta Decay of ^{48}Ca

1. Introduction

1.1 Neutrino Mass

Neutrinos are massless in the Standard Model of particle physics[1]. However, the discovery of neutrino oscillations indicates the existence of neutrino mass[2]. At same time, mass of neutrino proves that neutrino is Majorana particle. That is also one of the reasons why double beta decays attract great interests in the field of particle and nuclear physics[3]. Observation of neutrinoless double beta decay provides the direct information of neutrino Majorana property and neutrino mass[4].

1.2 Double Beta Decay

1.2.1 Mechanisms of double beta decay

In nuclear physics, double beta decay is a type of radioactive decay in which two neutrons are simultaneously transformed into two protons inside an atomic nucleus. Double beta decay is allowed although single beta decay is energetically forbidden or strongly suppressed due to large change of spin. There are two types of double beta decay: two neutrino double beta decay ($2\nu\beta\beta$) and neutrinoless double beta decay ($0\nu\beta\beta$). In $2\nu\beta\beta$, which has been observed in several isotopes, two electrons and two electron antineutrinos are emitted from the decaying nucleus. In $0\nu\beta\beta$, a hypothesized process that has never been observed, only two electrons are emitted.

There are many naturally occurring isotopes capable of double beta decay such as ^{48}Ca, ^{76}Ge, ^{130}Te, ^{136}Xe and so on. This happens for even-Z, even-N isotopes. In most cases, the double beta decay is so rare that it is nearly impossible to observe against the background. So for double beta decay experiments, reducing the background is the most important work.

1.2.2 Neutrinoless double beta decay

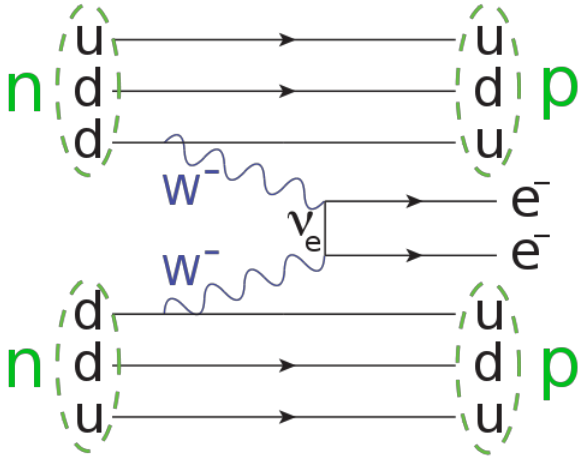

Fig 1.1 Feynman diagram of neutrinoless double beta decay, with two neutrons decaying to two protons.

Neutrinoless double beta decay is a lepton number violating process. The only emitted products in this process are two electrons, which can occur if the neutrino and antineutrino are the same particle (i.e. Majorana neutrinos) so the same neutrino can be emitted and absorbed within the nucleus. The detection of neutrinoless double beta decay is thus a sensitive test of whether neutrinos are Majorana particles[6].

1.2.3 Experiment Method and status

Early experiments did claim discovery of neutrinoless double beta decay[7], but modern searches have set limits disfavoring those results[8-10]. Recent published lower bounds for germanium and xenon indicate no sign of neutrinoless decay[11,12].

As of 2017, GERDA has reached much lower background, obtaining a half-life limit of 2.1×10^{25} years with 21.6 kg·yr exposure[13]. IGEX and HDM data increase the limit to 3×10^{25} yr and rule out detection at high confidence[14]. Searches with ^{136}Xe, Kamland-Zen and EXO-200, yielded a limit of 2.6×10^{25} yr[15,16]. Using the latest nuclear matrix elements, the ^{136}Xe results also disfavor the Heidelberg-Moscow claim.

1.2.4 CANDLES experiment with ^{48}Ca

The CANDLES (CAlcium fluoride for studies of Neutrino and Dark matters by Low Energy Spectrometer) is running at Kamioka Underground Laboratory by using CaF_2 scintillating crystals to detect the sum energy of 2 electrons from ββ decay of ^{48}Ca[17,18]. ^{48}Ca has the highest $Q_{\beta\beta}$ value (4.27MeV) among all double beta decay nuclei, ensuring a large phase space factor for the decay rate. In addition, its decay is above the energies from natural radioactivity of β^- (max 3.27MeV from ^{214}Bi) and γ-rays (max 2.6MeV from ^{208}Tl). Therefore, the background from natural radioactivity is limited in the Q value region.

The picture of the CANDLES system is shown in Fig.1.2. Pure CaF_2 scintillators with a dimension of 10 cm cube are immersed in the liquid scintillator (LS). Scintillation lights from both CaF_2 and LS are viewed by the large PMTs. The emission light of CaF_2 crystal has a peak in the UV region at the maximum of 285 nm. The LS acts as not only an active shield to reduce background events, but also a wave length shifter (WLS) to convert the UV light emitted by CaF_2 to the visible where the quantum efficiency of the large PMT is quite large (maximum at ~400 nm). The CaF_2 scintillator has a decay time of 1 μsec, although LS has a width of around a few tens nsec. Thus by observing pulse shape the signals from LS (background) can be discriminated.

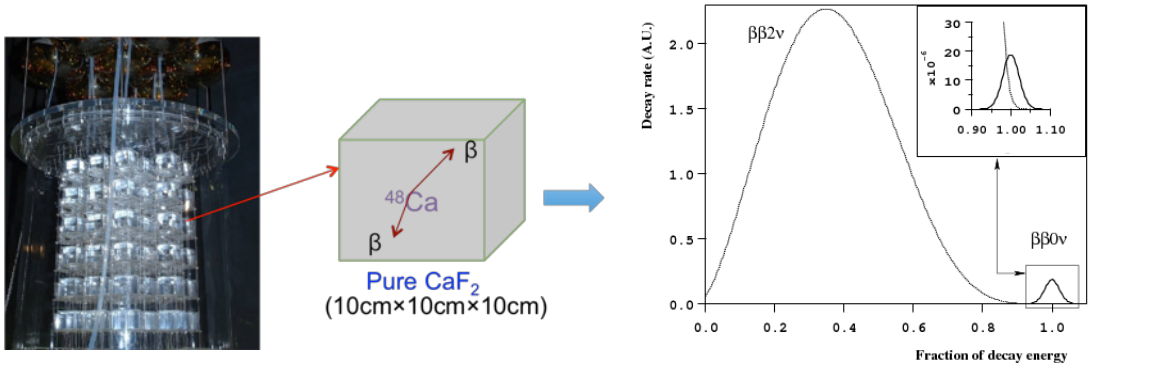

Fig.1.2 The picture of the CANDLES system (left side); double beta decay of ^{48}Ca in the CaF_2 scintillating crystal (middle); the concept spectrum of double beta decay, 2νββ would be the intrinsic background for 0νββ (right side).

As for the spectrums of double beta decay, the 2νββ is a continuous

spectrum to the end point of Q value. However, 2νββ has essentially same characteristics as the 0νββ except for its energy, thus it would be substantial background for the 0νββ spectrum (right side of Fig.1.2). The background contribution depends on the energy resolution of the detector and the half lifetime of the 2νββ decay of ^{48}Ca. We thus need to reduce it by improving energy resolution. We also need to know 2νββ lifetime to estimate the background contribution to 0νββ. ^{48}Ca is one of the two nuclides (^{48}Ca and ^{96}Zr) that can theoretically decay though single beta decay that is extremely suppressed and has never been observed[5]. For CANDLES, the β decay could give substantial contribution to 2νββ spectrum since it uses $(10\text{cm})^3$ CaF_2 crystals (describe later). Thus, the β decay of ^{48}Ca should be carefully studied.

2. Beta Decay of ^{48}Ca

2.1 Decay scheme

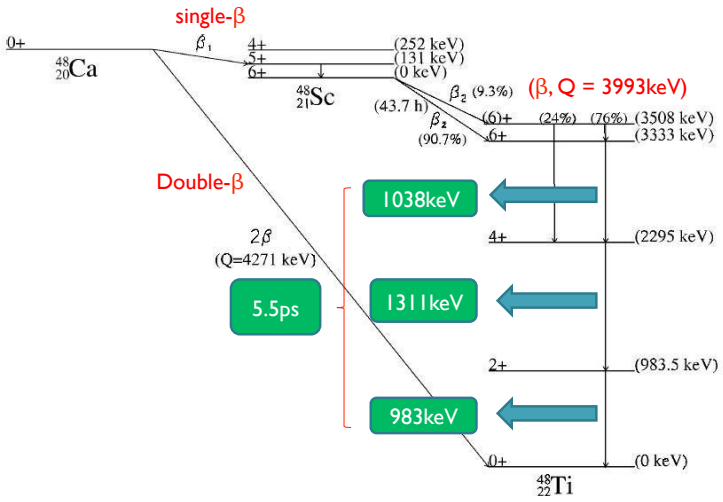

Fig.1.3 The decay scheme of ^{48}Ca

Fig.1.3 shows the decay scheme of ^{48}Ca. ^{48}Ca can decay to ^{48}Ti with double beta decay (include 2νββ and 0νββ) with Q value of 4.27MeV. ^{48}Ca can also has ß decay with Q value of 278keV. ^{48}Sc is the ß decay product and has half-life time of 43.7 h. Then ^{48}Sc decays to excited levels of ^{48}Ti and 3 γ rays with energy of 983, 1038 and 1311 keV are emitted simultaneously with 97.8% intensity per decay.

2.2 The theoretical interests

^{48}Ca is unique, since it is the only one, which can be treated "exactly" in the nuclear shell model by solving the problem of eight nucleons distributed within the fp shell without truncation[19]. However, calculations for β half lifetime of ^{48}Ca always have huge uncertainties (more than 70%) because the difference of NMEs. We have relationship as $ft_{1/2}$=6147s/<C> where f is the Fermi integral and $t_{1/2}$ is the half-life in seconds. <C> is the shape factor that includes the phase-space factors and nuclear matrix elements. Thus, the β half-life measurement provides a unique test of the nuclear physics involved in the matrix element calculation.

2.3 Studies so far

2.3.1 Theoretic predictions

(1). Calculations were made assuming a closed 2s, 1d shell at ^{40}Ca and a closed $f_{7/2}$-neutron subshell for ^{48}Ca, a $f_{7/2}$-neutron hole and a proton in the full 1f, 2p shell for ^{48}Sc. Harmonic oscillator radial wave functions were used. The theoretical beta-decay half-life of ^{48}Ca is found to be (7.6±5.3) ×10^{20} years [20].

(2). M. Aunola gave a theoretical prediction of (11±8) ×10^{20} years by using both the harmonic oscillator and the Woods-Saxon mean-field wave functions [21].

As we can see, calculations for β half lifetime of ^{48}Ca always have huge uncertainties (more than 70%) because the difference of NMEs. Thus, the β half-life measurement provides a unique test of the nuclear physics involved in the matrix element calculation.

2.3.2 Experiments

Experimental studies are quite limited, only a few experimental results are available.

(1). I did single beta decay experiment for my master thesis in 2012. The principle of the experiment was based on triple coincidence measurement of 3 gamma rays from ^{48}Sc. I used 6 NaI(Tl) scintillators with size of 10.5×10.5×21cm^3 to cover (4π solid angle) the sample space with 10.5^3 cm^3. We measured the 2kg CaF_2 crystals (natural abundance) sample with 249 days at surface laboratory and got a lower limit which was $T_{1/2} > 8.3\times10^{18}$ yr with 95% C. L.

(2). A $^{48}CaCO_3$ powder sample containing 3.71 g of ^{48}Ca was measured. The cascade γ rays of 983.5, 1037.5, and 1312.1 keV in the β decay of 44-h ^{48}Sc, were searched for in the HPGe spectrum by requiring coincidences with summed γ rays in the NaI(Tl) detector. The half-life was found to be $T_{1/2} > 6 \times 10^{18}$ y (95% confidence) [22].

(3). R. Bernabei et al gave $T_{1/2} > 2.4 \times 10^{18}$ y at 90% C.L. The β–γ coincidence technique has been applied by using a 1.11 kg CaF_2(Eu) scintillator partially surrounded by low background NaI(Tl) detectors [23].

(4). A $^{48}CaCO_3$ powder sample containing 20.18 g of ^{48}Ca was measured for 797 h with a 400 cm^3 low-background HPGe detector at underground lab by a French and Russian collaboration [24]. They got best-published experiment result $T_{1/2} > 1.1\times10^{20}$ yr that was almost an order of magnitude less than the theoretical prediction.

We realized the necessary requirements of experiment for higher sensitivity like the theoretical prediction would be (I) large amount of target atoms (II) low background and (III) high detection efficiency.

3. Single beta decay in CANDLES

The 2.6 MeV gamma rays in ^{208}Tl are naturally abundant in the energy spectrum for double beta decay research. Therefore, it will largely affect on a spectrum above 3 MeV for the study of 2νββ. The single β decay could be

substantial background for the 2vßß when γ rays and β ray deposit all their energy in the $(10cm)^3$ CaF_2 crystals in CANDLES (Fig. 4).

From the Monte Carlo simulation, 2vββ spectrum above 3 MeV is about 3.2% of its whole region. On the other hand β spectrum is 4.2% since probability to absorb the 3γ rays and β ray is relatively large in $(10cm)^3$ CaF_2 crystals. Thus the ß decay can contribute to background of 2vßß more than 5% if its half lifetime $T_{1/2}(\beta)=12.9\times10^{20}yr$ the upper limit of prediction. Therefore new experiment to precisely measure the lifetime of β decay is necessary in order to precisely estimate background for 2vββ decay.

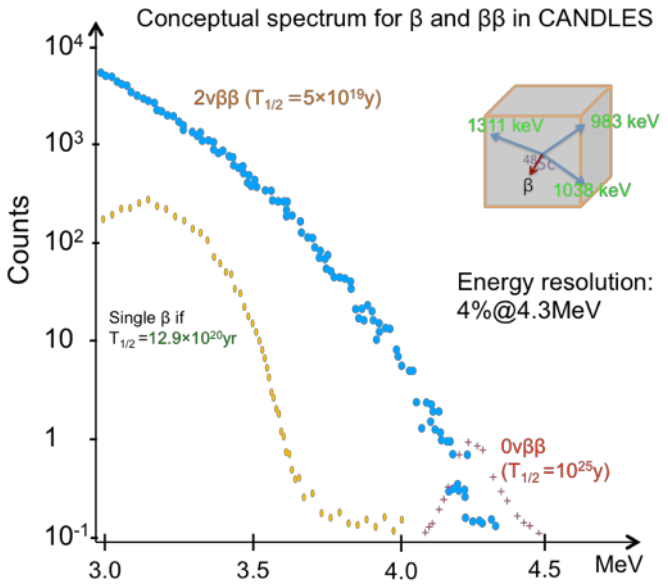

Fig.1.4 The concept spectrum of beta decay of ^{48}Ca for CaF_2 crystal. On the right up side is the single beta decay of ^{48}Ca in CaF_2 crystal; and left side is simulated spectrums of decay of ^{48}Ca, include single β decay, 2vββ and 0vββ decay and their relationship. Different half-life time of single β decay have different background contribution for 2vββ decay spectrum.

4. Experimental principle

It is extremely difficult to detect β decay directly by experiment because the energy of electron from ß decay of ^{48}Ca is too low. It will emit an electron with energy (Q value) 278 keV, or 147 keV (and then emit a photon with energy

131 keV). Instead, we take the experiment based on detecting the β decay product--^{48}Sc since its lifetime is short.

We will determine the half-life of β decay by detecting 3 γ rays (983, 1038 and 1311 keV) from ^{48}Sc (Fig.1.3) with triple coincidence technique.

5. Experimental target sensitivity

The target for the experiment was set as $T_{1/2} > 1.1\times10^{21}$ yr which was almost the upper limit of theoretic prediction. In order to reach to this limit, we made 3 major improvements.

(1). More target atoms (> 170g ^{48}Ca)

The natural abundance for ^{48}Ca is only 0.187% and ^{48}Ca enrichment is difficult. And 170g ^{48}Ca means 255kg high pure $CaCl_2$ powder. At same time, the experimental sample should be small size so new experiment technique is needed. We capture the ^{48}Sc with high efficiency Chelate resin from $CaCl_2$ solution. With 170g ^{48}Ca, the beta decay events would be over 1200/year for the target sensitivity.

(2). Lower backround:

We still take triple coincidence to measure 1038, 1311 and 983 keV gamma rays from ^{48}Sc. We use more CsI veto counter to reduce background further. And a plastic scintillator will veto the cosmic rays. With all those improvements, the background events will be less than 30/year

(3). Higher detection efficiency (>10%)

We apply 4-pi detection with 30 CsI(Tl) scintillators. With the segmentation of detectors, the detectable beta decay events will be over 120/year.

Chapter II: CsI(Tl) scintillators

1. Detector Description

1.1 CsI scintillator

1.1.1 Description of CsI scintillator

There were 30 CsI(Tl) scintillators in this experiment with dimension of 6.5 × 6.5 × 25 cm^3 and light guide and reflector (Fig.2.1). Since the experiment would also need $CaCl_2$ solution, we covered the scintillator with water proof sheets.

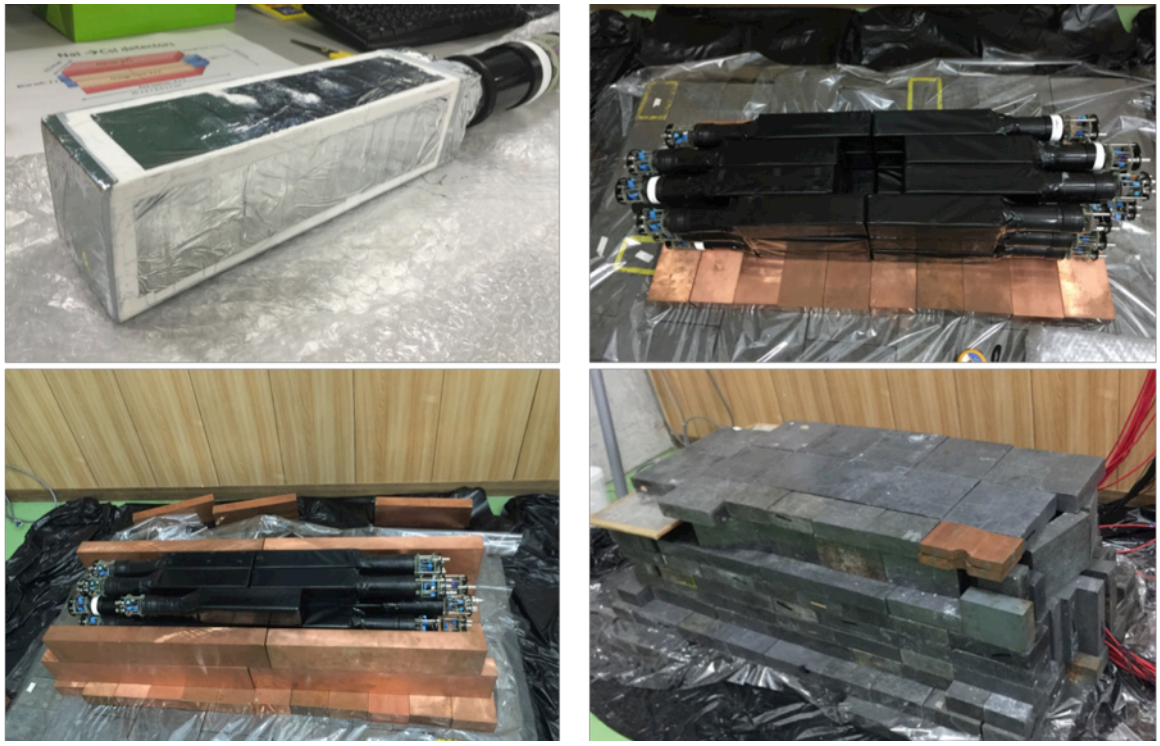

Fig.2.1 The CsI scintillator and arrays (The upper left picture showed the CsI crystal that covered with reflector and connect with PMT. The upper right showed the CsI crystal arrays that covered by water proof sheet; the sample space is in the middle of crystal arrays; the bottom is 10cm Pb and 5 cm Cu. The down left and right picture showed the CsI crystal arrays covered by 10cm Pb and 5cm Cu from all directions)

1.1.2 CsI arrays

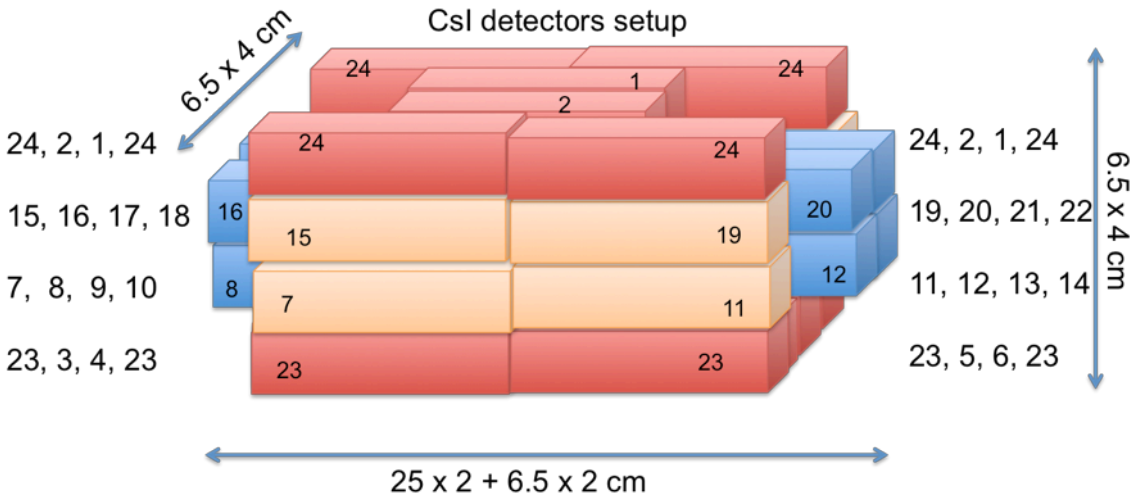

Fig.2.2 the CsI(Tl) scintillators arrays (those numbers correspond to the ADC channel in the experiment)

We arranged the 30 CsI(Tl) scintillators as Fig.2.2 with 4-π cover of a sample space of 13.0 × 13.0 × 13.0 cm^3 . On the top and bottom side, each has 4 scintillators share the same ADC channel (23 & 24); they didn't face to the sample space directly and works as veto counter. And on the topside, CsI scintillators 1 & 2 had double solid angle to the sample space, which worked for background and candidate events identification.

Outside of the CsI scintillators arrays, there were passive shield of 5cm Cu and 10cm Pb at all directions. A Radon free environment had also been ensured with radon purge system.

1.1.3 Energy Calibration

We calibrated the detector with radioactive sources of ^{22}Na (511 keV, 1275 keV and sum energy 1786 keV), ^{60}Co (1173 keV, 1333 keV and sum energy 2506 keV), and ^{137}Cs (662 keV) like Fig.2.3 showed. Those sources was thought as point source and put at the center of the sample space. We calibrated the energy of CsI detectors once every week. And we also calibrated them with natural radioactivity sources in detectors, shield

materials and so on, such as ^{40}K (1465keV) and ^{208}Tl (2614keV). Fig.2.4 shows the typical energy calibration for each ADC channel.

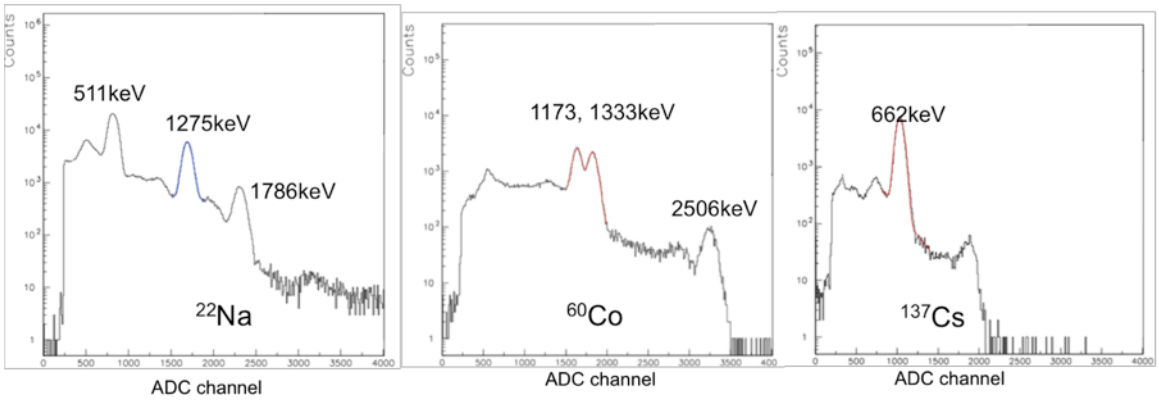

Fig.2.3 The calibration energy spectrum of ^{22}Na (left), ^{60}Co (middle) and ^{137}Cs (right)

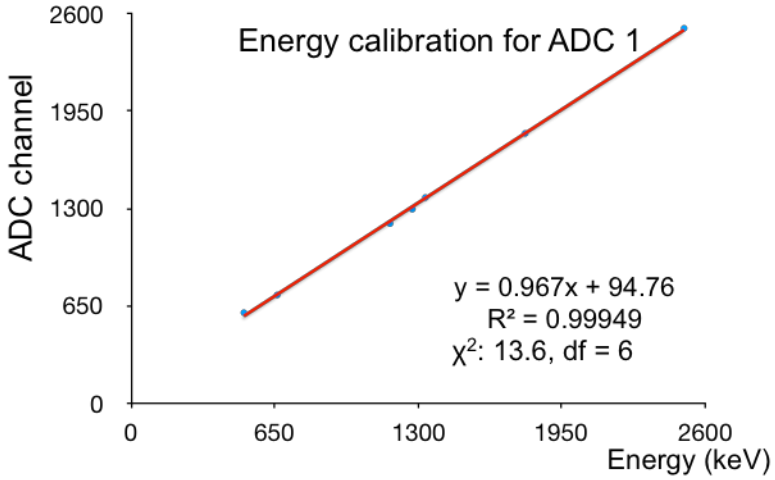

Fig.2.4 The typical energy calibration for ADC

1.1.4 Energy resolution

The energy resolution was measured by using standard γ sources of ^{22}Na (511 keV, 1275 keV and sum energy 1786 keV), ^{60}Co (1173 keV, 1333 keV and sum energy 2506 keV), and ^{137}Cs (662 keV) like Fig.2.3. Then we fitted the σ with following formula

$$\Delta E(\sigma)keV = A \times \sqrt{E},$$

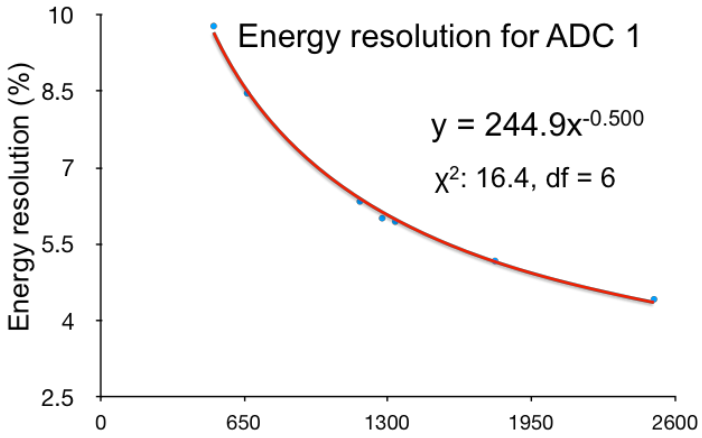

Fig.2.5 The typical energy resolution calibration

The fitting result example was like Fig.2.5. The best fitted curve had the function of $\Delta E(\sigma) = E(keV)^{1/2}$. We used the fitting function and calculated the energy resolution of interested of energy range at 1 MeV. The calculation result was showed in table.2-1. We calibrated the energy resolution once every two weeks in order to check the stability.

Table.2-1 The energy resolution @1MeV for each CsI scintillator

CsI scintillator	Resolution (FWHM)	CsI scintillator	Resolution (FWHM)	CsI scintillator	Resolution (FWHM)
CsI 1	7.41%	CsI 11	7.44%	CsI 21	7.78%
CsI 2	7.6%	CsI 12	7.46%	CsI 22	7.68%
CsI 3	7.38%	CsI 13	7.52%	CsI 23 (ADC23)	7.67%
CsI 4	7.45%	CsI 14	7.6%	CsI 24 (ADC23)	7.75%
CsI 5	7.51%	CsI 15	7.55%	CsI 25 (ADC23)	8.01%
CsI 6	7.5%	CsI 16	7.61%	CsI 26 (ADC23)	7.95%
CsI 7	7.67%	CsI 17	7.42%	CsI 27 (ADC24)	8.09%
CsI 8	7.58%	CsI 18	7.39%	CsI 28 (ADC24)	8.05%
CsI 9	7.55%	CsI 19	7.46%	CsI 29 (ADC24)	8.01%
CsI 10	7.62%	CsI 20	7.42%	CsI 30 (ADC24)	8.04%

1.2 Radon Purge System

The radon concentration in air at the laboratory was measured with alpha-particle detector made of PIN photo-diode. The measured concentration value was found to be 10-40Bq/m^3. We used radon purge system to reduce the Radon concentration around CsI scintillators and Cu and Pb shield. The radon purge system included airtight plastic sheets and N_2 gas supplier. N_2 gas flow speed was around 1L/minute during experiment. With the radon purge system, the radon concentration in scintillator arrays was around 0.1Bq/m^3 (we determined the ^{222}Rn by detecting the ^{214}Bi with coincidence measurement by CsI scintillators), which was suitable for this experiment.

1.3 Plastic Scintillator

A plastic scintillator with 4 PMT and size of 1m×1m×2cm had been installed on the top of detection system to reduce the background from cosmic rays. We asked the sum signal of all the 30 CsI(Tl) detectors to has coincidence with the signal from plastic scintillator (see the electric circuits at Fig.2.6). If those two signals have coincidence, then we could recognize it as the background from cosmic rays. We set the threshold at 1.5MeV for plastic scintillator because its thickness that could absorb the energy of cosmic rays. We used the ^{60}Co standard source to define energy threshold. Besides, the counting rate for the plastic scintillators should not be too high that could affect the live time of the CsI detectors. The veto time of plastic scintillator had been set at 20μs. Fig. 2.6 showed the CsI(Tl) energy spectrums when it had coincidence with the plastic scintillator. We could see the clear peak of 511keV in the coincidence spectrum. And there was no special peak in the interested energy regions around 1MeV and 1.3MeV.

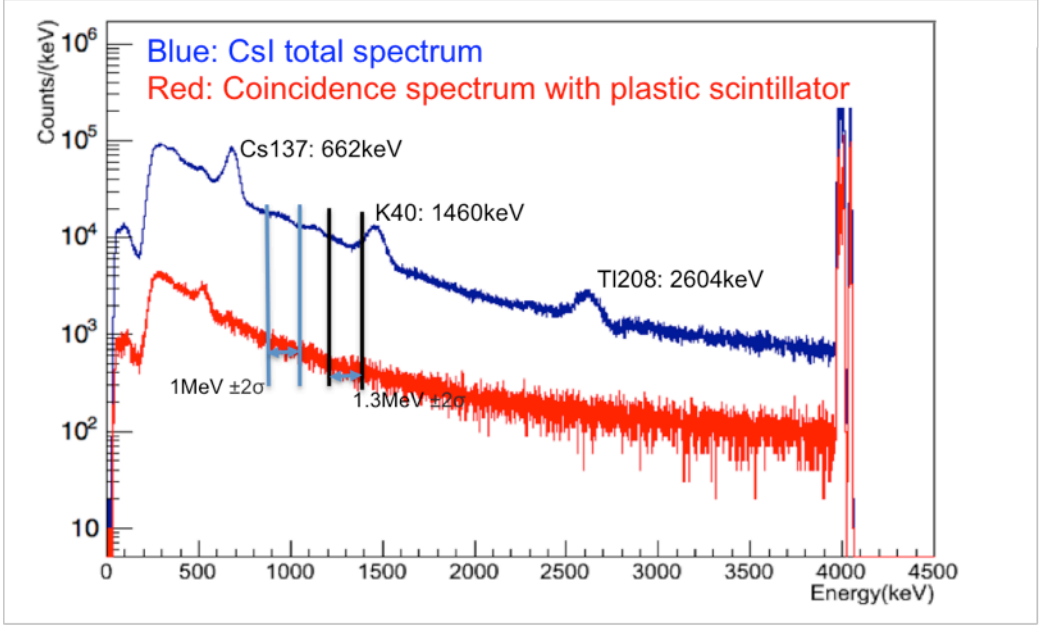

Fig.2.6 The coincidence spectrum with plastic scintillator

2. Data Acquisition System

2.1 Electric Circuits

Fig.2.7 showed the electric circuits of this experiment. Signals from the CsI(Tl) detectors got into Linear FAN IN/OUT module and then divided to two ways. One of them was delayed 200 ns to ADC module which installed in CAMAC system; another one went to Discriminator and also divided to two ways, and the energy threshold for discriminator was around 400 keV in order to keep the 511 keV peak since we used ^{22}Na as calibration source. One of the signals from discriminator went to a LOGIC FAN IN/OUT module at where those 30 CsI scintillators signal would be summed together. Another signal from discriminator had been delayed 200 ns, and then went to two modules in CAMAC system, Coincidence Register module and TDC module as stop signal, respectively.

On the other side, the signal from Logic FAN IN/OUT module went to coincidence module that vetoed by Computer CPU and started by a clock module with frequency 100Hz. We used two scalars to record the real time and live time, respectively. One of the output signals of Coincidence module

went to a Gate Generator and then went to TDC module with timing length of 50 ns as TDC start signal in CAMAC system. Another one would be the input signal for a different Gate Generator. And there were two output signals for this Gate Generator. One of them was going to be the gate signal for the ADC module in CAMAC system. Another one went though a Logic FAN IN/OUT module and then became gate signal for Coincidence Register in CAMAC and also had coincidence with the signal from plastic scintillator. For the signal of plastic scintillator, it went to a discriminator with threshold 1.5 MeV. And then to be the input signal for one Gate Generator, one of the output signals went to a scalar, which would record the counting rate of plastic scintillator. Another output had coincidence with the summed signal of those 30 CsI detectors. And output signal from this coincidence module would be delayed by 200ns and then went to the Coincidence Register in CAMAC system.

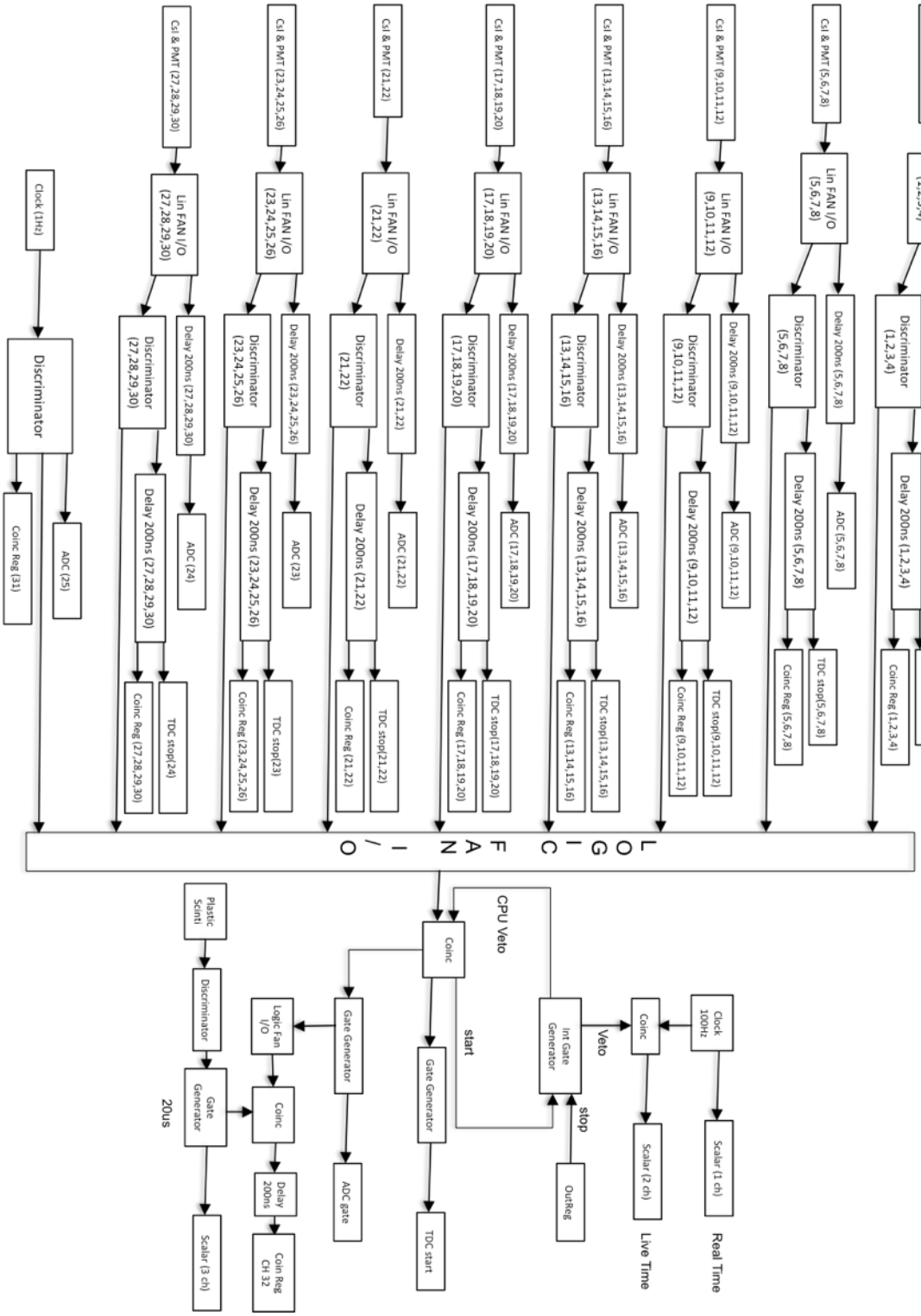

Fig.2.7 The electric circuits of beta decay experiment

2.2 Timing calibration for TDC

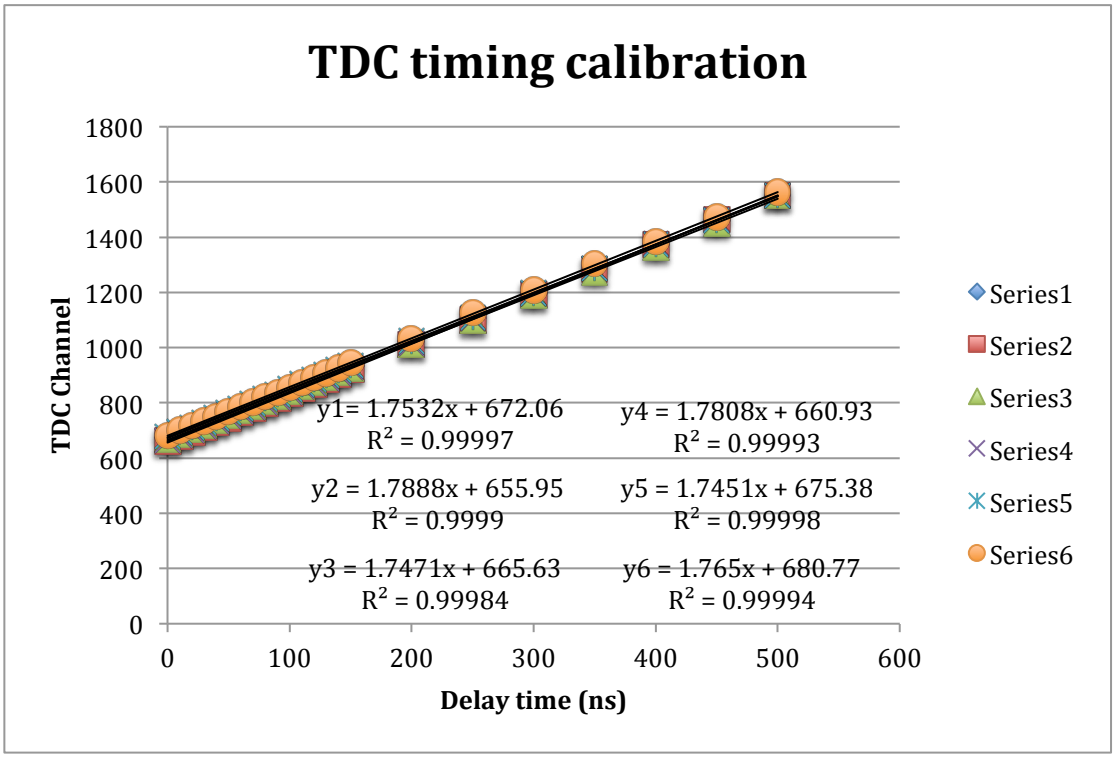

Fig.2.8 The TDC timing calibration for CsI 1-6

For the timing calibration, we changed the CsI(Tl) signals by 100Hz clock signal on electric circuits of Fig.2.7. Then we fixed the timing for TDC start signal and delayed different times for all the TDC stop signals individually. And we would find the peak on TDC spectrums respectively. We got the relationship between the delay time and TDC channel after that like Fig.2.8. Then we would know the timing for each channel on TDC spectrum. Like energy calibration, we did TDC timing calibration once every two weeks to check the stability of the TDC system.

2.3 Timing correction

2.3.1 Principle

There are time differences for different energies (Walk Effect) for CsI(Tl) detector. Like Fig.2.9, we could see the wave shape for low energy and high energy from the detector. There was a time difference when we set a

threshold and higher energy was a little earlier than the lower energy. And this time difference had strong relationship on energy. We would call this relationship as T-E function, where T means time and E means energy.

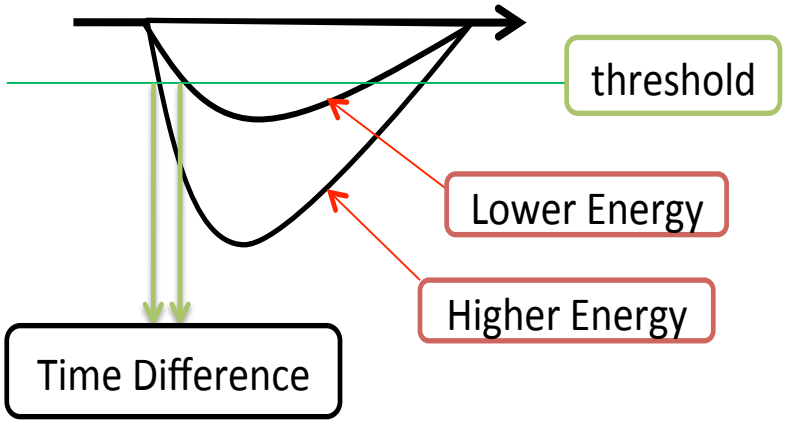

Fig.2.9 The principle for walk effect

The timing correction was based on the TDC spectrums such as TDC1-2, TDC1-3,…TDC1-24…TDC23-24. Where TDC1-2 means TDC spectrum 1 minus TDC spectrum 2, that is (TDC1-TDC2). Then we found a peak on TDC1-2, and shifted the peak to 0 in order to analyze easier in later analysis. We named this was the first step.

The second step was getting the T-E function. As we know that time differences between 2 detectors depended on energies of gamma rays. Thus we fixed the energy region for one detector and changed the energy region for another one, and then checked the time difference on each TDC spectrums respectively.

For example, we fixed the energy region for NO.1 detector at (983±2σ) keV. Then changed the energy of NO.2 detector from (800～1350)keV, and got time difference on TDC spectrums, TDC1-2 in this case. We got the Fig.2.10 as a result. Then we could draw those time differences on Fig.2.11 to get the T-E function at this case.

Those T-E functions were the basis for timing correction. On one hand, we could get the timing difference and its timing resolution between 983 keV on detector 1 and 1038 keV by fix those two energy regions on each detector, respectively. On the other hand, we could get a new time difference and resolution according to the T-E function that we got.

Just took the same steps as the example; we could fix any energy region that we interested (511, 1274keV for ^{22}Na and 983, 1038, 1311keV for ^{48}Ca) on ADC spectrum 1, and change energy region (400—1500keV for ^{22}Na and 800—1500 for ^{48}Ca) on ADC spectrum 2. We would get individual time difference on TDC1-2 and then got T-E function respectively. It was the same for ADC 1 and ADC 3, ADC 1 and ADC 4, until ADC 24 and same for ADC 2, ADC 3… until ADC23 like ADC 23 and ADC 24.

Timing correction was one of the most important parts for this experiment to reduce the background from accidental coincidence.

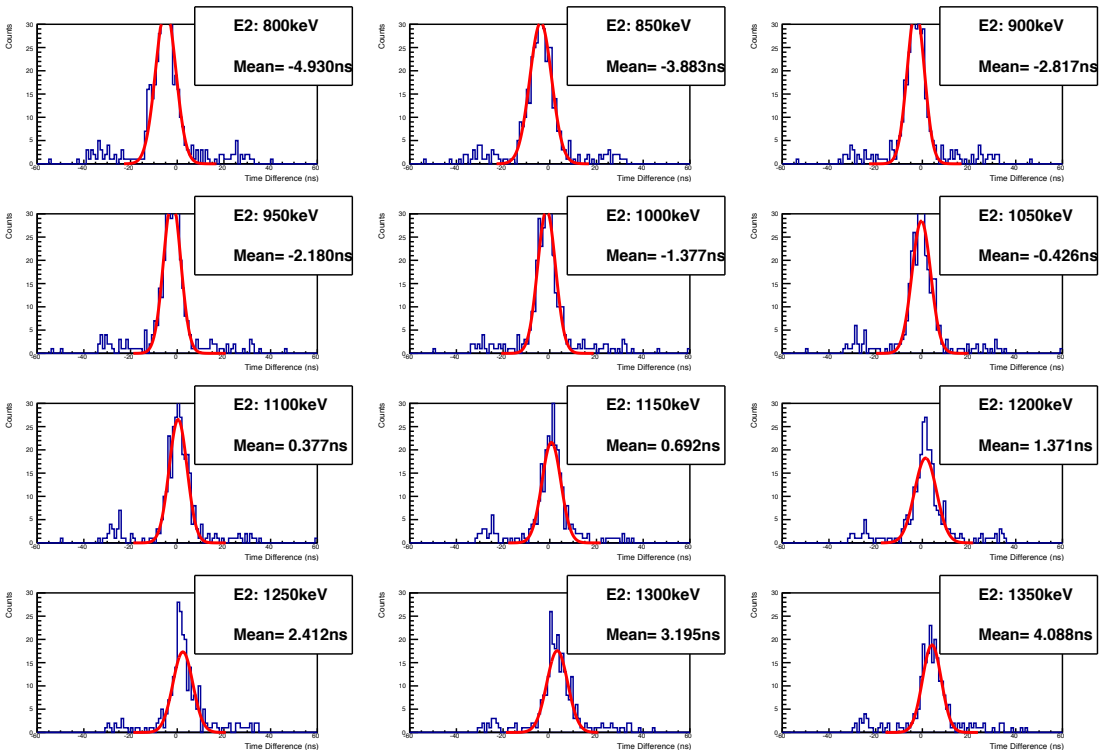

Fig.2.10 The time difference for detector 1 (983keV) and detector 2 (800—1350keV)

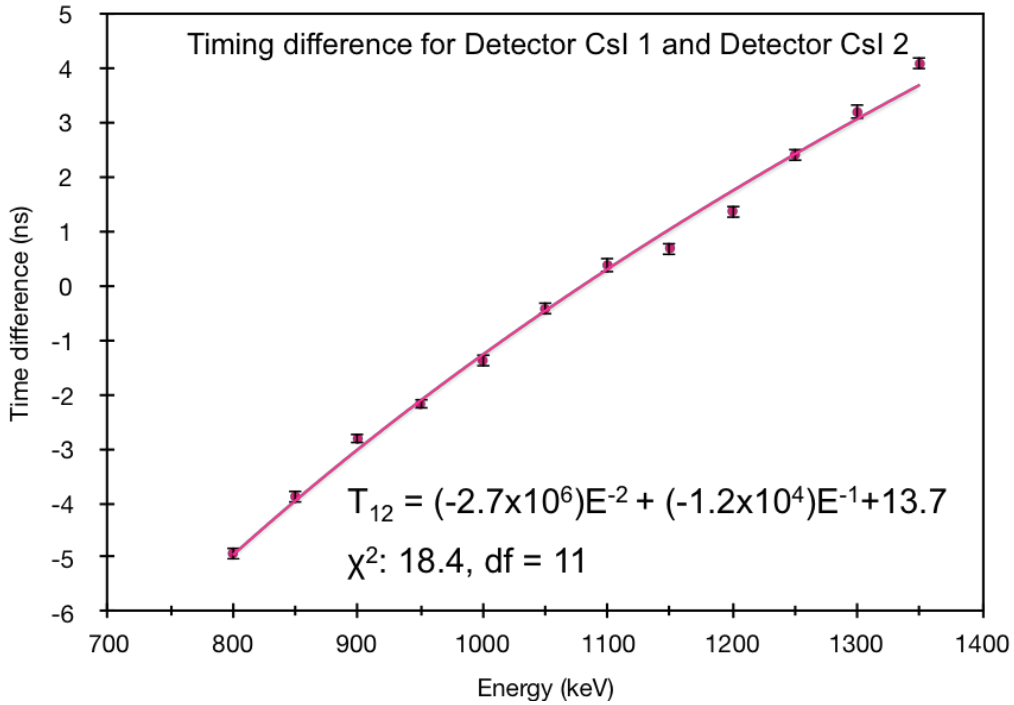

Fig.2.11 T-E function for Detector 1 (983keV) and detector 2 (800—1350keV)

Fitted Function: Fitting time difference by $a_0E^{-2} + a_1E^{-1}+a_2$

2.3.2 Timing resolution improvement

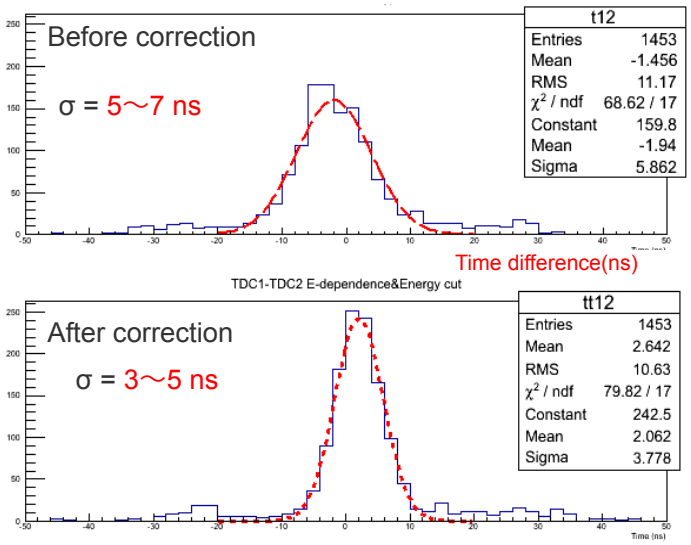

Fig.2.12 The timing resolution improvement example (the time difference between CsI 1 and CsI 2 around 1 MeV)

We had already got the T-E function in part 2.3.1. We could improve the timing resolution by applying the T-E function. Time differences between 2 detectors depended on energies of gamma rays which absorbed by each CsI(Tl)

detector. We improved the time resolution by using this relationship for timing correction. For example, it would reject around 80% of background from accidental coincidence with improvement of the time resolution from 5~7 ns to 3~5 ns (Fig.2.12). One of the most important features of this experiment was that we could reduce the background from accidental coincidence effectively with better time resolution.

Chapter III: ^{48}Sc Enrichment

1. Sc Enrichment with Ion Exchange Method

1.1 Ion exchange method

Ion exchange is an exchange of ions between two electrolytes or between an electrolyte solution and a complex. In most cases the term is used to denote the processes of purification, separation, and decontamination of aqueous and other ion-containing solutions with solid polymeric or mineralic "ion exchangers".

1.1.1 Sc capture

In this experiment, Sc was the decay product of ^{48}Ca. In that case, the solution was full of Ca ions and only had few Sc ions. And Sc ions were randomly distributed in the $CaCl_2$ solution. Since our sample space was very limited, we had to capture all of Sc ions into the sample space to measure the ^{48}Sc decay gamma rays. The important requirement for the ion exchange resin was that the resin should have almost 100% efficiency to capture the Sc ions and almost 0% efficiency for the Ca ions. It took us few years to search such kind of special resin and finally we found one chelate resin exactly marched this requirement. That was NOBIAS-CHELATE-PA1 made by Hitachi High Technology Ltd.

1.1.2 Chelate resin in this experiment

The resin we used for the ^{48}Sc enrichment was NOBIAS-CHELATE-PA1 as Fig.3.1. The diameter of the chelate resin was 45-90μm. The chelate resin we used was white powder as the left size of the Fig.3.1.

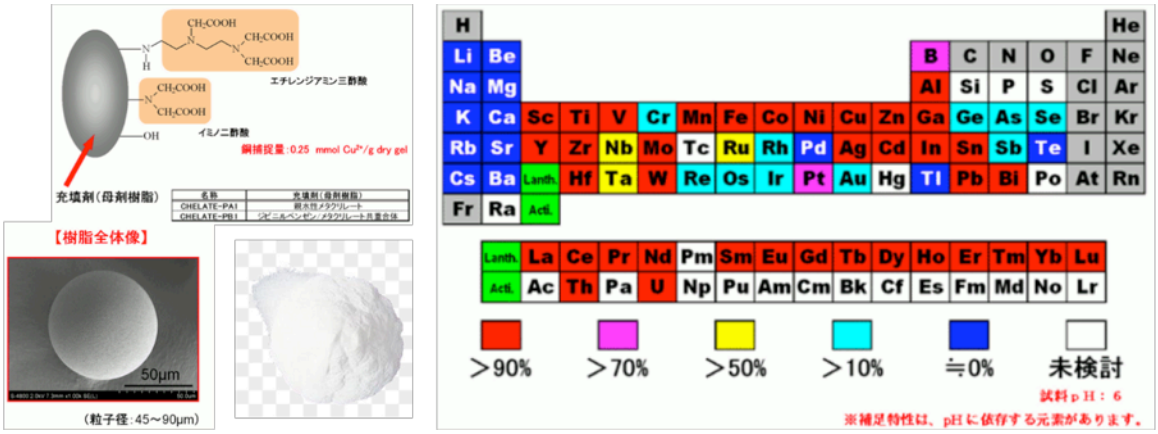

Fig.3.1 The NOBIAS-CHELATE-PA1 resin and its capture efficiency for different elements

As we could see from the right side of Fig.3.1, the resin was really good at capturing the Sc ion and almost no ability of capturing Ca ion. This Resin was also good at capturing the Fe, Cu, Pb and Bi. So the resin could also easily be contaminated by those ions such as Fe, Cu, Pb and Bi. We should take out those elements before the solution pass though the NOBIAS-CHELATE-PA1 resin.

1.2 Ion exchange setup

The ion exchange setup (Fig.3.2) mainly contained a solution tank, a pump for solution circulation and holder for resin. The circulation flow had to be carefully controlled because the resin was sensitive on the contact time of ion exchange process.

We had lots of efficiency would be described in this chapter. So we made definition here for each of them.

(1) Capture efficiency of resin: the efficiency that target ions be captured after target ions passed though the resin.

(2) Circulation efficiency: the efficiency that Radioactivity target atoms were captured before those atoms decay in the tank.

(3) Enrichment efficiency: the efficiency for this ^{48}Sc enrichment experiment that combined the capture efficiency and circulation efficiency.

(4) Gamma detection efficiency: detection efficiency for gamma rays.

(5) Experimental detection efficiency: the total efficiency for this experiment that combined with enrichment efficiency and gamma detection efficiency.

1.2.1 Demonstration setup

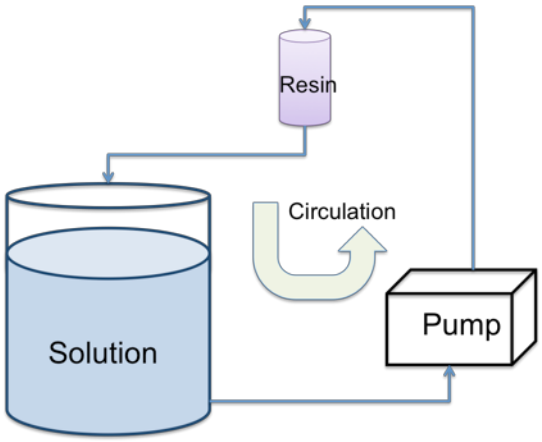

Fig.3.2 The conceptive setup of ion exchange

The demonstration setup like Fig.3.2 mainly worked for setting parameters of best conditions for highest capture rate of ^{48}Sc.

First of all, we estimated the circulation efficiency for ^{48}Sc, the conceptive setup was like Fig.3.3. Part of 48Sc would decay in the tank before passed though the resin.

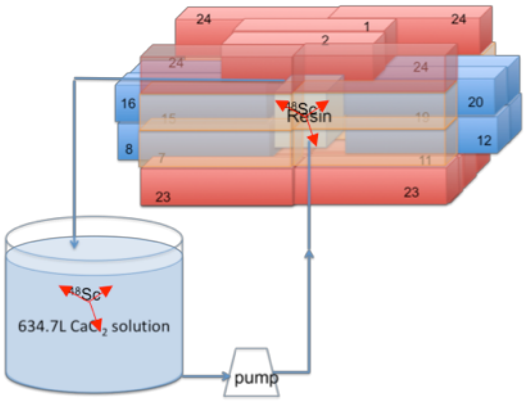

Fig.3.3 The circulation efficiency for ^{48}Sc

For the ^{48}Sc half-life time is 43.7h. So during the $CaCl_2$ solution circulation, part of the ^{48}Sc would decay in the tank, and that part we couldn't detect with CsI scintillators like Fig.3.3. The lost part of the efficiency is

$$\sum_{n=1}^{\infty}\left(1-e^{\frac{-t}{\tau}}\right)^{n}$$

Where t is the circulation time with unit of hours; τ is mean-life time τ= 63.06h. If we set the lost of efficiency less than 10%, thus we calculated the maximum circulation time would be t<5.3hours for this beta decay experiment.

Then we tried to know if there was Ca density dependence for the capture efficiency. Only we set the Ca density that we could calculate the volume of $CaCl_2$ solution in order to design the size of tank. Then we needed to know if there was Sc density dependence for the capture efficiency. Finally, we set the solution flow rate and mass of resin and calculated the enrichment efficiency. The above-mentioned demonstration was for the macro level (ppm) for Sc density. However, in the beta decay experiment, there would be only a few Sc atoms/day in the solution. So we needed demonstrate that the resin could still capture those few Sc atoms with high capture efficiency.

1.2.1.1 The previous demonstration

Undergraduate students in Kishimoto Lab did this demonstration experiment in 2015. Here I would mainly mention Mr. Fujiwara's experiment because he used the same resin as this beta decay experiment.

Firstly, I reproduced Fujiwara's experiment about the pH and buffer for the resin and confirmed that the best pH was 5.6 with buffer of HNO_3 (0.1mol/L) and CH_3COONH_4 (0.1mol/L).

Then I checked the capture efficiency with different density of Ca in $CaCl_2$ solution in order to get to know the best Ca density for the beta decay

experiment. Table.3-1 showed the capture efficiency result for different Ca density. The result confirmed that the Ca density almost not affect the capture efficiency for this resin. So we could make the $CaCl_2$ solution with Ca maximum density of 12% (4mol/L). And the capture efficiency was 93.5±1.7% when did test in a very small scale (100ml) of $CaCl_2$ solution. The capture efficiency was calculated based on measurement result of Sc with ICP-MS before and after the circulation.

Table. 3-1 The capture efficiency result for different Ca density

Ca density	Resin (g)	Sc content	Solution volume	Solution flow	Circulation time	Capture efficiency
3%	1	100 ppb	100ml	10ml/min	90min	94.7±2.1%
6%	1	100 ppb	100ml	10ml/min	90min	94.0±2.2%
9%	1	100 ppb	100ml	10ml/min	90min	93.1±1.9%
12%	1	100 ppb	100ml	10ml/min	90min	93.5±1.7%

I also checked the capture efficiency when increasing the density of Sc ions. I set the Ca density at 12%, and 10g resin, 10ml/min solution flow, with 100ml solution. The circulation time was still 90 minutes. I changed the Sc density as 1ppm, 10ppm, 50ppm each time. The capture efficiency was measured and the result was 94±3% for all set Sc density. It confirmed that the capture efficiency was stable when increase the target ions with enough resin.

I tested the Sc contamination with ICP-MS in pure water for making $CaCl_2$ solution, and the buffer of HNO_3 and CH_3COONH_4. It turned out the Sc was less than 0.5ppb in pure water, less than 1 ppb in HNO_3(0.1mol/L) and less than 0.5 ppb in CH_3COONH_4(0.1mol/L).

In conclusion, there was no Ca density and Sc density dependence for the capture efficiency of resin. The capture efficiency was 94±3%. The Ca density could be set as 12% in the solution. In that case, we calculated the solution size would be 634.7L for 255kg $CaCl_2$ powder. Since we set the minimum

circulation efficiency at 90%, which corresponded the circulation time was 5.2 hours. We calculated the circulation flow should be 2.0L/min.

1.2.1.2 The 10 times scale up demonstration

Since we would use 634.7L $CaCl_2$ solution, we needed estimate how much resin to use to keep high capture efficiency. We also needed to make sure that the capture efficiency would be always stable in big scale. So we designed a 10 times scale up demonstration.

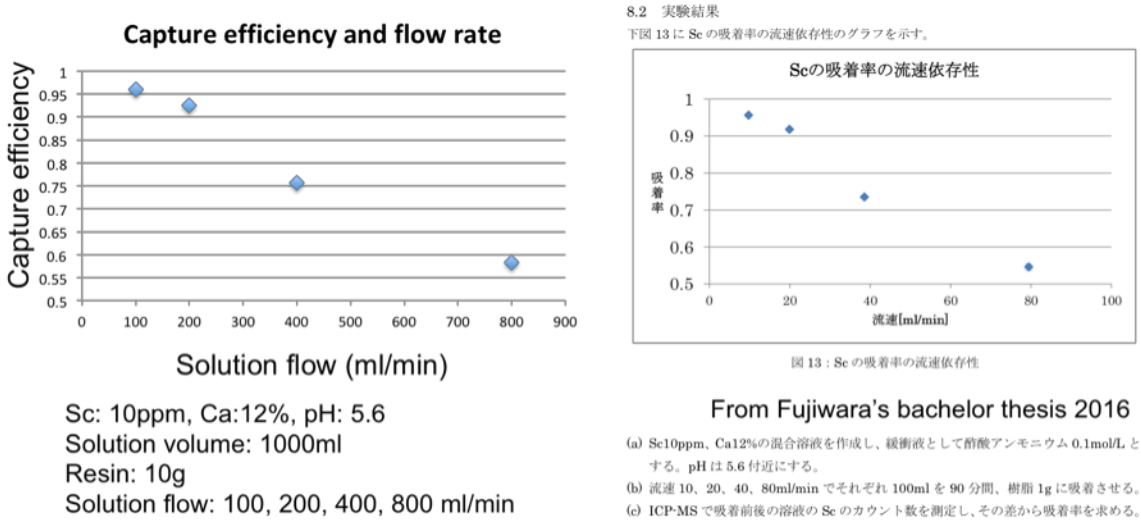

Fig.3.4 The capture efficiency and solution flow rate [The left one is 10 times scale up compare with the right side one (from Mr. Fujiwara's experiment), the two experiment showed the same relationship and the capture efficiency decrease when flow speed increase]

We still set the Sc at 10ppm in $CaCl_2$ solution with Ca density of 12%. pH was still 5.6 and buffer was HNO_3(0.1mol/L) and CH_3COONH_4(0.1mol/L). We used 10g ion exchange resin and made 1000ml $CaCl_2$ solution. In order to compare the capture efficiency for different solution flow speed, we did the experiment with solution flow of 100 ml/min, 200 ml/min, 400 ml/min. The circulation time was the same for 90 min. We measured the Sc in $CaCl_2$ solution before and after the circulation with ICP-MS. Fig.3.4 showed the experiment result for 10 times scale up and compared with the right side one which was the result from Mr. Fujiwara. From the experiment, we realized that if we increased the solution flow to 10 times, we need also increase the mass of resin at least 10 times to keep the same capture efficiency. That

demonstrated the minimum mass of enrichment resin was 100g. For safety and economical reason, we set the mass of chelate resin at 138.5g.

1.2.2 Full scale experiment setup

For the full-scale ^{48}Sc enrichment, we used 634.7L $CaCl_2$ solution and pH was 5.6. The mass of enrichment ion exchange resin was 138.5g. The $CaCl_2$ solution flow was 2.0L/min. So one circulation time was 311.1 min. From the demonstration experiments, the ^{48}Sc capture efficiency was 94±3%.

1.3 Capture efficiency

1.3.1 Efficiency for $CaCl_2$ solution circulation

For the ^{48}Sc half-life time is 43.7h. The lost part of the efficiency is

$$\sum_{n=1}^{\infty}\left(1-e^{\frac{-t}{\tau}}\right)^{n}$$

Where t is the circulation time t = 311.1min; τ is mean-life time τ= 63.06h

The lost of efficiency would be 8.9±0.3%, thus we calculated the circulation efficiency is 91.1±0.3% for this beta decay experiment.

1.3.2 Efficiency at atoms level of targets

1.3.2.1 Radon-rich water experiment

For the beta decay measurement, the atom number of ^{48}Sc was very small (about 3--4 atoms/day ($T_{1/2}(^{48}Ca(\beta))$--10^{21} y). Thus we also had to confirm the enrichment efficiency under extremely low target atoms number.

The best way was use ^{48}Sc isotopes and measured with CsI scintillators. However, it was impossible to make it because of short lifetime. Then the other good choice was use ^{46}Sc (produce with $^{45}Sc + n \rightarrow {}^{46}Sc$ by accelerator).

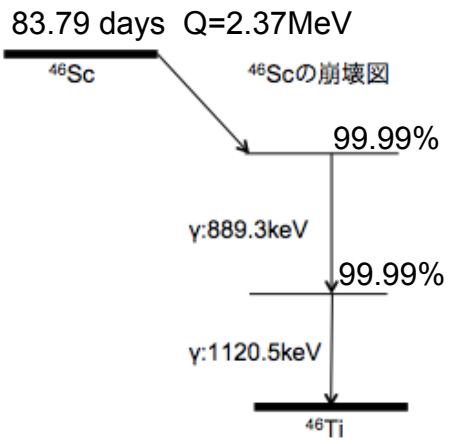

Fig.3.4 Decay scheme of ^{46}Sc

As we could see from Fig.3.4, the ^{46}Sc with half-life time is 63.8 days. ^{46}Sc decays to ^{46}Ti and emits 2 gamma rays with energy of 889keV and 1120keV. We could easily detect those two gamma ways with coincidence measurement. However, the accelerator was not available to make such isotope in 2016.

We finally found out that ^{222}Rn was also very good to make test about the ion exchange resin. As we could see from the decay chain of ^{222}Rn like Fig.3.5, among those decay products, the ion exchange resin could not capture Po, Tl and Hg (see Fig.3.1). However Pb and Bi were highly efficient for the capture of ion exchange.

For the isotopes of Pb and Bi, there are 3 candidates like below:

(1) ^{214}Pb
- (gamma, 295keV[energy], 26.8m[half-life time], 19%[decay branch ratio])
- (gamma, 352keV, 26.8m, 36%)

(2) ^{210}Pb
- (gamma, 47keV)

(3) ^{214}Bi
- (gamma, 609keV, 19.7minutes, 47%)
- (gamma, 1120keV, 19.7m, 17%)
- (gamma, 1764keV, 19.7m, 17%)

We had to measure the isotope by detecting the gamma rays with CsI

scintillators. For ^{210}Pb, the energy was too low to detect by CsI. ^{214}Pb and ^{214}Bi were possible to detect, however ^{214}Bi was better to detect because of the gamma energies were perfect for CsI to detect.

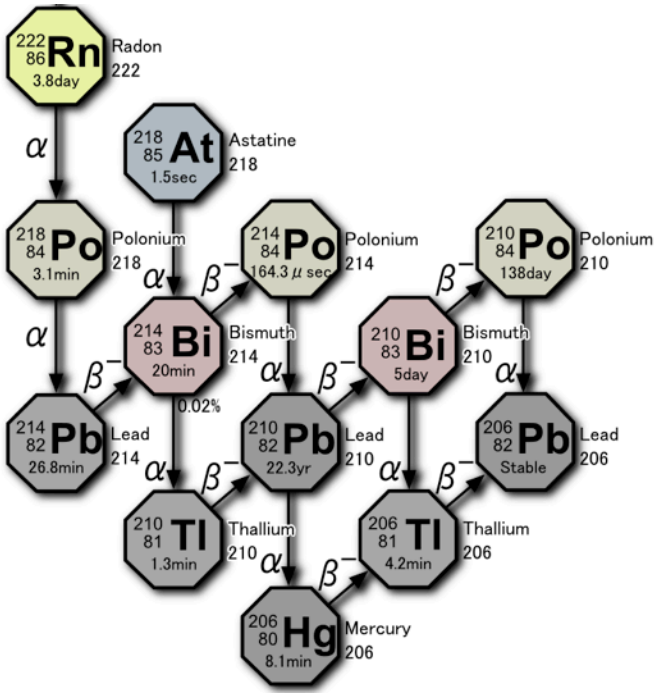

Fig.3.5 The decay chain of ^{222}Rn

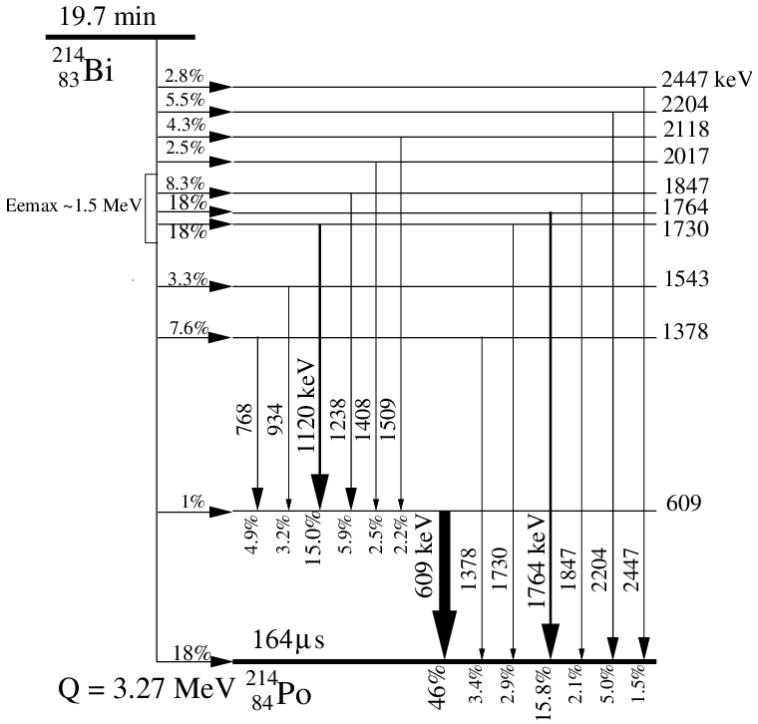

Fig.3.6 The decay scheme of ^{214}Bi

1.3.2.1.1 Experiment method

Radon is relatively easy to dissolve into water. The radon level in Kamioka underground Lab was higher than Osaka University surface lab. So we made radon rich water in Kamioka lab that had Radon level over 200Bq/m^3. We used 30L pure water and pumped Kamioka Lab air with speed 20L/min into the pure water. The air pumping time was 8 hours.

Then we measured the radon rich water in Osaka University with CsI scintillators. There were two independent experiments.

(1) Used CsI scintillators array to measure 2L radon rich water directly.

(2) There was 28L Radon rich water passed though the chelate resin and measured with CsI scintillators array.

We compared those two experiments and checked the difference of detected events, from that we could calculate the capture efficiency of ion exchange resin.

1.3.2.1.2 Detect ^{214}Bi decay

We used coincidence method to detect the ^{214}Bi. There were 3 coincidence measurements independently. We got the detection efficiency from Monte Carlo simulation that would be introduced in next chapter. And the detection efficiency for each coincidence showed like table 3-2.

Table 3-2 The detection efficiency for each coincidence pair

Coincidence pair	Branching ratio	Detection efficiency
1120keV & 609keV	15%	19.0%
1120keV & 609keV	5.9%	18.7%
1120keV & 609keV	4.9%	22.4%

1.3.2.1.3 Background Measurement

We measured the background for 241.2 hours live time, the sample space set

as normal pure water. We got the background events like table 3-3:

Table 3-3 The background measurement for each coincidence pair

Coincidence pair	Total events	Counting rate
1120keV & 609keV	649	21.5 /8hours
1120keV & 609keV	251	8.3 /8hours
1120keV & 609keV	315	10.5 /8hours

1.3.2.1.4 Experiment result for 2L direct measurement

The energy spectrum of 2L radon-rich water measurement showed in Fig.3.7.

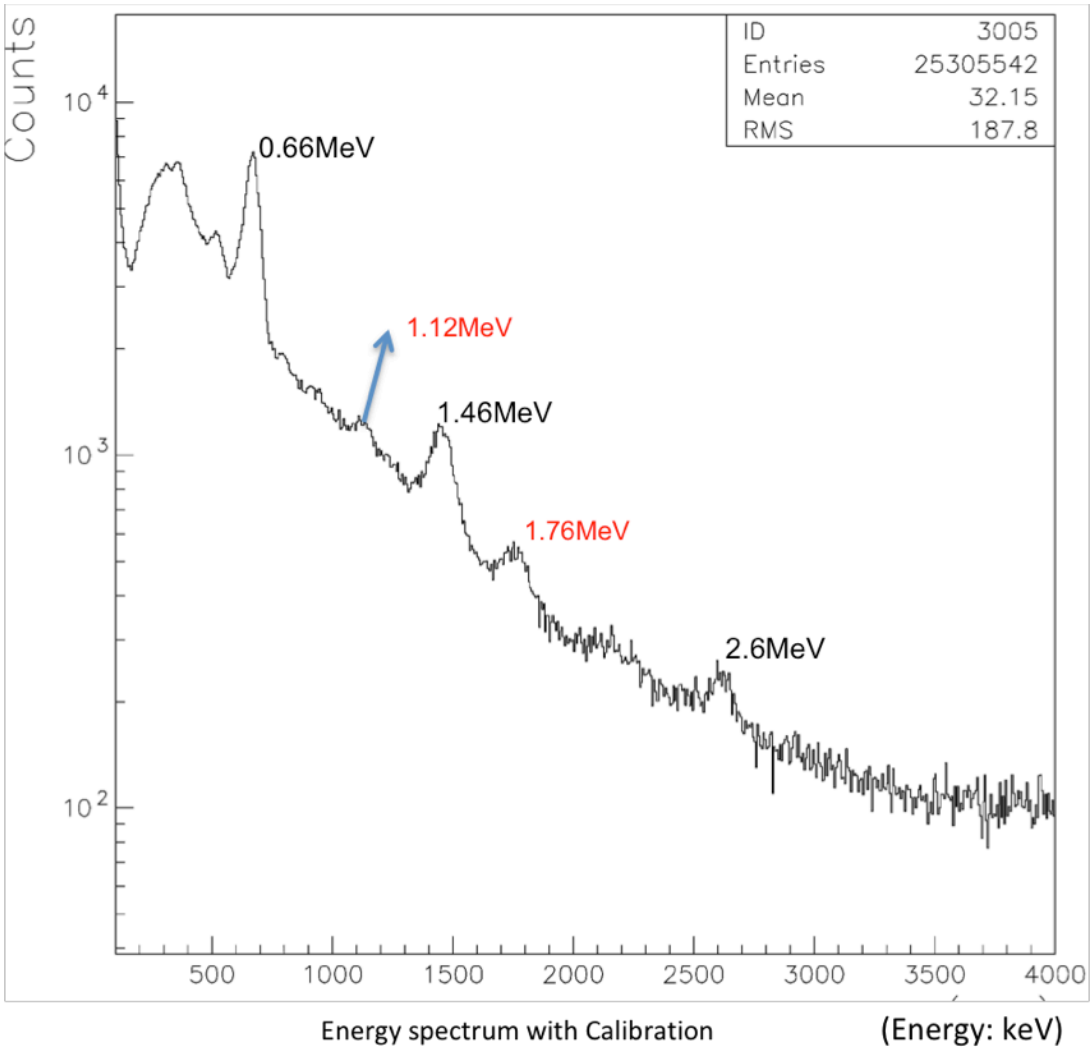

Fig.3.7 Energy spectrum for 2L radon rich water measurement

From the energy spectrum, we could see the clear energy peak of ^{137}Cs (662keV), ^{40}K (1.46MeV) and ^{208}Tl (2.6MeV). We could also see the energy peak of ^{214}Bi at energy of 1120keV and 1764keV, however, with huge amount of background. Thus we measured the counting rate of ^{214}Bi by coincidence measurement. Fig.3.8 showed the coincidence spectrum of ^{214}Bi with fixed energy of 609keV±2σ. We could clearly see the coincident peaks of 768keV, 934keV, 1120keV and so on.

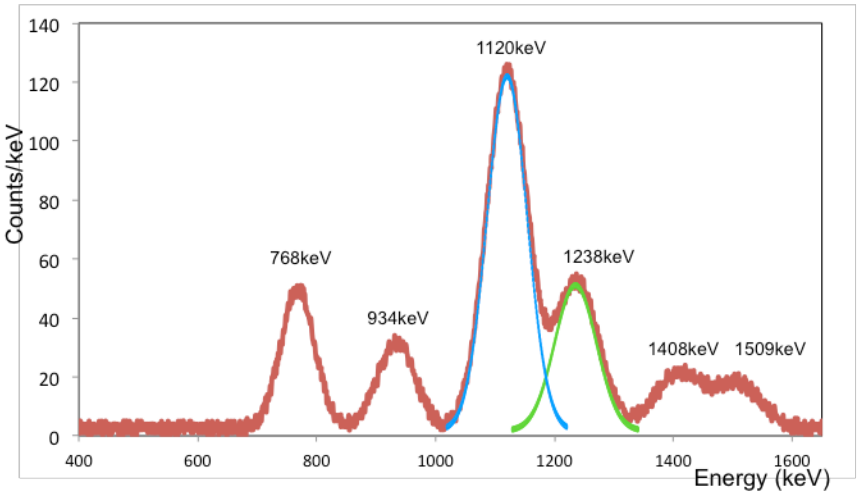

Fig.3.8 The coincidence spectrum for ^{214}Bi measurement

We put the 2L radon rich water in a 2mm thick plastic box and started the measurement from 2017/1/21 10am to 2017/1/23 10am, analyze data every 8 hours. Fig.3.9 showed the measurement data for each point.

Table.3-4 Measurement events for 2L radon rich water

Time (hour)	Coincidence 1 events	Background subtracted 1	Coincidence 2 events	Background subtracted 2	Coincidence 3 events	Background subtracted 3
8	332	310.4	128	120.0	131	119.6
16	314	292.2	119	111.0	121	110.5
24	296	274.7	115	106.2	114	103.8
32	279	257.6	108	99.6	106	96.2
40	265	243.6	102	94.2	103	92.8
48	252	230.4	95	86.7	97	86.4

*Coincidence 1 means 1120keV & 609keV; coincidence 2 means 1238keV & 609keV; coincidence 3 means 768keV & 609keV.

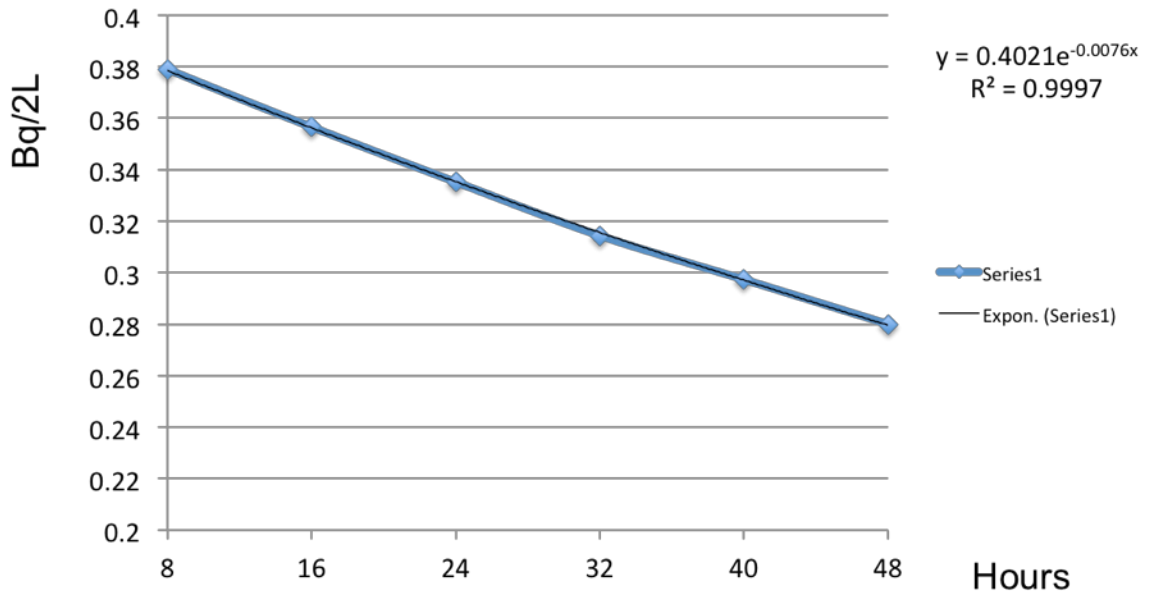

Fig.3.9 The measurement result for 2L radon rich water measurement

We could calculate the half lifetime for ^{222}Rn was 91.2h (3.80days). Comparing with the half-life for ^{222}Rn-222 was 3.82days. Thus the experiment error for this measurement was about 0.5%.

1.3.2.1.5 Measurement with CsI :28L with resin enrichment

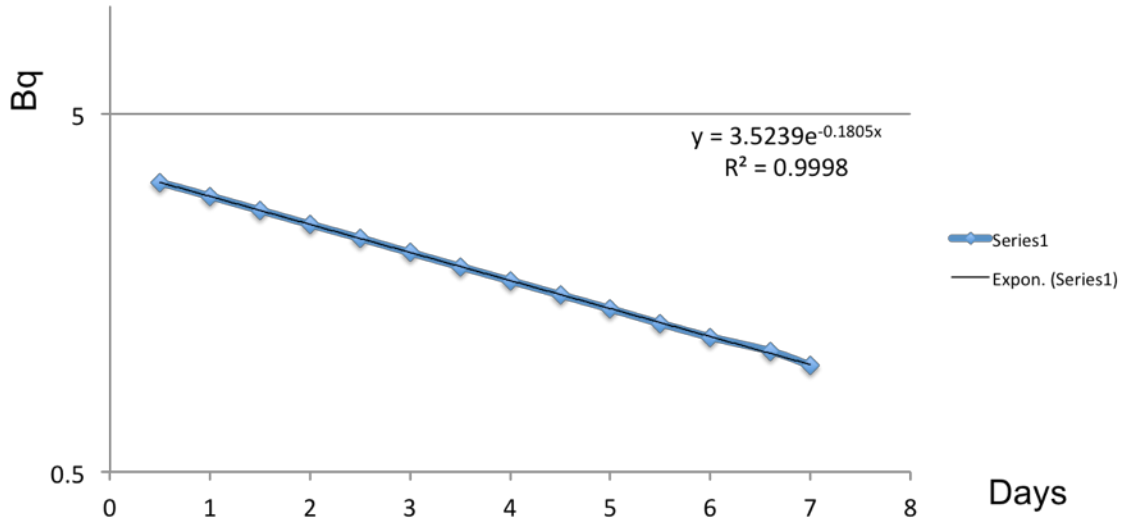

Fig.3.10 The measurement result for 28L radon rich water ^{214}Bi enrichment measurement

Measurement condition for radon-rich water with ^{214}Bi resin enrichment

by CsI scintillators array was like below:

- Sample: 28L radon-rich water
- Ion-exchange resin: 5g
- Water flow: 0.5L/min (61min/circulation)
- Measurement time: 7 days

The Measurement started from 2017/1/23 11am to 2017/1/30 11am. We analyzed the data every 0.5day. The measurement result showed in Fig.3.10. We could calculate the half lifetime for ^{222}Rn was 3.84days. Comparing with the half-life for ^{222}Rn was 3.82days. Thus the experiment error for this measurement was about 0.6%.

1.3.2.1.6 experiment result

(1) Capture efficiency of ^{214}Bi

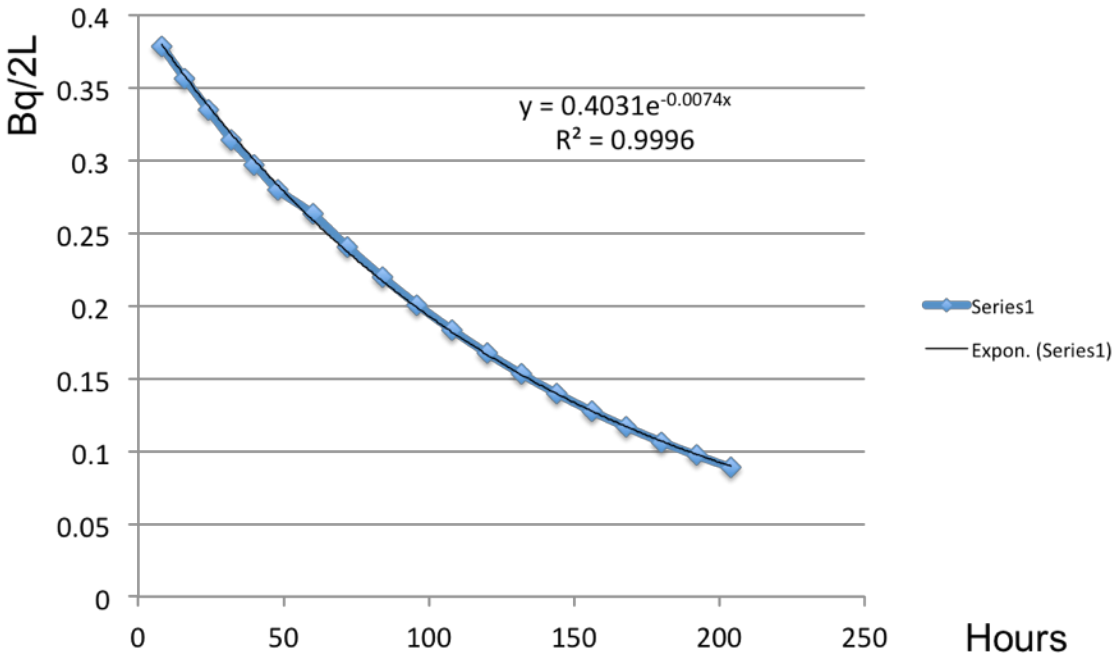

Fig.3.11 The normalized measurement result for radon rich water measurement

We compared the two results that mentioned above. The 28L radon rich water should had 14 times events be detected by the CsI detectors if we assume both of the capture efficiency and circulation efficiency were 100%.

Since we calculated that the circulation efficiency was 82.3%, so the capture efficiency of ^{214}Bi was 94.8±1.8%.

(2) Capture efficiency of ^{48}Sc

Since the ^{214}Bi and ^{48}Sc have mostly the same capture efficiency, we got to know the capture efficiency for ^{48}Sc could still be over than 94% at few atoms level.

1.3.2.2 Radon-rich $CaCl_2$ solution experiment

We used the $CaCl_2$ solution for beta decay experiment, thus we also needed to know the affect of $CaCl_2$ for the few atoms level enrichment.

1.3.2.2.1 Prepare $CaCl_2$ solution

We took 5.0 kg $CaCl_2$ powder and made it to 12.0L solution. We still used the as buffer and pH set as 5.6. We divided the 12.0L solution into 2 parts and each part had 6.0L. One part had been made for Radon-rich $CaCl_2$ solution and another part had been set as background check.

1.3.2.2.2 Prepare Radon rich $CaCl_2$ solution

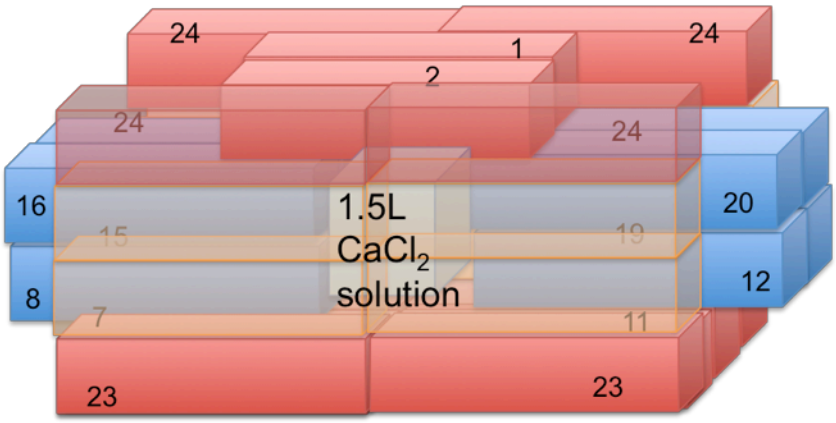

Fig.3.12 Setup for 1.5L radon-rich solution direct measurement

We made the Radon-rich $CaCl_2$ solution in Osaka University at Radon level of 80Bq/m^3. We pumped the air with flow of 8 L/min and continued for 54 hours. Then we divided the solution into 2 parts, one with 1.5L for direct measurement (as Fig.3.12) and another one with 4.5L for resin enrichment

circulation (as Fig.3.13). We used 1.5g resin for the ^{214}Bi enrichment experiment.

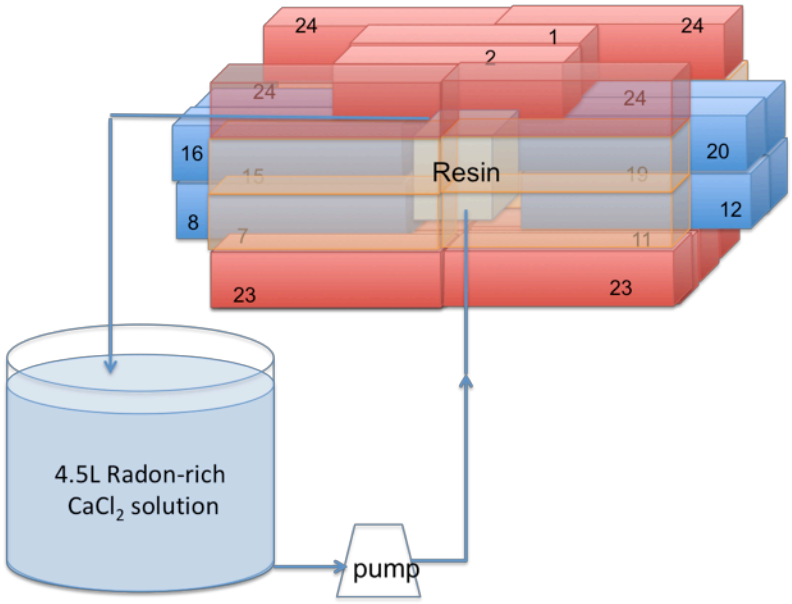

Fig.3.13 Setup for 4.5L radon-rich solution enrichment measurement

1.3.2.2.3 Background test

(1) Background for direct measurement

The condition for the background measurement set as the same for radon rich $CaCl_2$ solution direct measurement, except we used 1.5L normal $CaCl_2$ solution. There was a 2mm plastic box with 1.5L $CaCl_2$ Solution and N_2 gas purge detector system. The measurement started after 4 hours gas purge to make sure the radon free environment.

We still detected the ^{214}Bi with 3 different of coincidence measurement. Measurement time set as 48 hours. The background coincidence events for 1.5L normal $CaCl_2$ solution direct measure was like below:

(I) 1120keV & 609keV: 62 events/48hours;
(II) 1238keV & 609keV: 32 events/48hours;
(III) 768keV & 609keV: 36 events/48hours.

(2) Background for resin enrichment measurement

The condition for the background measurement set as the same for ^{214}Bi

enrichment radon rich $CaCl_2$ solution direct measurement, except we used 4.5L normal $CaCl_2$ solution. There was a 2mm plastic box with pipe that contained 1.5g resin for enrichment of $CaCl_2$ Solution. Also there was N_2 gas purge system. The measurement started after 4 hours gas purge to make sure the radon free environment.

We still detected the ^{214}Bi with 3 different of coincidence measurement. Measurement time set as 48 hours. The background coincidence events for 4.5L normal $CaCl_2$ solution with resin enrichment was like below:

(I) 1120keV & 609keV: 53 events /48hours;
(II) 1238keV & 609keV: 27 events/48hours;
(III) 768keV & 609keV: 30 events /48hours.

The background rate had little difference for the previous two background measurements. The background rate for direct solution measurement was little higher than the resin enrichment. The reason was the difference of sample space. For the resin enrichment, 85% of the sample space was N_2 gas, however, almost all of the sample space for direct measurement was $CaCl_2$ solution that might contain some ^{214}Bi.

1.3.2.2.4 Measurement result

(1) Measurement for 1.5L radon rich $CaCl_2$ solution

Table.3-5 Measurement events for 1.5L radon rich $CaCl_2$ solution

Time (hour)	Coincidence 1 events	Error 1	Coincidence 2 events	Error 2	Coincidence 3 events	Error 3
8	1387	37.4	538	23.3	535	23.2
16	1306	36.3	507	22.6	504	22.5
24	1228	35.2	477	21.9	474	21.8
32	1152	34.1	447	21.2	445	21.2
40	1089	33.2	423	20.6	421	20.6
48	1026	32.2	398	20.0	396	20.0

*Error = SQRT(Coin events + BG/8hours); Measurement time: 48hours: start from 2017/2/13

at 20:00 and stop at 20:00, 2017/2/15.

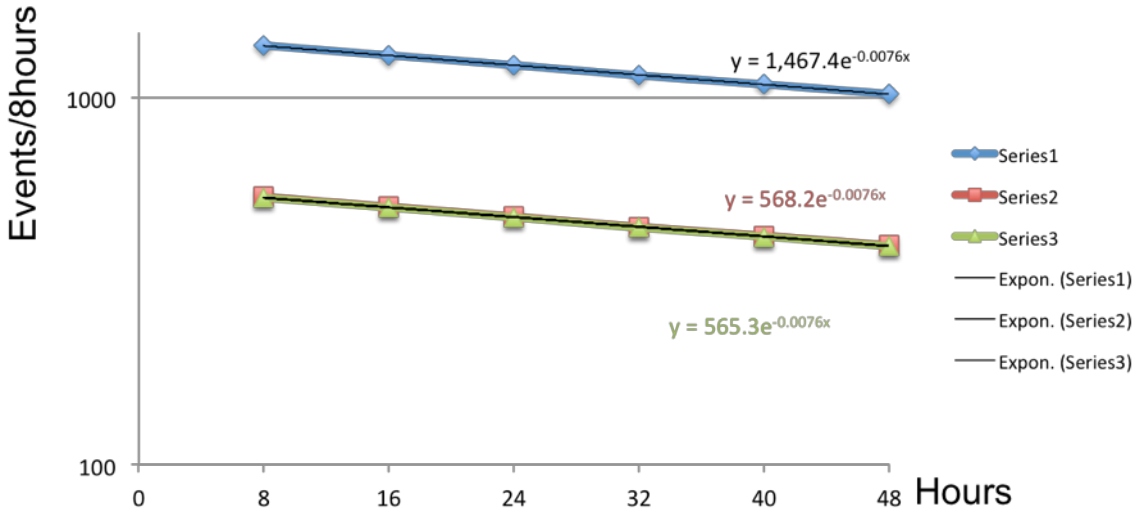

Fig.3.14 The fitting histogram for the 3 coincidence measurements [Series 1, 2, 3 for coincidence 1, 2, 3, respectively]

We analyzed the data every 8 hours, and the ^{222}Rn concentration at 48th hour was 1.41/(min・L). The half-life time for ^{222}Rn we measured was 91.2±0.5 hours.

(2) Measurement of radon-rich $CaCl_2$ solution with resin enrichment

The sample was 1.5g ion exchange resin and circulated with 4.5L radon-rich $CaCl_2$ solution with flow of 0.2L/min (22.5min/circulation). Measurement time was 7.1 days.

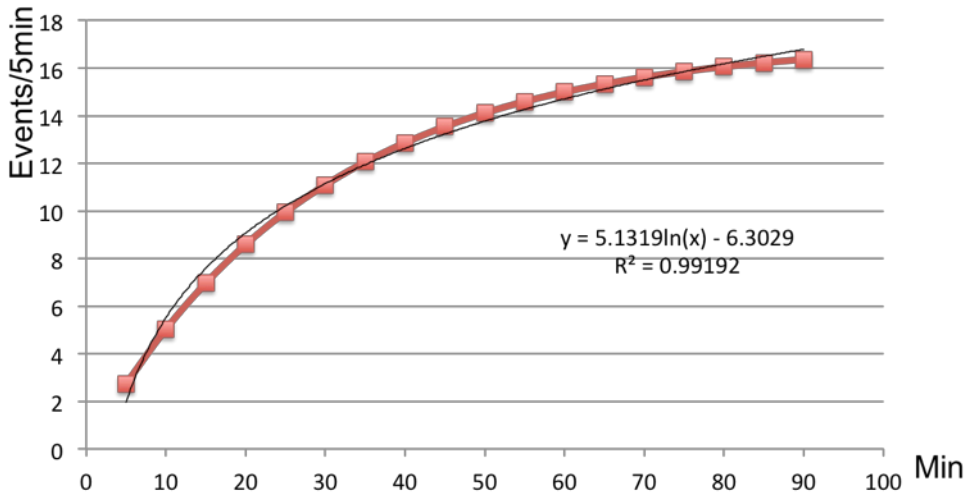

Fig.3.15 The counting rate of ^{222}Rn in the first 90 minutes of $CaCl_2$ circulation

For the data of the first 1.5 hours, we analyzed data every 5 minutes. Fig.3.15 showed the measurement result. The decay speed increase with time confirmed that the enrichment worked in good condition.

In Fig.3.15, we only showed the events for coincidence measurement of 1120keV and 609keV. The measurement started from 2017/02/16 at 4am.

Table.3-6 showed the measurement result for 4.5L radon rich $CaCl_2$ solution with resin enrichment. We took 8 hours to make radon free detection environment with N_2 purge system at flow of 2L/min. The measurement time started from 56^{th} hour comparing with the start time of 1.5L radon rich $CaCl_2$ solution direct measurement. The 4.5L radon rich $CaCl_2$ solution should had the same decay rate if we normalized it to 1.5L with assumption that the capture efficiency and circulation efficiency both were 100%. From the calculation, the circulation efficiency was 90.5%, so the capture efficiency of ^{214}Bi was 94.5±0.8%.

Table.3-6 Measurement events for 4.5L radon rich $CaCl_2$ solution with resin enrichment

Time (hour)	Coincidence 1 events	Error 1	Coincidence 2 events	Error 2	Coincidence 3 events	Error 3
64	2216	47.1	860	29.4	857	29.7
72	2034	45.2	787	28.1	783.3	28.1
80	1858	43.2	719	26.9	715.4	26.8
88	1697	41.3	657	25.7	653.4	25.6
96	1550	39.5	600	24.6	596.8	24.5
104	1415	37.7	548	23.5	545.1	23.4
112	1293	36.0	500	22.4	497.9	22.4
120	1181	34.5	457	21.5	454.7	21.4
128	1078	32.9	417	20.5	415.3	20.5
136	985	31.5	381	19.6	379.3	19.6

* We took 8 hours to make radon free detection environment with N_2 purge system. The measurement time start from 56^{th} hour comparing with the start time of 1.5L radon rich $CaCl_2$ solution direct measurement. The coincidence events were result of 8 hours measurement.

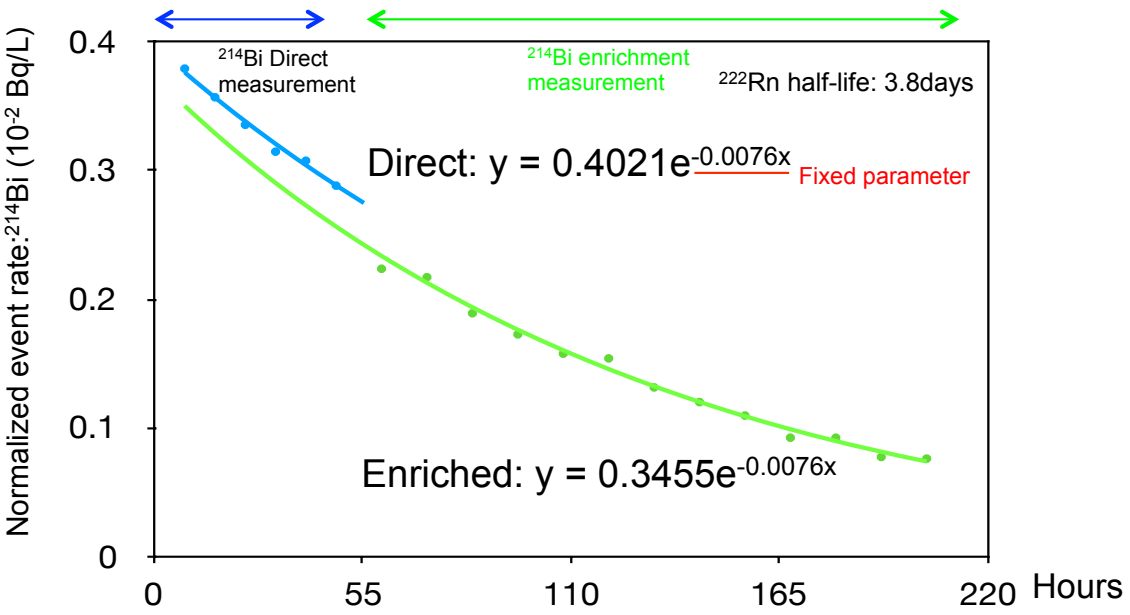

Fig3.16 The measurement result for direct measurement and enrichment measurement

Fig.3.16 showed the measurement result for 1.5L direct measurement and 4.5L enrichment measurement. The difference of the two fitting was the capture efficiency for ^{214}Bi combined with circulation efficiency. The capture efficiency of ^{214}Bi was 94.8±1.2%. It confirmed the high capture ability of resin for hundred of target atoms. It also confirmed the detection ability for CsI scintillators for coincidence measurement.

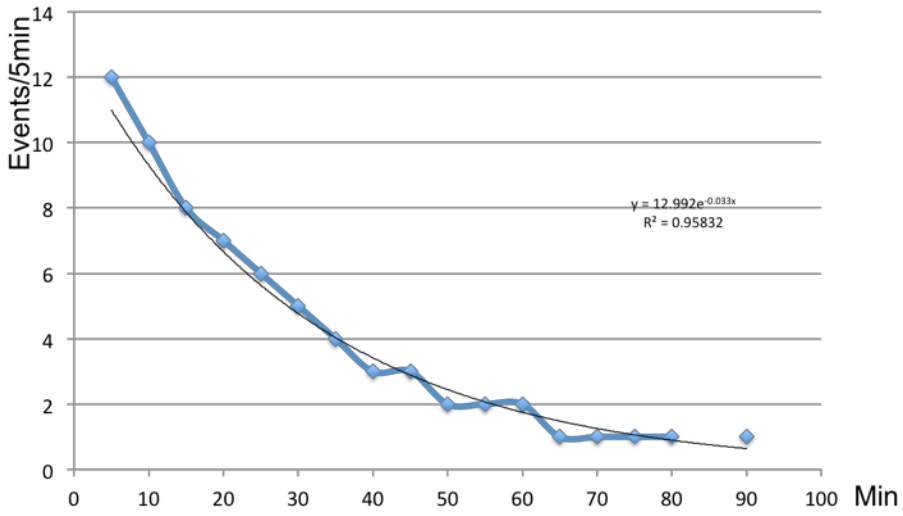

Fig.3.17 The measurement result after stopped the $CaCl_2$ solution circulation

We continued to take 1.5 hours data after we stopped the circulation, and

analyzed the data very 5 minutes. The result showed in Fig.3.17 and it followed the ^{214}Bi decay rate.

1.3.2.3 Conclusion of Radon Test

We did radon test with ^{222}Rn rich pure water and Radon rich $CaCl_2$ solution. The combined capture efficiency for ^{214}Bi was 94.6±0.9%.

Since the ^{214}Bi and ^{48}Sc had same capture property for the resin we used, we assumed the capture efficiency for ^{48}Sc was over than 94%. According to the experiment of Sc-$CaCl_2$ solution, the capture efficiency for ^{48}Sc that we got was 94.1±0.5%.

2. ^{48}Ca sample

We used the Ca sample with ^{48}Ca natural abundance of 0.187%. In order to have the best efficiency of ion exchange enrichment of ^{48}Sc, this experiment took the $CaCl_2$ powder as ^{48}Ca source.

2.1 $CaCl_2$ powder

The $CaCl_2$ powder we used in this experiment was special pure level. It had few contamination elements like Cu (<2ppm), Fe (<2ppm) and Pb (<5ppm). Each contamination had been showed in Fig.3.18. We used ion exchange method the make further purification of those contaminations before the measurement.

In total, we had 255.1kg $CaCl_2$ powder for the experiment. We measured the abundance of ^{48}Ca with ICP-MS method and confirmed the natural abundance. We measured the total amount of ^{48}Ca in the $CaCl_2$ powder, that was 171.0±0.9g.

HPC
林 純薬工業株式会社

製　品　規　格

規格番号 ： 7-72
制定記号 ： AAM06
資源番号 ： 03000705

製品名 ： 塩化カルシウム

（別　名 ：　　）
等　級 ： 特 級
容　量 ： ５００ｇ
分　類 ： －

〒540-0037 大阪市中央区内平野町3-2-12
林 純薬工業株式会社
環境安全・品質保証部

No.	試　験　項　目	(単位)	規　格　値	試　験　方　法
1	外　観　(形　状)	－	潮解性の結晶又は粒塊	JIS K8123-1994による
2	(色　相)	－	白　色	
3	含　量	%	９５．０　以上	
4	水溶状	－	ほとんど澄明以内	
5	ｐＨ　(50g/L, 25℃)	－	８．０～１０．０	
6	硝酸塩　(NO_3)	%	０．００３　以下	
7	硫酸塩　(SO_4)	%	０．００５　以下	
8	りん酸塩　(PO_4)	%	０．００１　以下	
9	アンモニウム　(NH_4)	%	０．００１　以下	
10	ひ　素　(As)	ppm	１　以下	
11	バリウム　(Ba)	%	０．００６　以下	
12	銅　(Cu)	ppm	２　以下	
13	鉄　(Fe)	ppm	２　以下	
14	カリウム　(K)	%	０．０１　以下	
15	マグネシウム　(Mg)	%	０．０１　以下	
16	ナトリウム　(Na)	%	０．０１　以下	
17	鉛　(Pb)	ppm	５　以下	
18	ストロンチウム(Sr)	%	０．０１　以下	

Fig.3.18 The contamination elements in $CaCl_2$ powder

2.2 $CaCl_2$ Solution

2.2.1 Steps to make $CaCl_2$ solution

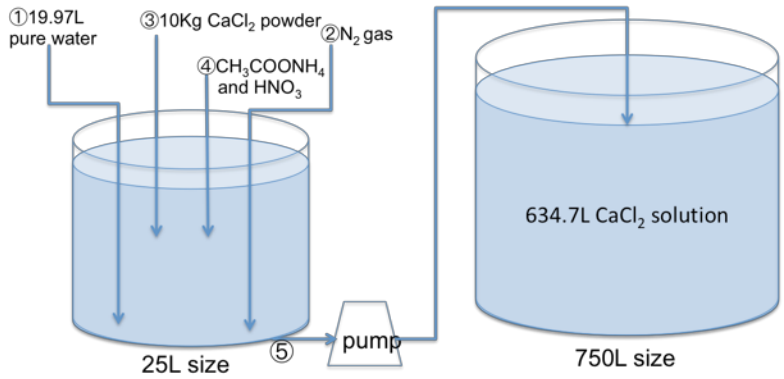

Fig.3.19 The steps to make $CaCl_2$ solution

Fig.3.19 showed the mainly steps for making 634.7L $CaCl_2$ solution with 255.1kg $CaCl_2$ powder. We made solution several times and each time with 10kg $CaCl_2$ powder.

(1). Take 10.0000kg $CaCl_2$ powder into 25L-size small tank; prepare radon

free pure water (N_2 gas circulation).

(2). Purge N_2 gas into small tank and circulate with flow 1.5L/min.

(3). Take 19.97L pure water to small tank.

(4). Close small tank and shake small tank until all $CaCl_2$ powder dissolved in the pure water.

(5). Put 28.4ml CH_3COONH_4 (0.1mol/L) and 1.6ml HNO_3 (0.1mol/L) into the small tank and shake the tank.

(6). Circulate N_2 gas to main tank; small tank is still in N_2 gas circulation.

(7). Pump $CaCl_2$ solution from small tank to 750L-size main tank.

(8). Repeat 25 times until dissolve all the 255.1kg $CaCl_2$ powder.

(9). Check pH value in main tank after pump all 634.7L $CaCl_2$ solution into it. The pH in main tank should be 5.6.

(10). Always keep air tight for all system during make and transfer the $CaCl_2$ solution.

2.2.2 Purification of $CaCl_2$ solution

In order to protect the ion exchange efficiency for the enrichment of ^{48}Sc, we had to clean the contamination of $CaCl_2$ solution, especially the Cu, Fe and Pb. The method was also ion exchange, we used the resin that was sensitive to absorb the Cu, Fe and Pb, and not absorb Ca at same time.

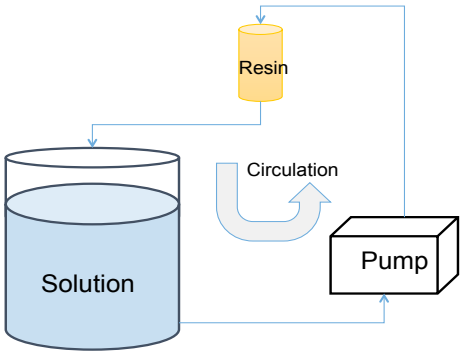

Fig.3.20 The purification setup

We used 1600g ion exchange resin (AG MP-50 made by Bio-Rad) for purification like Fig.3.20. We passed all the $CaCl_2$ solution though it and keep circulation with pump at 2L/min. $CaCl_2$ solution clean circulation time was 72 hours. Then we checked the contents of contaminations in solution by ICP-MS. It turned out that the Fe content was less than 10ppb, Cu content was 10 ppb and Cu content was 50ppb. Contaminations in these levels would not affect the ^{48}Sc enrichment efficiency of ion exchange resin. With less than 1 g of Chelate resin could capture all those contaminations in the experiment.

3. The enrichment efficiency of ^{48}Sc

The full scale of beta decay experiment had 634.7L $CaCl_2$ solution. The mass of enrichment ion exchange resin was 138.5g. The $CaCl_2$ solution flow was 2.0L/min.

From the demonstration experiments with Sc^{3+}, the ^{48}Sc capture efficiency was 94±3%. The Radon rich experiments showed the capture efficiency when the number of target atoms was in few level and the capture efficiency still been around 94%.

In conclusion, the capture efficiency for ^{48}Sc in beta decay experiment was 94±3%. With the circulation efficiency at 91.1±0.3%, we calculated the enrichment efficiency was 85.6±3.2%.

Chapter IV: Detection Efficiency

1. Monte Carlo Simulation

1.1 Regards Geant 4

In order to understand the detection efficiency of triple coincidence measurement of single beta decay of ^{48}Ca, the best way would be using ^{48}Sc isotope for both experiment and simulation by measuring 3 gamma rays. However, the ^{48}Sc isotope was not available. Instead, we used Geant 4 for the simulation.

Geant4 (for GEometry ANd Tracking) is a platform for "the simulation of the passage of particles through matter," using Monte Carlo methods. Main features for Geant 4 include:

(1) Geometry is an analysis of the physical layout of the experiment, including detectors, absorbers, etc., and considering how this layout will affect the path of particles in the experiment.

(2) Tracking is simulating the passage of a particle through matter. This involves considering possible interactions and decay processes.

(3) Detector response is recording when a particle passes through the volume of a detector, and approximating how a real detector would respond.

There were mainly three steps for Geant 4 simulation in this experiment.

1.1.1 Experimental environment and setup

We installed those CsI scintillators and all the materials around scintillators, such as PMT, air, Cu, Pb and son on. We also needed the reproduction of describing the substance composition, structure, arrangement and so on.

1.1.2 Particles generator

The particles generator required the precise selection of particles such as

alpha, beta, and gamma rays. We also precisely set the position of particle source, the momentum (direction), and initial energies.

1.1.3 Tracking of Particles

This step was the most important part to record the reaction information. We took the needed information such as information of particle movement and particle position before and after Compton scattering, etc. include pre-step point and post-step point. The most important information among them was the information of energy deposit in detector and surrounded materials. Fig.4.1 showed the concept of particles tracking by Geant 4 simulation.

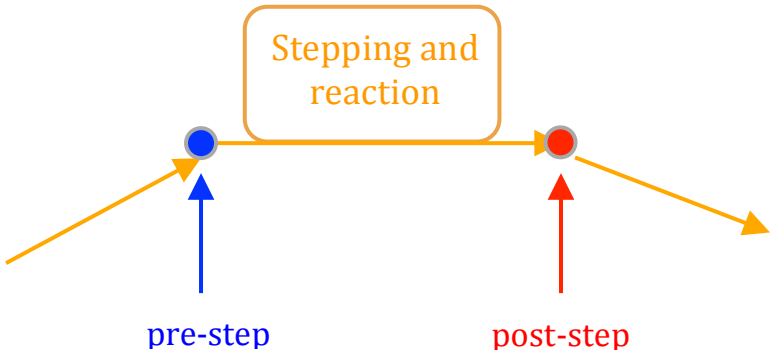

Fig.4.1 The concept for tracking of particles in Geant 4 simulation

1.2 Geometry

Fig.4.2 showed the simulation geometry of beta decay experiment with 30CsI scintillators. Each CsI scintillator had the same size of 6.5 × 6.5 × 25 cm^3. Just exactly like the experiment, we set the 30 CsI(Tl) scintillators with 4-π cover of a sample space of 13.0 × 13.0 × 13.0 cm^3 . On the top and bottom side, each had 4 scintillators shared the same ADC channel (23 & 24); they didn't face to the sample space directly. And on the topside, CsI scintillators 1 & 2 had double solid angle to the sample space.

Outside of the CsI scintillators arrays, there were passive shield of 5cm Cu and 10cm Pb at all directions. N_2 environment had also been ensured with radon purge system.

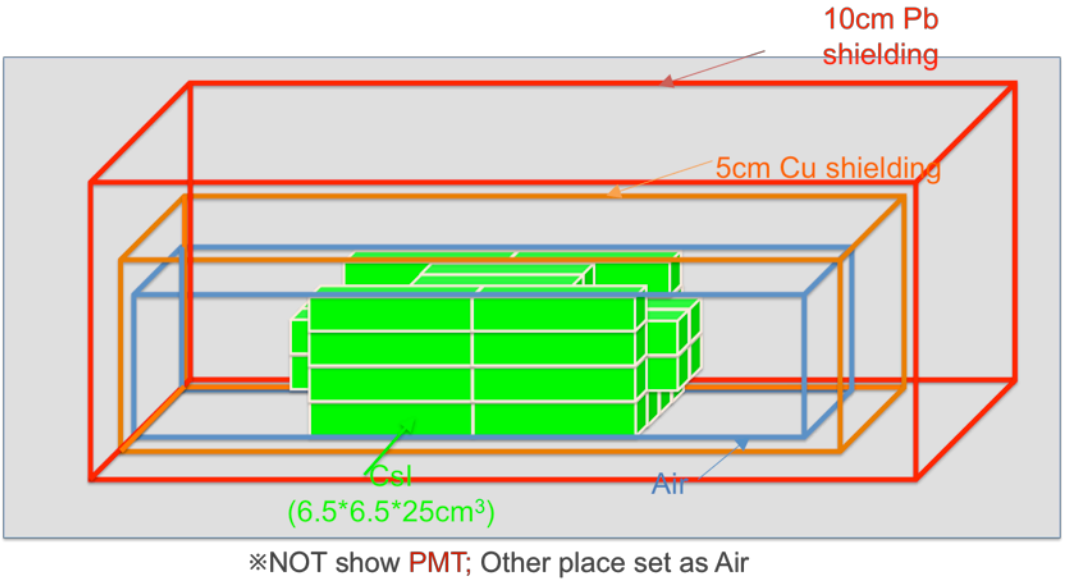

Fig.4.2 The geometry of CsI array setup in simulation

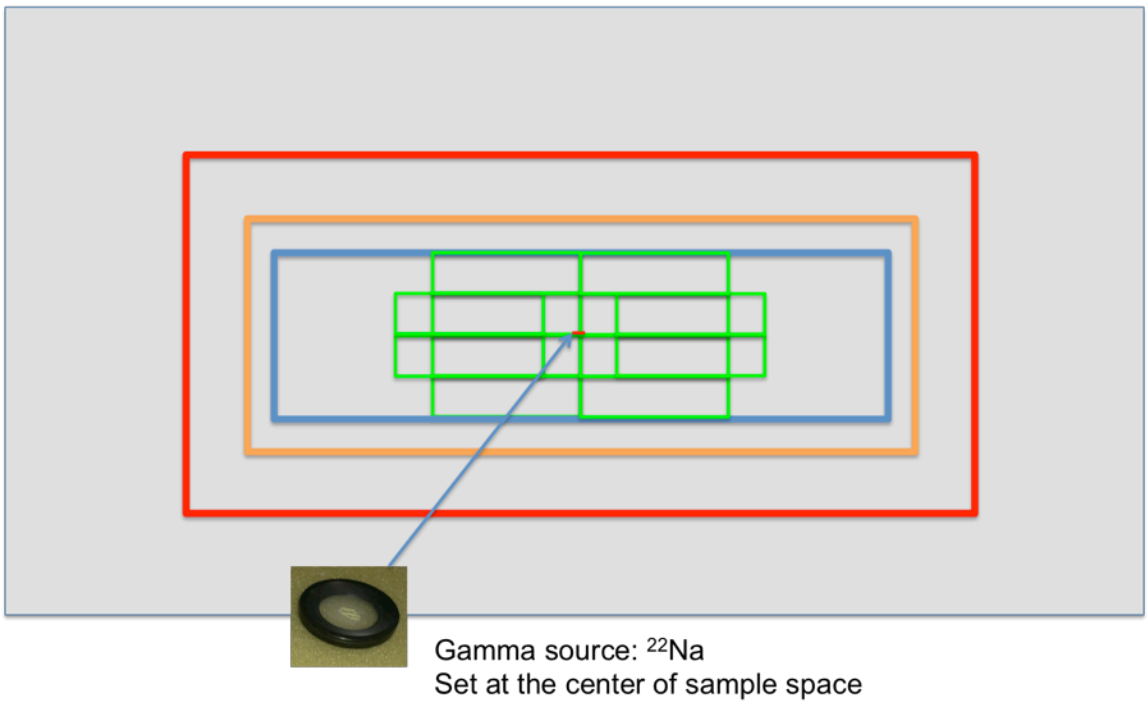

Fig.4.3 The geometry of setup the standard source of ^{22}Na

Fig.4.3 showed the example setup when we used the ^{22}Na source for calibration. In this case, we put the source in the geometry center. And we also set the source in different place or even randomly in order to check the response of each scintillator.

1.3 Appropriate evaluation

There were many points to confirm about the Geant 4 simulation such as position of CsI scintillators, the shape of surrounded materials and position of gamma source and radiation directions and so on.

The confirmation of detection efficiency simulation for this experiment was comparing the energy spectrum from simulation and experiment. The target isotope source was ^{22}Na because it also had 3 gamma rays as output, two 511 keV rays and one 1274.5 keV gamma ray like Fig.4.4. We could use triple coincidence for both simulation and experiment.

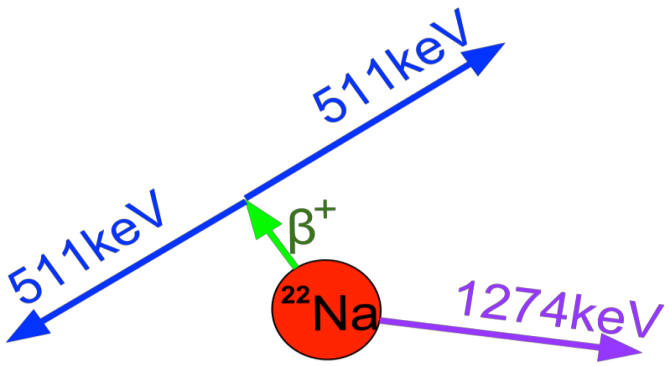

Fig.4.4 The gamma rays radiation of ^{22}Na

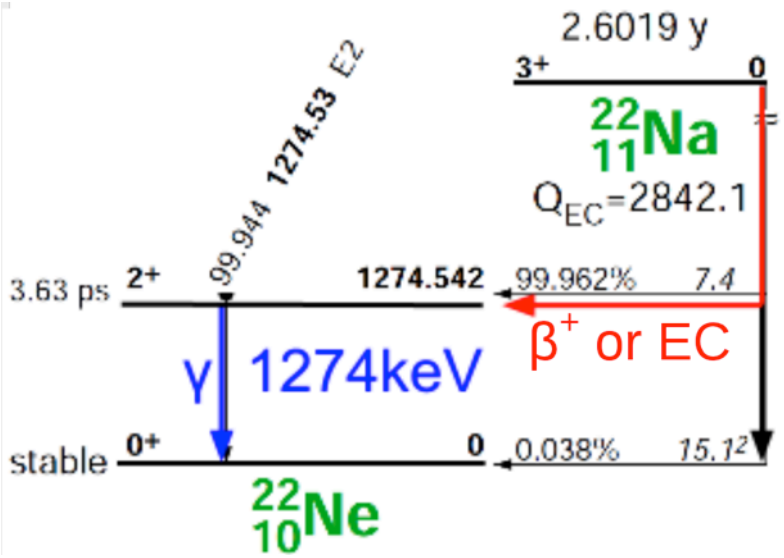

Fig.4.5 The decay scheme of ^{22}Na

We set the simulation generator for β^+ decay of ^{22}Na as Fig.4.5. There was 10% of EC decay and emitted 1274.5 keV gamma rays. There was another 90% of β^+ decay with Q value of 1567keV and emitted 1274.5 keV gamma rays. We set the generator position at center of the sample space and the radiation direction set as randomly. We got the simulation result for the β^+ decay as Fig.4.6. The simulation perfectly marched the theoretic result.

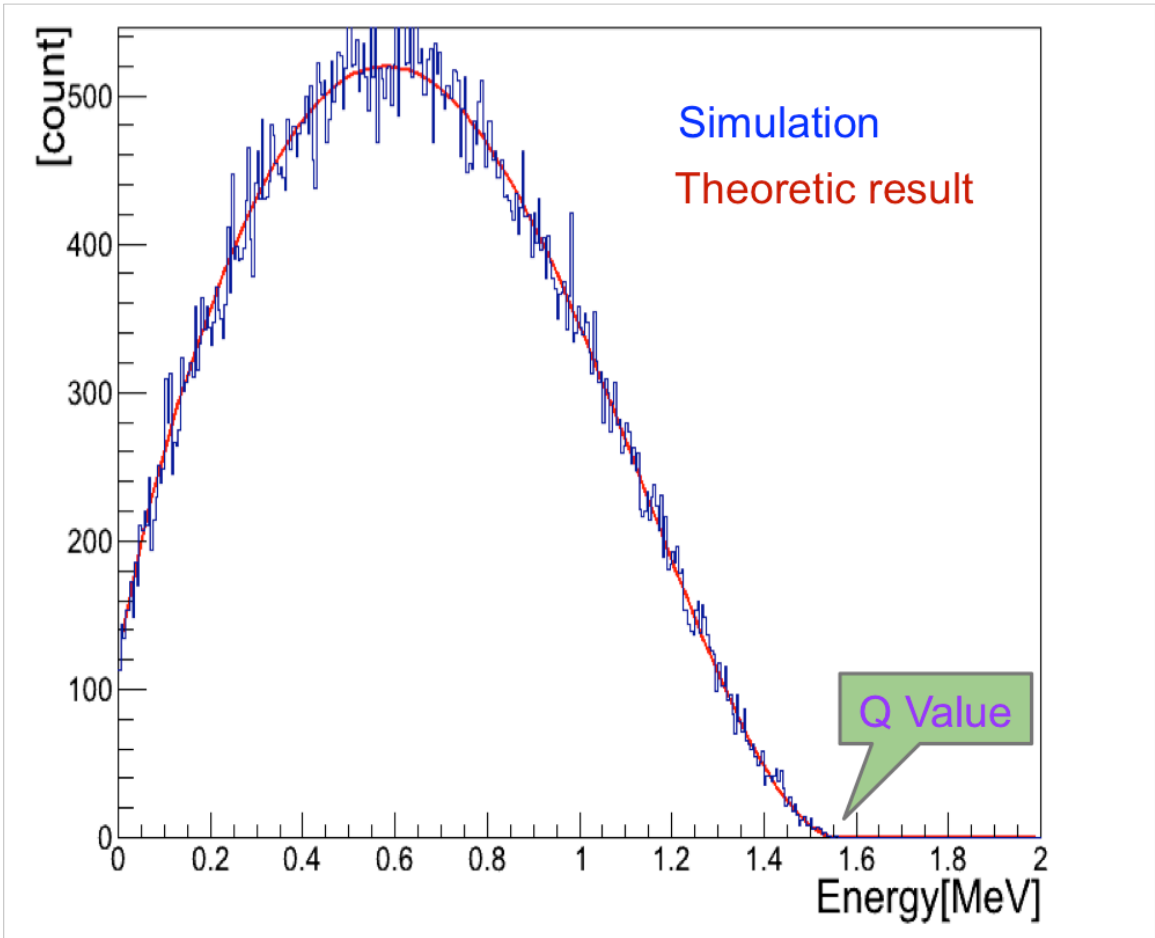

Fig.4.6 The beta decay simulation and theoretic result of ^{22}Na

We also got the energy spectrum for CsI scintillators like Fig.4.7. We did experiment and set the ^{22}Na standard source at the center of sample space. The blue line showed the simulation and red one as experiment result. The simulation spectrum and experimental spectrum marched perfectly. It showed the reliability of Geant 4 simulation.

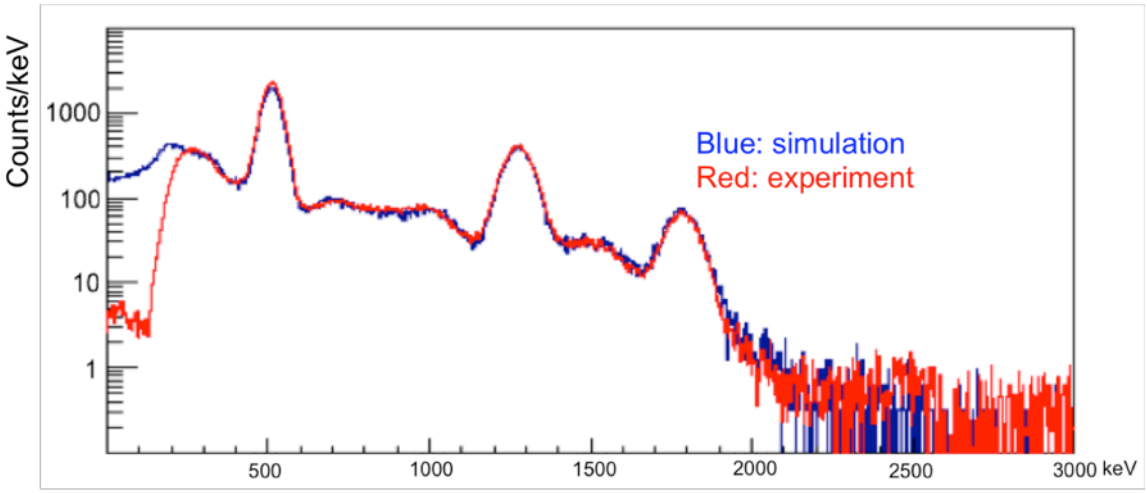

Fig.4.7 The CsI energy spectrum of simulation and experiment of ^{22}Na

1.4 Simulation Generator

We did simulation for the beta decay of ^{48}Ca. It was following the decay scheme as Fig.4.8. The decay chain for ^{48}Ca→^{48}Sc → ^{48}Ti had been precisely set in the program. The 3 gamma rays were 983, 1038, and 1311keV from decay of ^{48}Sc. And the gamma rays generator position was set at random place in ion exchange resin and radiation direction set as randomly.

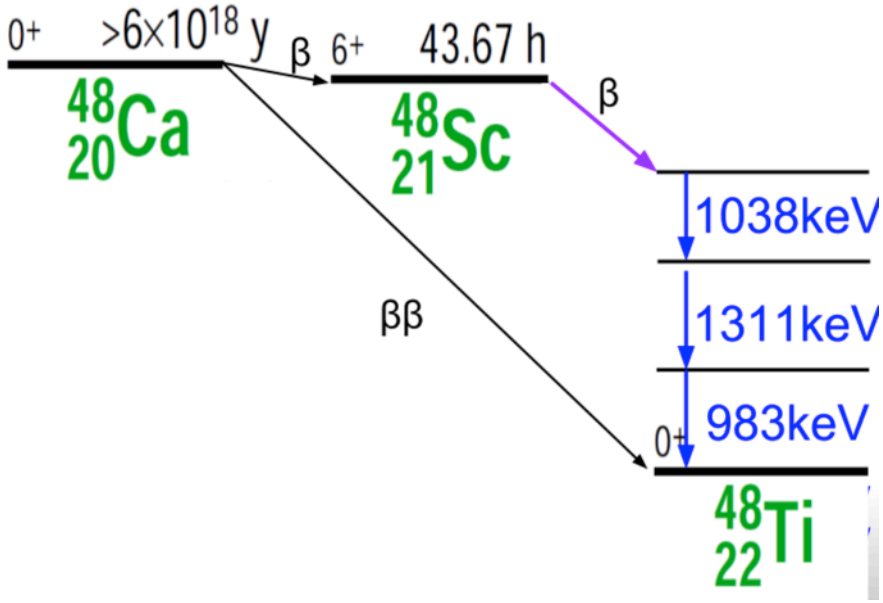

Fig.4.8 The Decay scheme of ^{48}Ca and ^{48}Sc

2. Experimental and Simulated Detection efficiency

2.1 ^{22}Na standard source

For both triple coincidence and double coincidence, the source for simulation and experiment all set at the same position in the center of sample space.

2.1.1 Triple coincidence

The detection efficiency of triple coincidence (511 keV, 511 keV and 1274.5 keV) for ^{22}Na at center were like bellow:

- Detection Efficiency from simulation: 17.2%
- Detection Efficiency from experiment: 16.8%

About the events selection, we set the energy region as 2 sigma and timing selection also as 2 sigma. The detail about the events selection would be introduced in next chapter of data analysis.

2.1.2 For double coincidence

There were two situations for double coincidence of ^{22}Na. First situation was two of the gamma rays (511keV and 1274.5keV) detected by a single CsI scintillator and another 511keV gamma ray detected by another scintillator. And the two 511 keV gamma rays should be opposite directions. Second situation was that we lost one of those 3 gamma rays. That was 511keV + 511keV or 511keV + 1274.5keV. Different scintillator would detect each gamma ray.

- 511, 511+1274keV
  - From simulation: 2.6%
  - From experiment: 2.7%
- 511 + 511 or 511 + 1274keV (lost 1 gamma)
  - From simulation: 34.3%
  - From experiment: 33.8%

2.2 ^{208}Tl source

2.2.1 Radioactivity of ^{208}Tl

Fig.4.9 The ^{208}Tl source and measurement setup

The ^{208}Tl sample measurement live time was 40.3 hours. Fig.4.10 showed the energy spectrum of ^{208}Tl source. We could see the very clear peak of 2.6MeV and also the sum energy of 3.2MeV.

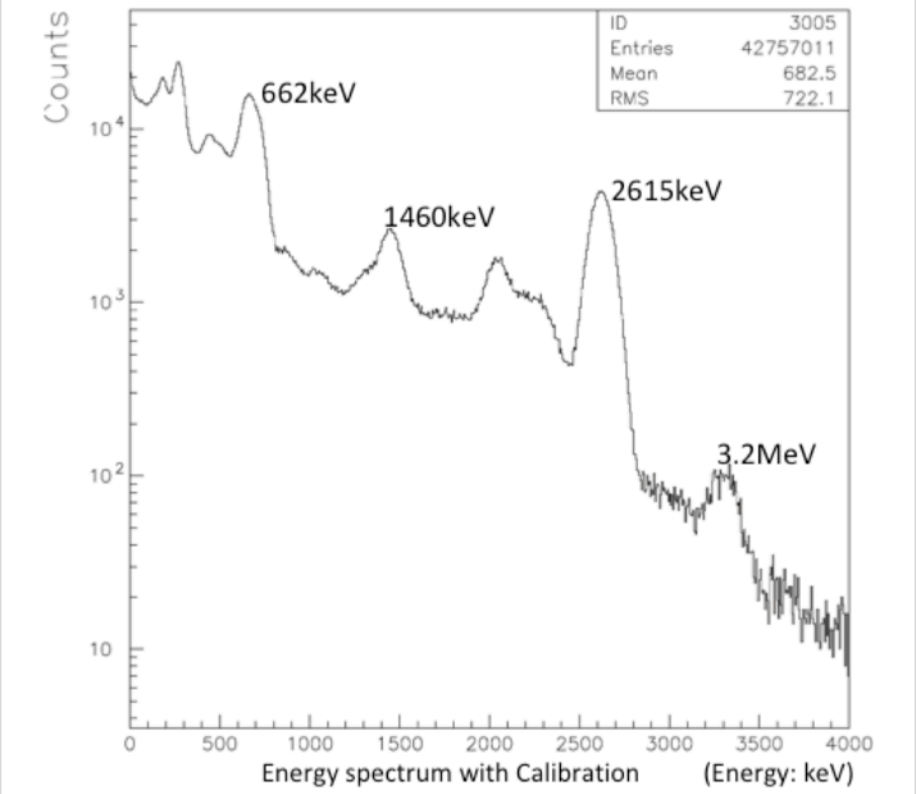

Fig.4.10 The energy spectrum of ^{208}Tl source measurement

The activity from the direct measurement (check the events for peak of 2.6MeV) was 52±3 Bq. The activity was about 85 times over the environmental ^{208}Tl background.

2.2.2 Simulation

We set the activity of ^{208}Tl source as 52 Bq just like measurement. Fig.4.11 showed the decay scheme of ^{208}Tl. And the shape of the source was also the same as the sample. The radiation direction set as randomly.

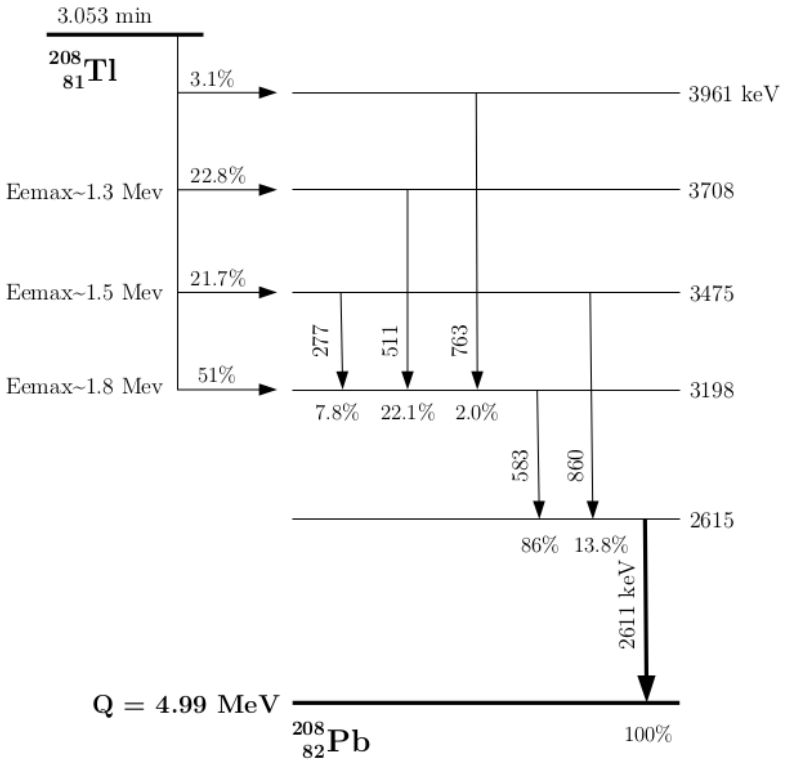

Fig.4.11 The decay scheme of ^{208}Tl

2.2.3 Simulation result

We checked the peak of 2.6MeV at both simulation and experimental spectrum and the events difference was less than 2.2%.

2.3 Beta decay of ^{48}Ca experiment simulation

2.3.1 Simulation condition

We put the 138.5g ion exchange resin in a PTFE pipe with plastic connector at both side of pipe. Then set the pipe in a 2mm thick water proof plastic box with size of $(13cm)^3$. The diameter of pipe was 2.0cm and length was 35.0cm. The pipe was set uniformly in the box. In the pipe, along with ion exchange resin, would be 70ml 4mol/L $CaCl_2$ solution. The radiation direction for 3 gamma rays (983keV, 1038keV and 1311keV) from ^{48}Sc was randomly. And the radiation position was randomly in the resin and $CaCl_2$ solution. The self-absorption for gamma rays of those materials was less than 1%.

We simulated both triple coincidence and double coincidence. Triple coincidence means 3 gamma rays hit 3 different scintillators; all other 27 CsI scintillators have no hit. Double coincidence means 2 of these 3 gamma rays hit 2 different scintillators and one scintillator might hit by Compton scattering ray or no hit and all other 27 scintillators has no hit. We lost 1 gamma, and 2 others detected by two different detectors: there were 3 situations 983keV+1038keV, 983keV+ 1311keV and 1038keV+1311keV. The detection efficiency for double coincidence would include all those 3 situations.

2.3.2 Simulation result

(1) The detection efficiency for triple coincidence was 9.8±0.4% for beta decay measurement with ion exchange resin enrichment of ^{48}Sc.

(2) The detection efficiency for double coincidence was 19.1±0.8%.

2.4 Background from ^{208}Tl for ^{48}Ca beta decay experiment

We analyzed the measurement data with ^{208}Tl source; measurement live time was 8.6 days. We also had the background measurement data, which was the same experiment condition: the sample space was empty and only had N_2 gas. We measured the background for 35.6 days with live time. We

analyze the data with both triple coincidence and double coincidence method with 3 gamma rays (983keV, 1038keV and 1311keV) from ^{48}Sc.

Table.4-1 showed the measurement result for both triple and double coincidence for background data and ^{208}Tl source data. From this experiment, we could understand that one of the main background sources was ^{208}Tl.

Table.4-1 Background contribution from ^{208}Tl to ^{48}Ca beta decay research

	Measurement time	Triple coincidence			Double coincidence		
		±1σ	±2σ	±3σ	±1σ	±2σ	±3σ
Background	35.6 days	0	1	3	8	18	28
^{208}Tl source	8.6 days	1	2	4	4	7	13

3. ^{48}Ca Beta Decay Detection Efficiency

The ^{48}Ca beta decay detection efficiency would mainly include those parts: the $CaCl_2$ solution circulation efficiency, the ion exchange capture efficiency and the CsI scintillators detection efficiency.

3.1 Capture efficiency

Firstly, we need calculate the circulation efficiency for ion exchange enrichment. We used 634.7L $CaCl_2$ solution and the circulation flow speed was 2.0L/min. The circulation efficiency we got here was 91.1±0.3%.

We also considered that part of the circulated solution might stay in the main tank for longer or shorter than the circulation time. If there were 1/e part of solution stay in tank, there would be same part of solution go out earlier. And the possibility for that 1/e (stay) part decay in the tank was equal to that 1/e (earlier) part decay in the resin. So the effect of mixture of $CaCl_2$ solution could be neglected in this calculation.

3.2 Ion exchange capture efficiency

From the demonstration experiments with Sc^{3+}, the ^{48}Sc capture efficiency was 94±3%. The Radon rich experiments showed the capture efficiency when the number of target atoms in few level and the capture efficiency still be

around 94%. In conclusion, the capture efficiency for ^{48}Sc in beta decay experiment was 94±3%.

3.3 Detector efficiency

From Monte Carlo simulation, the detection efficiency for triple coincidence was 9.8±0.4% for beta decay with ion exchange resin enrichment of ^{48}Sc. The detection efficiency for double coincidence was 19.1±0.8%.

3.4 Combined experimental efficiency

For the total detection efficiency for triple coincidence, 3 different CsI detectors detected 3 different gamma rays from beta decay of ^{48}Sc. The final efficiency was the multiply of detector efficiency, ion exchange capture efficiency and circulation efficiency, that was (9.8±0.4%) × (94±3%) × (91.1±0.3%) = 8.4±0.5%.

For the total detection efficiency for double coincidence, 2 different CsI detectors detected 2 different gamma rays from beta decay of ^{48}Sc. The final efficiency was the multiply of detector efficiency, ion exchange capture efficiency and circulation efficiency, that was (19.1±0.8%) × (94±3%) × (91.1±0.3%) = 16.3±1.0%.

Chapter V: Data Analysis and Result

1. Data Analysis

1.1 Data taken condition

For background measurement, we circulated 40L pure water without $CaCl_2$ to pass though resin. The measurement started from 2016.10.18 to 2017.03.20 at Lepton Lab, Osaka University. The background measurement live time was 69.8days.

For beta decay measurement, we circulated 634.7L $CaCl_2$ solution with speed of 2.0L/min. The measurement started from 2017.03.27 to 2017.06.24 at Lepton Lab, Osaka University. The beta decay measurement live time was 70.7days.

1.2 Selection of Analyzed Modules

For the beta decay of ^{48}Ca, decayed events were extremely rare. It was impossible to see the energy peak on the energy spectrum directly. We had to analyze the spectrum event by event. The candidate event had to following all the requirements such as the triple hit or double hit, the energy region, the time difference, and the sum energy spectrum and candidate event energy distribution.

We analyzed the background event with the same condition for measurement spectrum. We calibrated the detectors system every two weeks for both energy and timing. We also checked the stability every day with ^{137}Cs, ^{40}K, ^{208}Tl for peaks, counting rates and energy resolutions.

1.3 Event Selection

1.3.1 Hit selection

Rejecting the possible background events was the most important process in the data analysis of this experiment. One of the most efficient ways was the coincidence measurement.

For triple coincidence analysis, we required 3 different CsI scintillators to be hit. And all other 27 CsI scintillators were out of hit (energy threshold <pedestal + 3σ). Similarly, for double coincidence, 2 different CsI scintillators to be hit and other scintillators were out of hit. Fig.5.1 showed the typical energy spectrum for triple coincidence hit and double coincidence hit. We could clearly see the energy peak of ^{137}Cs, ^{40}K and ^{208}Tl from the single hit spectrum. We could also find the 511keV peak on double coincidence hit and triple coincidence hit spectrum. The interested energy regions at 1MeV±2σ and 1.3MeV±2σ were flat and no particular peaks.

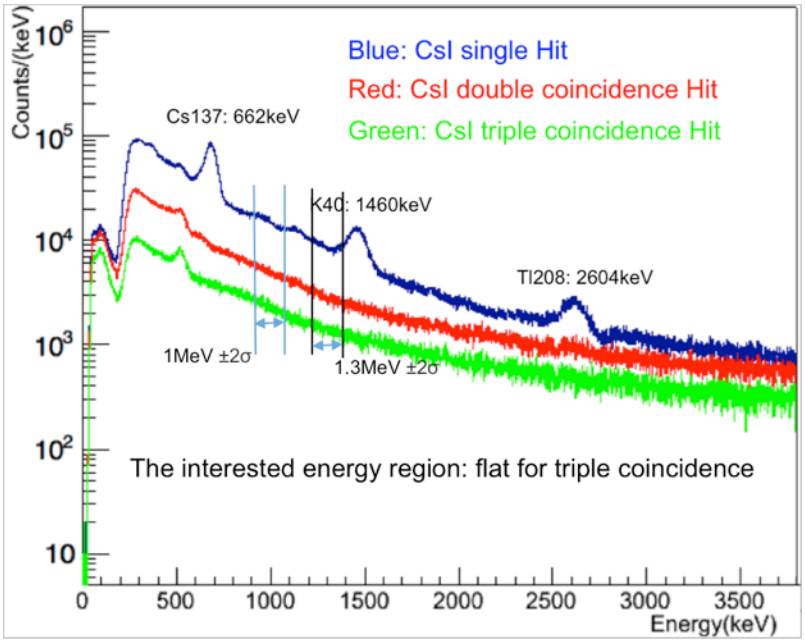

Fig.5.1 The energy spectrum and its double and triple coincidence

1.3.2 Energy Selection

The target was to detect 3 gamma rays (983keV, 1038keV and 1311keV) from beta decay of ^{48}Sc. The energy selection for each scintillator was based on the energy resolution (σ) for that energy. So the energy calibration and energy resolution calibration were extremely important. We had to calculate the energy resolution of target energy for each scintillator. In the analysis, we analyzed the data with energy region for ±1σ, ±2σ, ±3σ, ±4σ.

For the real events of beta decay of ^{48}Sc, they had to follow the Gaussian distribution, and the background events would be flat distribution. This rule also helped to identify the background events from candidates.

Table 5-1 The example of energy selection for triple coincidence of beta decay of ^{48}Ca

Detector NO.	1	2	3	4	5	…	30
Energy	$(983\pm2\sigma_1)$keV	$(1038\pm2\sigma_2)$keV	$(1311\pm2\sigma_3)$keV	0	0	…	0
Energy resolution(σ)	32.0keV	33.5keV	37.5keV				

For the case of ^{48}Ca, 3 of the CsI detectors had energies $983\pm2\sigma_1$, $1038\pm2\sigma_2$, $1311\pm2\sigma_3$, respectively. Where σ_n are correspondent energy resolutions. If other CsI detectors all gave 0 (pedestal) then it was a true triple coincidence candidate event. Otherwise it was accidental coincidence events. Table.5-1 just showed the one example of combination of 3 detectors got 3 different energies with correspondent energy resolution.

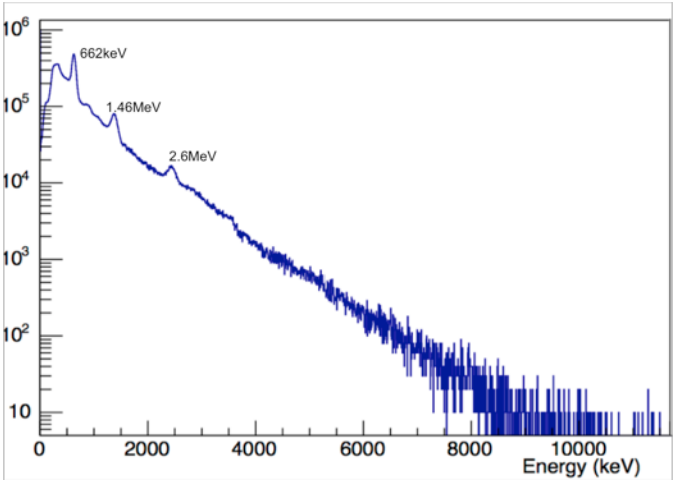

Fig.5.2 The sum energy spectrum of all 30 CsI scintillators

We still could see the clear peaks from ^{137}Cs, ^{40}K and ^{208}Tl from the sum energy spectrum of all 30 CsI scintillators. There was a small break around 3.2MeV, might be the sum peak of ^{208}Tl.

1.3.3 Timing Selection

There were time differences (T) for different energies (Walk Effect) for CsI(Tl) detectors. The time difference ΔT: $T-2\sigma<\Delta T<T+2\sigma$ where σ was the corresponded time resolution. For example, if the time difference between 983 keV for ADC1 and 1311keV for ADC2 on TDC12 was 5ns, with sigma was 3ns; then the time range for our analysis was from -1 (5-6)ns to 11 (5+6)ns. We choose 2σ as the range because to get 95% C.L for the final result.

2. Result for beta decay of ^{48}Ca

2.1 Background measurement result

2.1.1 Background measurement condition

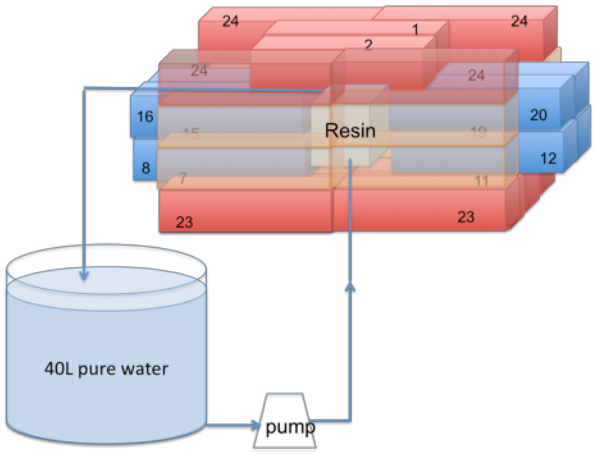

Fig.5.3 The setup for background measurement

Measurement condition was the same experimental condition as beta decay experiment. As showed in Fig.5.3, in the sample space, a box container with tube, and 138.5g resin in that tube. The background measurement was done by circulation of 40L pure water without $CaCl_2$ solution. The circulation speed was set as 2.0L/min. The N_2 gas purge system worked on 1L/min for the radon free environment. And the plastic scintillator with 4 PMTs and size of 1m×1m×2cm had been installed on the top of detection system as veto for cosmic rays.

The background measurement time live time was 69.8 days in total.

2.1.2 Background analysis method

The background analysis method was the same as beta decay analysis. For the hit selection, there were triple hit and double hit. For the energy selection, the 3 gamma rays (983keV, 1038keV and 1311keV) from beta decay of ^{48}Sc had energy region of ±1σ, ±2σ, ±3σ, ±4σ, where σ was the energy resolution. For the timing selection, we set the region of ±2σ, where σ was the timing difference resolution.

2.1.3 Background analysis result

2.1.3.1 Triple coincidence analysis result for background

Table.5-2 showed the background events for both triple coincidence and double coincidence. There were 4 energy regions from ±1σ to ±4σ. For triple coincidence, there were 3 events in total in ±2σ and 8 events in ±4σ. For double coincidence, there were 21 events in ±2σ and 40 events in ±4σ.

Table. 5-2 The background measurement result for triple coincidence and double coincidence

	Measurement time	Triple coincidence events				Double coincidence events			
		±1σ	±2σ	±3σ	±4σ	±1σ	±2σ	±3σ	±4σ
Background	69.8 days	1	3	6	8	9	21	28	40

*σ here means energy resolution, for 983±1σ keV as example: energy region is (983-σ to 983+σ) keV

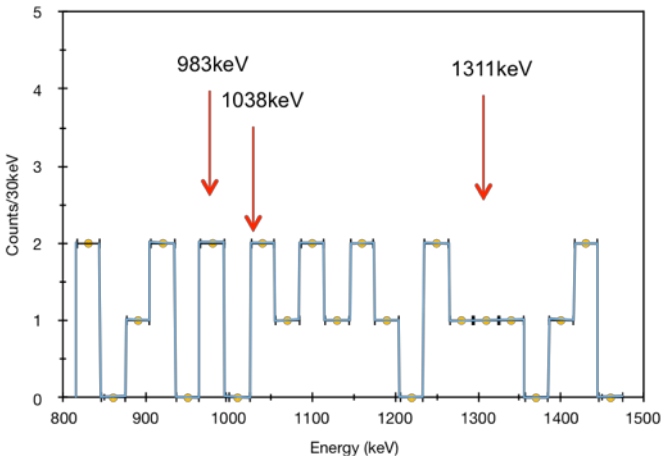

Fig.5.4 The background events energy distribution for triple coincidence

We checked the background events energy distribution for triple coincidence. We listed all the energies of each background events in Fig.5.4. We could find that the energies were almost flat and no peak could be found at the interested energy region of 983keV, 1038keV and 1311keV.

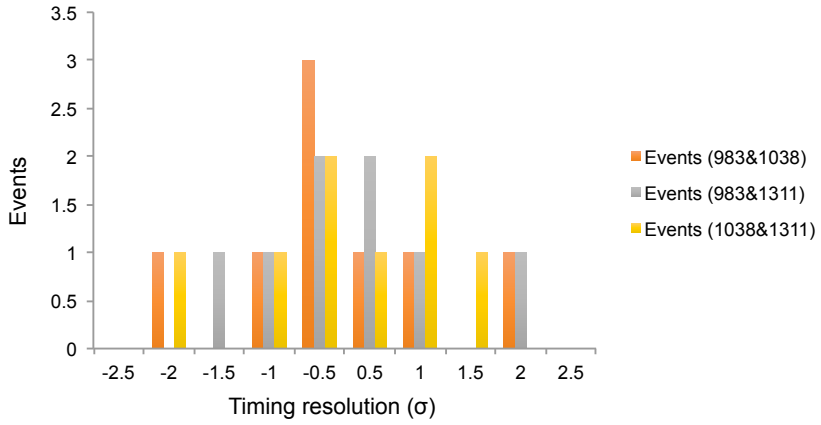

Fig.5.5 The background events timing difference distribution for triple coincidence

We also checked the background events timing difference for the triple coincidence. We showed the timing difference with unit of resolution like Fig.5.5.

Table.5-3 The background events distribution for triple coincidence

Events NO.	Energy Window	Timing Window	CsI Hit NO.1 (983keV)	CsI Hit NO.2 (1038keV)	CsI Hit NO.3 (1311keV)	Sum Energy (keV)
1	±1σ	±2σ	7	28	12	3208.4
2	±2σ	±2σ	25	20	1	3375.9
3	±2σ	±2σ	2	15	22	3293.1
4	±3σ	±2σ	17	30	6	3402.5
5	±3σ	±2σ	19	9	26	3104.7
6	±3σ	±2σ	16	8	13	3555.8
7	±4σ	±2σ	28	18	4	3175.4
8	±4σ	±2σ	11	17	5	3503.6

We analyzed the sum energies of 3 gamma rays for each background events of triple coincidence analysis. There was no peak around 3335keV.

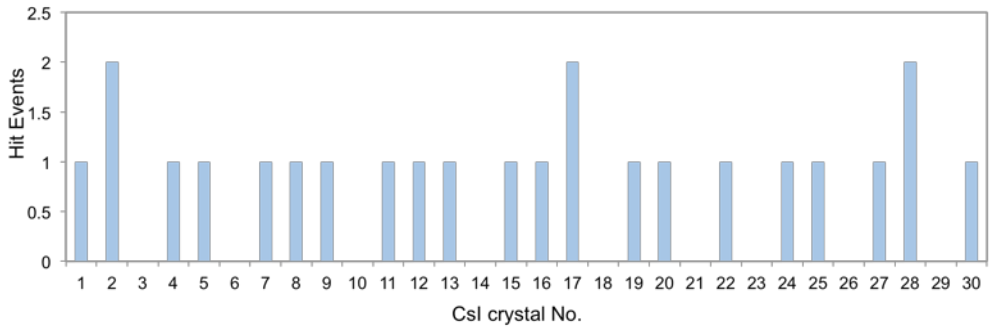

Fig.5.6 The CsI scintillator hit distribution of triple coincidence events

We analyzed the CsI scintillator hit distribution for triple coincidence events and showed it on Fig.5.6. We found that ADC 23 (CsI 23-26) and ADC 24 (CsI 27-30) had higher hit rate than most other ADCs. The reason was because both ADC 23 and ADC 24 had 4 CsI scintillators. So ADC 23 and ADC 24 were easier to catch the background events. We also estimated the background source, 2 events from accident coincidence according to the single hit rate; 3 events from cosmic ray according to the plastic scintillator veto efficiency; and 3 other events from intrinsic gamma rays background.

2.1.3.2 Double coincidence analysis result for background

We also analyzed the energy distribution for the 40 double coincidence events (±4σ) as Table 5-2. There were 2 gamma rays for each event and there were 40 events in total. The energy spectrum was showed in Fig.5.7 and it was almost flat and no obvious peak had been found.

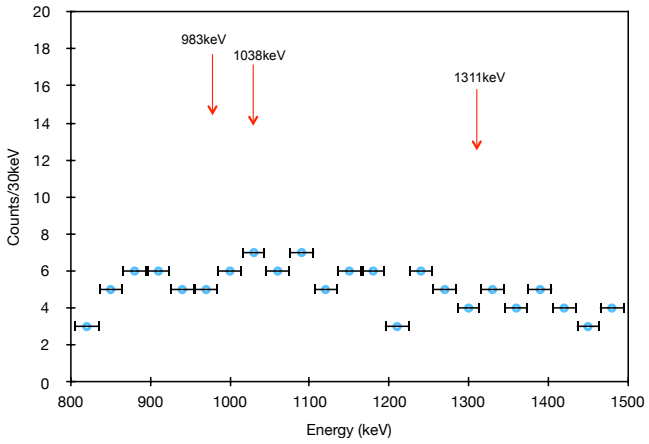

Fig.5.7 The background events energy distribution for double coincidence

We checked the timing difference distribution for background events of double coincidence. The distribution for all 3 combinations of energies as showed in Fig.5.8.

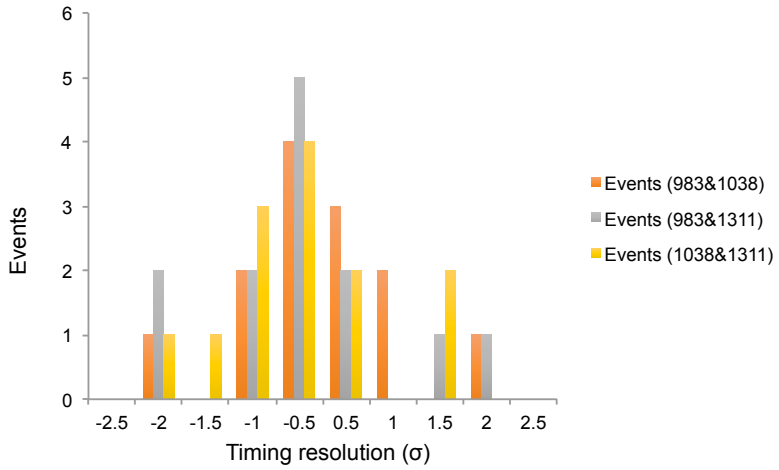

Fig.5.8 Background events timing difference distribution for double coincidence

2.2 ^{48}Ca Beta decay measurement

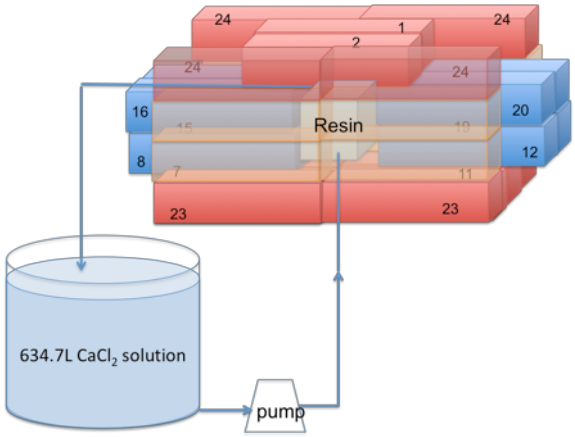

Fig.5.9 The setup for beta decay measurement

As showed in Fig.5.9, in the sample space, a box container with tube, and 138.5g resin in that tube. The background measurement was done by circulation of 634.7L $CaCl_2$ solution. The circulation speed was set as 2.0L/min. The N_2 gas purge system worked on 1L/min for the radon free environment. And the plastic scintillator with 4 PMT and size of

1m×1m×2cm had been installed on the top of detection system as veto for cosmic rays.

The measurement time live time was 70.7 days in total. We showed the energy spectrum with various cut in Fig.5.10.

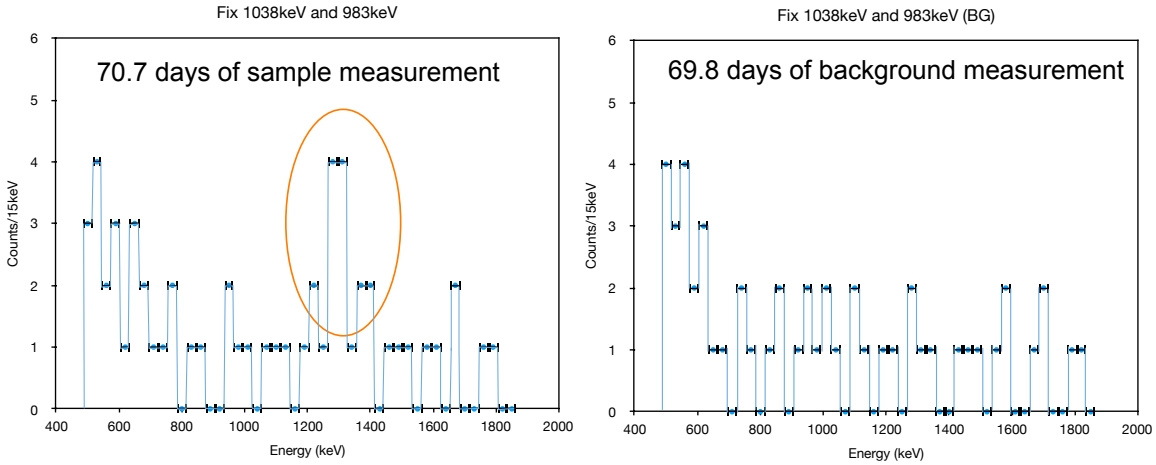

Fig.5.10-A1 The background reduction with various cut: Fix energy 983keV±2σ and 1038keV±2σ for two CsI scintillators, The 3rd CsI scintillator energy range rom 500keV to 1850keV,Others 27 CsI energy threshold: <pedestal + 3σ

We found the peak at 1300keV in Fig5.10-A1 at sample measurement spectrum (left) and no peak at background measurement spectrum (right).

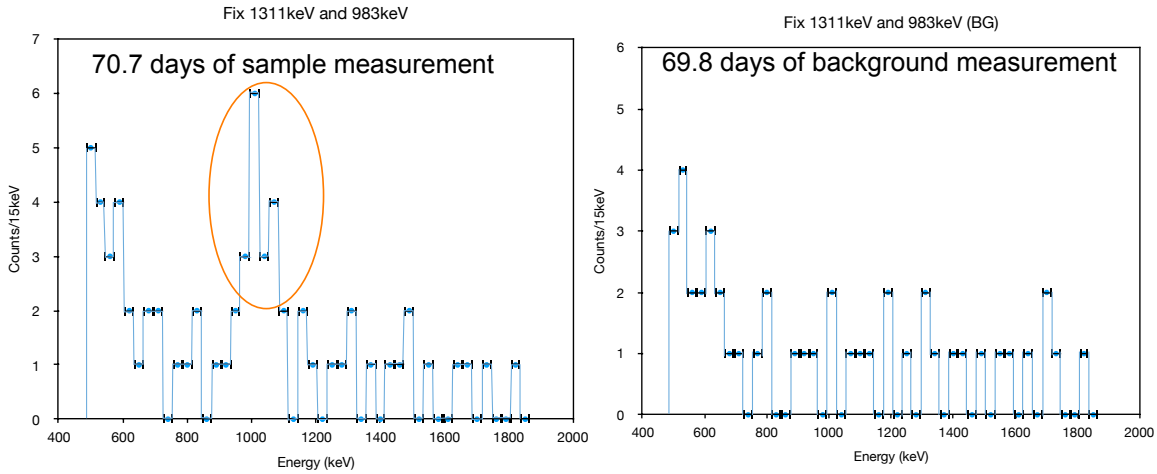

Fig.5.10-A2 The background reduction with various cut: Fix energy 983keV±2σ and 1311keV±2σ for two CsI scintillators, The 3rd CsI scintillator energy range rom 500keV to 1850keV,Others 27 CsI energy threshold: <pedestal + 3σ

We found the peak at 1030keV in Fig5.10-A2 at sample measurement spectrum (left) and no peak at background measurement spectrum (right).

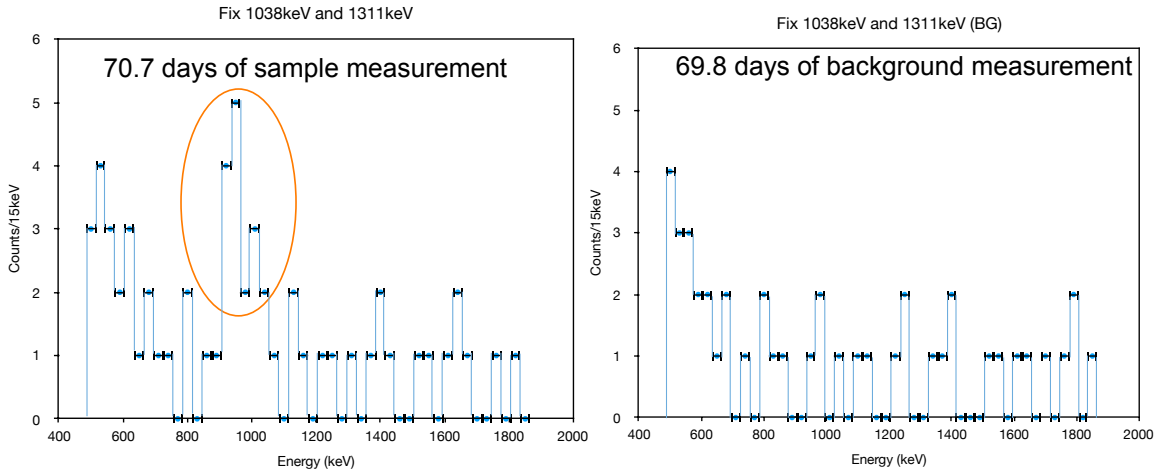

Fig.5.10-A3 The background reduction with various cut: Fix energy 1311keV±2σ and 1038keV±2σ for two CsI scintillators, The 3rd CsI scintillator energy range rom 500keV to 1850keV,Others 27 CsI energy threshold: <pedestal + 3σ

We found the peak at 970keV in Fig5.10-A3 at sample measurement spectrum (left) and no peak at background measurement spectrum (right).

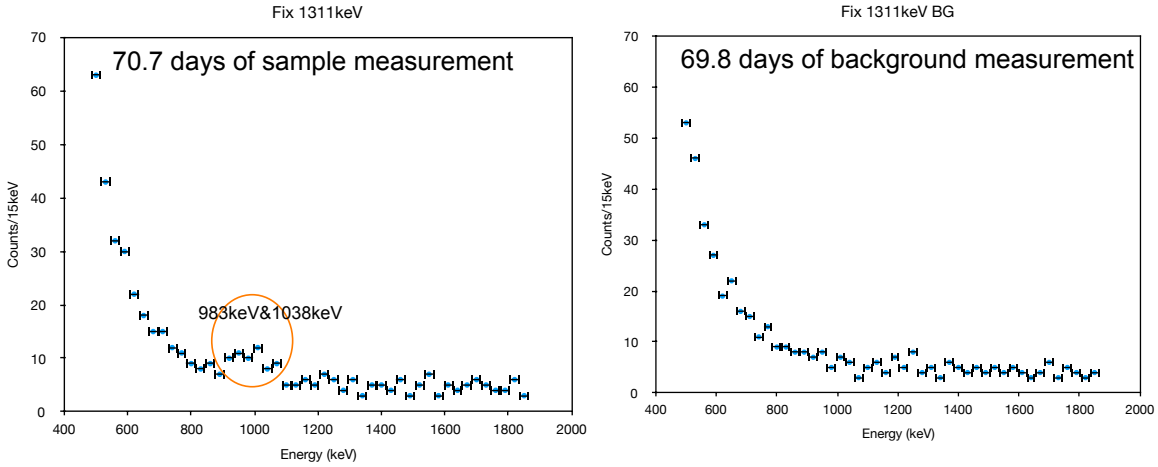

Fig.5.10-B1 The background reduction with various cut: Fix energy 1311keV±2σ for one CsI scintillators, the 2nd and 3rd CsI scintillator energy range rom 500keV to 1850keV , others 27 CsI energy threshold: <pedestal + 3σ

We found the peak around 1000keV (the sum of 983keV and 1038keV) in Fig5.10-B1 at sample measurement spectrum (left) and no peak at

background measurement spectrum (right).

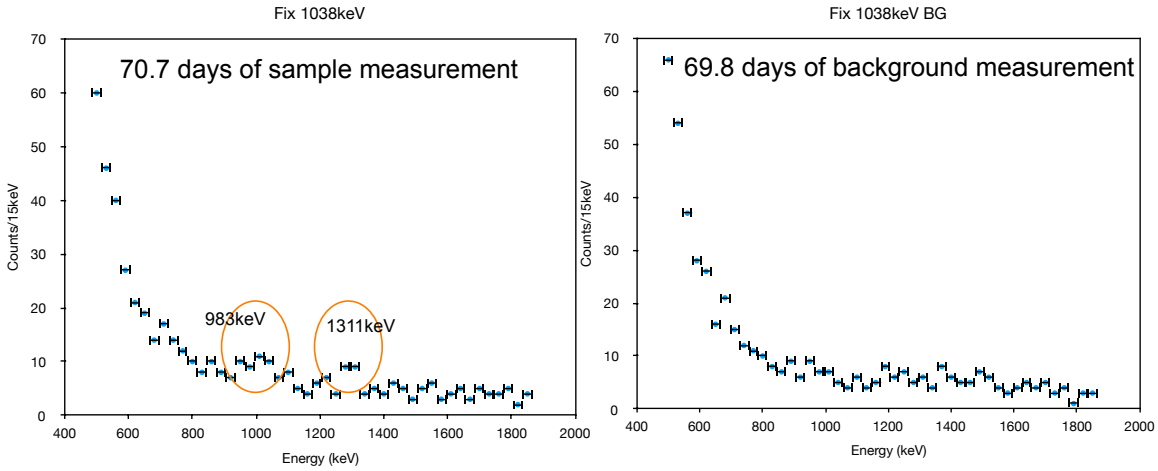

Fig.5.10-B2 The background reduction with various cut: Fix energy 1038keV±2σ for one CsI scintillators, the 2nd and 3rd CsI scintillator energy range rom 500keV to 1850keV , others 27 CsI energy threshold: <pedestal + 3σ

We found the peak around 980keV and 1300keV in Fig5.10-B2 at sample measurement spectrum (left) and no peak at background measurement spectrum (right).

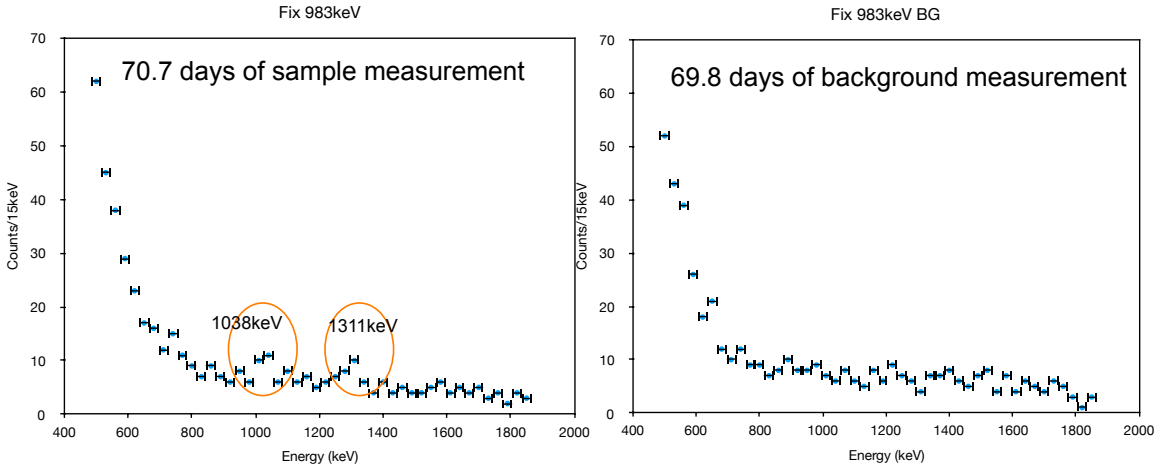

Fig.5.10-B3 The background reduction with various cut: Fix energy 983keV±2σ for one CsI scintillators, the 2nd and 3rd CsI scintillator energy range rom 500keV to 1850keV , others 27 CsI energy threshold: <pedestal + 3σ

We found the peak around 1030keV and 1300keV in Fig5.10-B3 at sample measurement spectrum (left) and no peak at background measurement

spectrum (right).

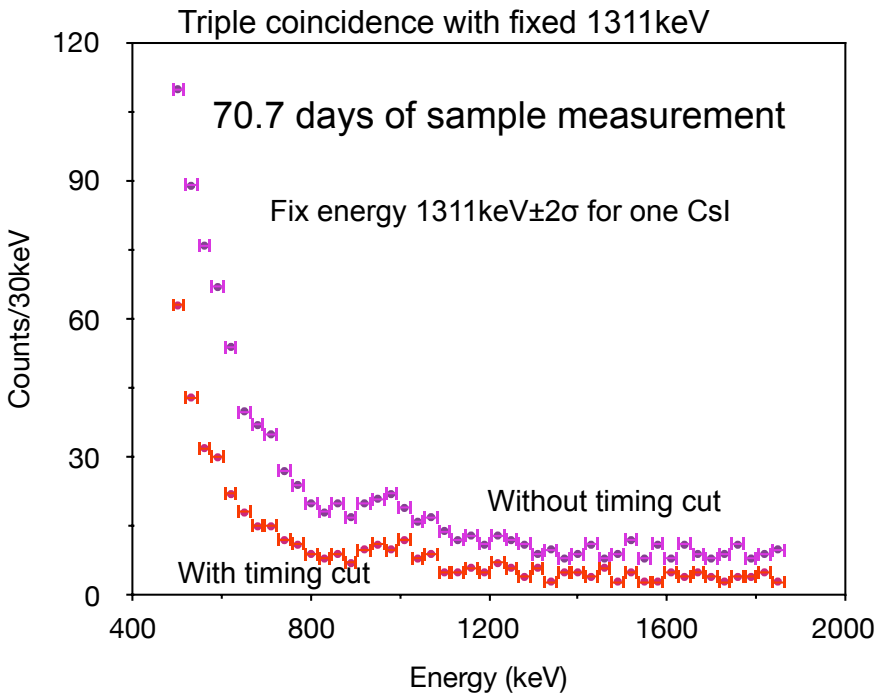

Fig.5.10-C The background reduction with various cut: Fix energy 1311keV±2σ for one CsI scintillators, the 2nd and 3rd CsI scintillator energy range rom 500keV to 1850keV , others 27 CsI energy threshold: <pedestal + 3σ. The red one showed the spectrum with timing cut and purple one showed the spectrum without timing cut.

In summarize, we found the peak with energy of 970keV, 1030keV and 1300keV from the beta decay measurement spectrum. Meanwhile, we didn't find any peak that corresponds to the decay of ^{48}Sc from the background measurement spectrum with same analysis. So it is reasonable to claim that those gamma rays come from the beta decay of ^{48}Sc. Since the only source of ^{48}Sc is the single beta decay of ^{48}Ca, it is clear that we found the signature of beta decay of ^{48}Ca.

2.2.1 The analysis condition for beta decay

For the hit selection, there were triple hit and double hit. For the energy selection, the 3 gamma rays (983keV, 1038keV and 1311keV) from beta decay of ^{48}Sc had energy region of ±1σ, ±2σ, ±3σ, ±4σ, where σ was the energy resolution. For the timing selection, we set the region of ±2σ, where σ was the timing difference resolution.

2.2.2 Candidate events for beta decay

Table.5-2 showed the beta decay candidate events for both triple coincidence and double coincidence. There were 4 energy regions from ±1σ to ±4σ. For triple coincidence, there were 14 events in total in ±2σ and 18 events in ±4σ energy region. For double coincidence, there were 44 events in ±2σ and 67 events in ±4σ energy region. We also showed the events for background measurement in table.5-2.

Table. 5-2 The background measurement result for triple coincidence and double coincidence

	Measure time	Triple coincidence events				Double coincidence events			
		±1σ	±2σ	±3σ	±4σ	±1σ	±2σ	±3σ	±4σ
Beta decay measurement	70.7 days	8	14	16	18	25	44	55	67
Background	69.8 days	1	3	6	8	9	21	28	40

*σ here means energy resolution, for 983±1σ keV as example: energy region is (983-σ to 983+σ) keV

2.2.3 Triple coincidence measurement result

We checked the candidate events energy distribution for triple coincidence. We listed all the energies of each candidate event in Fig.5.11. We could find the energies peak at the interested energy region of 983keV, 1038keV and 1311keV. We made Gaussian fitting for each energy region and showed in Fig.5.14. Both the peak energy and resolution marched the requirements for the beta decay of ^{48}Sc. On the other words, we found the ^{48}Ca beta decay events on the spectrum.

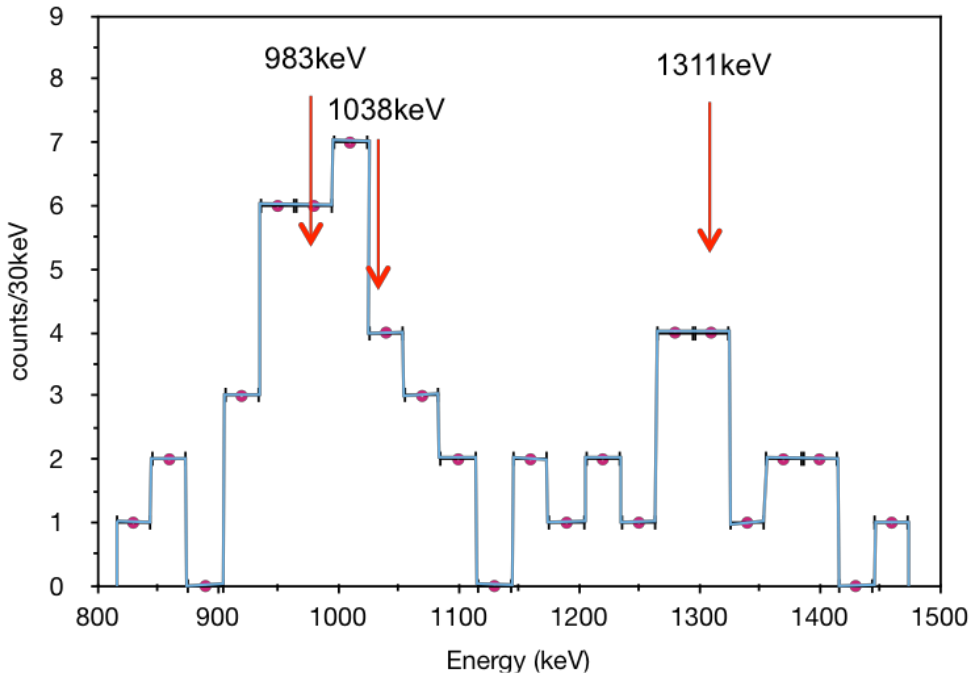

Fig.5.11 The energy distribution for triple coincidence candidate events

We also checked the candidate events timing difference for the triple coincidence. We showed the timing difference for each energy pair with unit of resolution like Table.5-4.

Table.5-4 Time Difference for 3 gamma rays of triple coincidence candidate events

Events NO.	dt for 983 & 1038 (ns)	dt for 983 & 1311 (ns)	dt for 1038 & 1311 (ns)	Events NO.	dt for 983 & 1038 (ns)	dt for 983 & 1311 (ns)	dt for 1038 & 1311 (ns)
1	1.1	6.9	6.2	10	2.4	7.5	5.7
2	1.7	7.3	6.8	11	1.4	6.6	6.9
3	0.6	8.1	7.4	12	3.3	7.9	2.1
4	-2.1	5.5	5.5	13	-1.2	6.2	6.4
5	2.7	4.1	3.4	14	2.8	3.1	7.0
6	-0.3	2.2	6.9	15	4.6	2.4	5.6
7	1.5	7.3	9.1	16	1.9	6.3	8.9
8	4.7	8.6	8.7	17	0.7	7.1	1.2
9	5.6	6.2	6.4	18	1.3	10.1	6.6

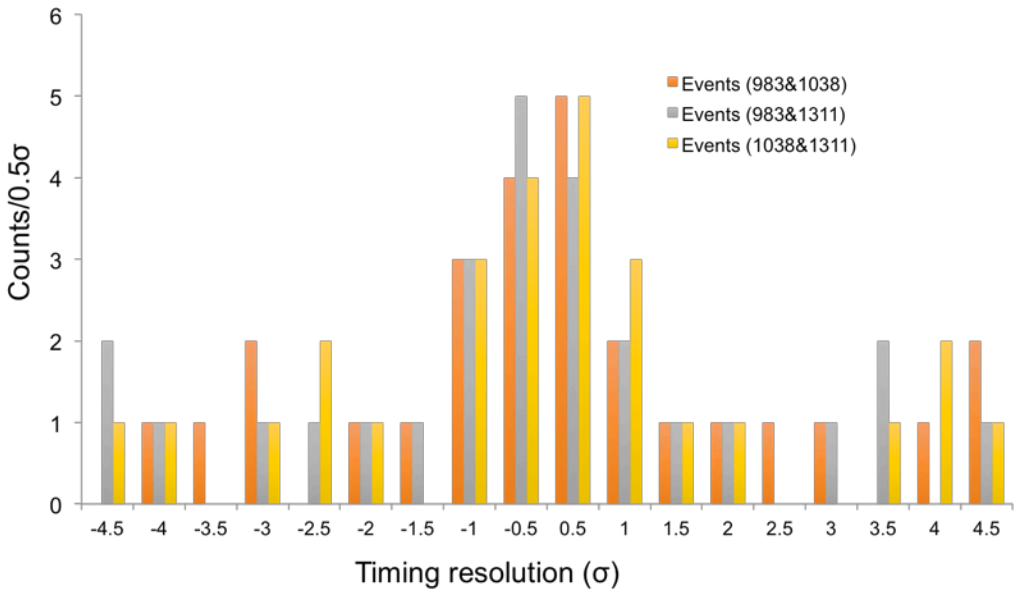

Fig.5.12 The time difference for triple coincidence candidate events

Fig.5.12 showed the timing difference for each pair of energies, 983keV & 1038keV, 983keV & 1311keV and 1038keV & 1311keV. We could see the peak for each pair around timing resolution of 0. That also implied the candidate events were quite possibly from the beta decay of ^{48}Sc. Meanwhile, we also found some events for timing resolution beyond ±1σ, which implied the sideband background. Totally, we found 3 sideband background events for ±2σ energy region and 9 sideband background events for ±4σ energy region.

Table.5-5 CsI scintillator distribution for triple coincidence candidate events

Events NO.	Energy Window	Timing Window	CsI Hit NO.1 (983keV)	CsI Hit NO.2 (1038keV)	CsI Hit NO.3 (1311keV)	Sum Energy
1	±1σ	±2σ	2	19	10	3309.1
2	±1σ	±2σ	13	8	21	3387.2
3	±1σ	±2σ	1	9	15	3299.4
4	±1σ	±2σ	14	2	7	3340.5
5	±1σ	±2σ	22	18	13	3290.6
6	±1σ	±2σ	7	30	1	3355.1
7	±1σ	±2σ	15	2	27	3327.8
8	±1σ	±2σ	25	21	19	3364.2

9	±2σ	±2σ	9	16	5	3287.6
10	±2σ	±2σ	5	20	8	3307.1
11	±2σ	±2σ	1	8	2	3387.6
12	±2σ	±2σ	12	3	6	3406.2
13	±2σ	±2σ	2	19	16	3388.3
14	±2σ	±2σ	27	3	14	3315.6
15	±3σ	±2σ	21	6	5	3418.9
16	±3σ	±2σ	20	18	12	3234.1
17	±4σ	±2σ	13	23	7	3476.1
18	±4σ	±2σ	4	1	29	3412.3

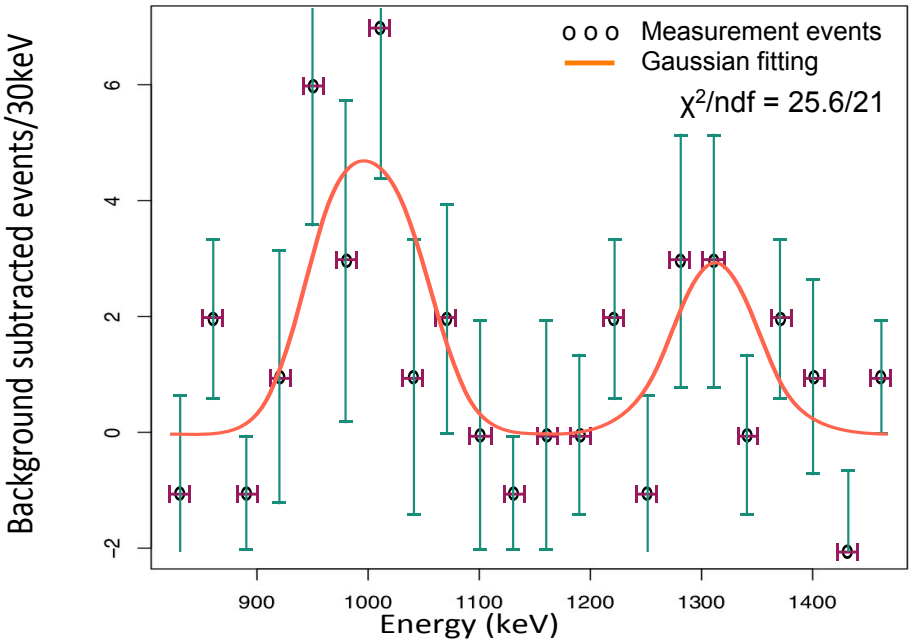


```
Formula: cnt ~ (A1 * exp(-(energy - 983)^2/(2 * 32^2))) + (A2 * exp(-(energy -
    1038)^2/(2 * 33^2))) + (A3 * exp(-(energy - 1311)^2/(2 *
    37^2)))
```

Fixed A1 =3.5; A2 = 3.4; A3 = 3.0

Fig.5.13 Background subtracted triple coincidence events energy distribution

We showed both candidate events and background events. We could clearly found the events that beyond the background level at the 3 interested energy regions of 983keV, 1038keV and 1311keV.

Then we showed the background subtracted triple coincidence events on

Fig.5.13. Those 3 peaks still could be clearly checked. We simulated the idea distribution for triple coincidence events of beta decay of ^{48}Sc, like the red line in Fig.5.13. I set the energy resolution for the 3 energies, and Gaussian distribution. I fixed the total events as 10 the same with experiment. Finally, I compared the experiment result and simulation result in events/30keV at same energy. I calculated the χ^2 based on the difference of simulation and experiment, χ^2/ndf = 25.6/21.

We also did the same analysis for 0.6, 1.2 and 1.5MeV, there was no peak found. The ^{208}Tl could contribute the background (583+2604keV = 3.2MeV), so we did coincidence analysis with sum energy of 3.2MeV and got the Fig.5.14. We could clearly get the peak with energy of 580keV and 2.61MeV.

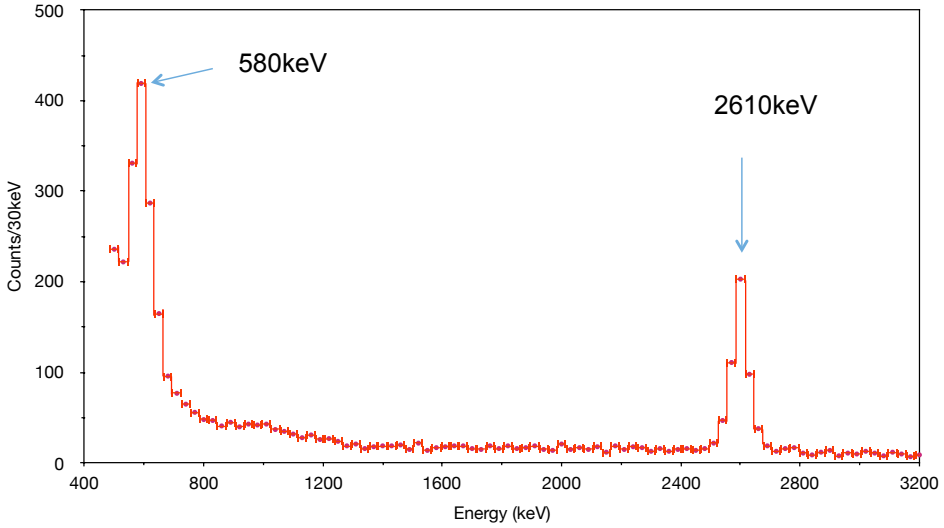

Fig.5.14 Triple coincidence analysis for 0.6, 1.2 and 1.5MeV

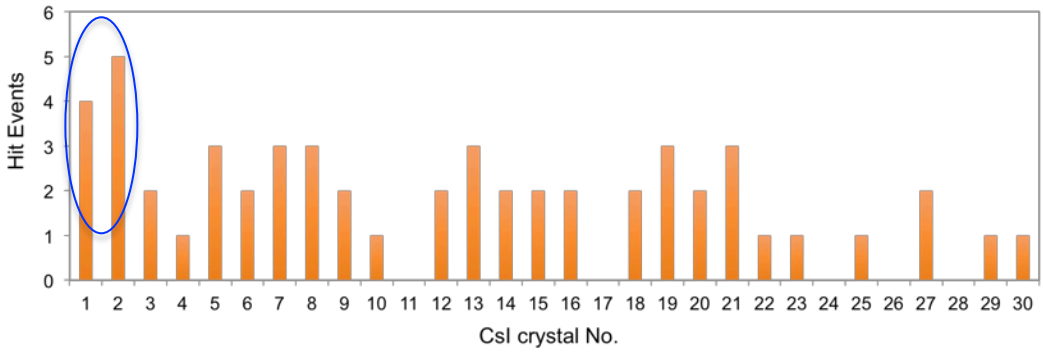

Fig.5.15 CsI scintillators hit distribution for triple coincidence candidate events

We analyzed the CsI hit distribution for triple coincidence events and showed it on Fig.5.15. We found that CsI 1 and CsI 2 had higher hit rate than most other CsIs. The reason was because both CsI 1 and CsI 2 had double solid angle for the sample space. So CsI 1 and CsI 2 were 2 times easier to catch the beta decay events from sample space. The CsI hit result also implied the candidate events from beta decay of ^{48}Sc.

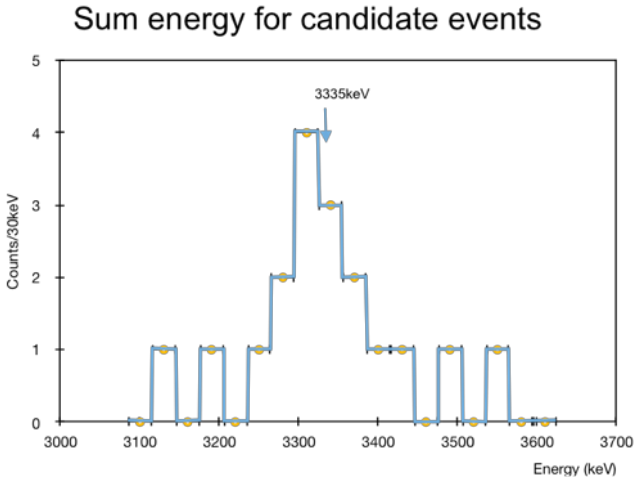

Fig.5.16 Sum energy spectrum for triple coincidence candidate events

Finally, we showed the sum energy (total energy for 3 gamma rays) spectrum in Fig.5.16 for triple coincidence and made Gaussian fitting for the peak. We got the fitting peak at 3313.8keV with energy resolution of 105.4keV. The fitting result implied the peak were the sum energy of 3 gamma rays from ^{48}Sc (983, 1038, 1311keV) with error less than 4%.

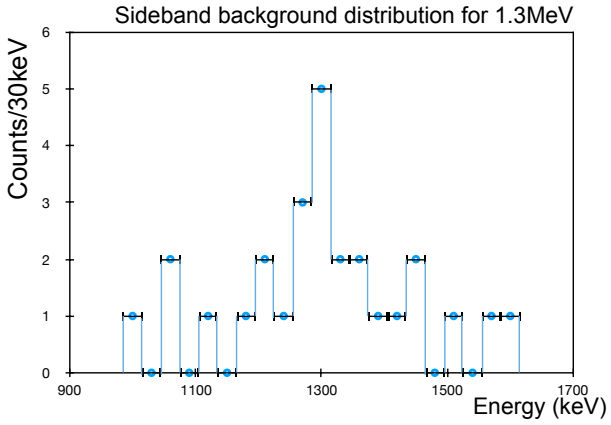

Fig.5.17 The sideband background distribution for 1.3MeV

We got the sideband background distribution for 1.3MeV by fixing energy 983keV±2σ and 1038keV±2σ for two CsI scintillators, the 3rd CsI scintillator energy range ±7σ from 1.0 MeV to 1.6MeV and others energy threshold: <pedestal + 3σ. The spectrum was showed in Fig.5.17 and it was consistent with the sideband background analysis with timing difference.

2.2.4 Triple coincidence result calculation

We have the well known relationship for radioactivity decay $N(t) = N e^{-\lambda t} \approx N(1-\lambda t)$, for the $-\lambda t$ almost equal 0. That means

$$N_0 = N\lambda t$$

$$T_{1/2} = \ln 2/\lambda = \ln 2\, \varepsilon N t/N_0$$

and $N_0=N_s-N_b$.

where N is the nuclei number of ^{48}Ca and N_0 is the number of decay events. N_s is the number of decay events from sample. N_b is the number of decay events from background. t is measurement time and ε is detection efficiency.

Table.5-6 Triple coincidence with ±2σ energy scale

	Measurement time (t: days)	Events (N_b, N_s)	Detection Efficiency	^{48}Ca Atoms (N)
Background	69.8	3		0
Sample	70.7	14	8.47%	2.16×10^{24}
Sideband background	70.7	3		

As listed in Table.5-6 for measurement of ±2σ energy scale, and from the half-life time formula $T_{1/2}=\ln 2/\lambda=\ln 2\times\varepsilon\times N\times t/N_0$, where the background events were integrated from background measurement and sideband background. We got $T_{1/2} = \ln 2\, \varepsilon N t/N_0=(2.2\pm0.8_{[\text{statistic error}]})\times10^{21}$ yr with 68% C.L., about 2.5σ excess was observed.

Since we didn't test the Sc capture efficiency at atoms level. So there is possibility of difference capture efficiency at atoms level and ppm level of Sc. We listed the dependence of detection efficiency for ±2σ with different Sc

capture efficiency at atoms level as table.5-7. We also calculated the correspondent half-life time for triple coincidence at 68% C.L. We could see the significant difference of half-life time because of the Sc capture efficiency. Thus the measurement of Sc capture efficiency at atoms level with Sc^{46} is extremely important. In the following part of thesis, we calculated half-life time based on the ppm level of Sc capture efficiency at 94%.

Table.5-7 The detection efficiency and Sc capture efficiency at atoms level

Sc capture efficiency at atoms level	Detection efficiency for ±2σ	$T_{1/2}$ (yr) (68% C.L.)
5%	0.45%	$(1.2\pm0.4)\times10^{20}$
10%	0.9%	$(2.3\pm0.8)\times10^{20}$
50%	4.5%	$(1.2\pm0.4)\times10^{21}$
94%	8.4%	$(2.2\pm0.8)\times10^{21}$
100%	8.9%	$(2.3\pm0.8)\times10^{21}$

Table.5-8 Triple coincidence with ±4σ energy scale

	Measurement time (t: days)	Events (N_b, N_s)	Detection Efficiency	^{48}Ca Atoms (N)
Background	69.8	8		0
Sample	70.7	18	8.82%	2.16×10^{24}
Sideband background	70.7	9		

As listed in Table.5-8 for measurement of ±4σ energy scale, and from the half-life time formula $T_{1/2}=\ln2/\lambda=\ln2\times\varepsilon\times N\times t/N_0$, where the background events were integrated from background measurement and sideband background. We got $T_{1/2} = \ln2\ \varepsilon Nt/N_0=(2.7\pm1.3_{[\text{statistic error}]})\times10^{21}$ yr with 68% C.L.

2.3 Double coincidence measurement

In order to check the reliability of the triple coincidence, we also analyzed the half lifetime with double coincidence method.

Fig.5.18 showed the candidate events energy distribution for double coincidence. We could find the energies peak at the interested energy region

of 983keV, 1038keV and 1311keV. On the other words, we found the ^{48}Ca beta decay events on the spectrum.

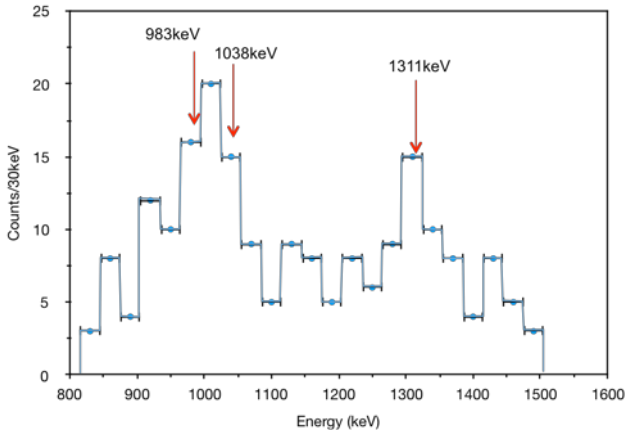

Fig.5.18 Candidate events energy distribution for double coincidence

We also checked the candidate events timing difference for the triple coincidence. We showed the timing difference for each energy pair with unit of resolution. Fig.5.19 showed the timing difference for each pair of energies, 983keV & 1038keV, 983keV & 1311keV and 1038keV & 1311keV. We could see the peak for each pair around timing resolution of 0. That also implied the candidate events were quite possibly from the beta decay of ^{48}Sc. Meanwhile, we also found some events for timing resolution beyond ±1σ, which implied the sideband background. Totally, we found 28 sideband background events for ±2σ energy region and 48 sideband background events for ±4σ energy region. The sideband background events were much higher than triple coincidence analysis.

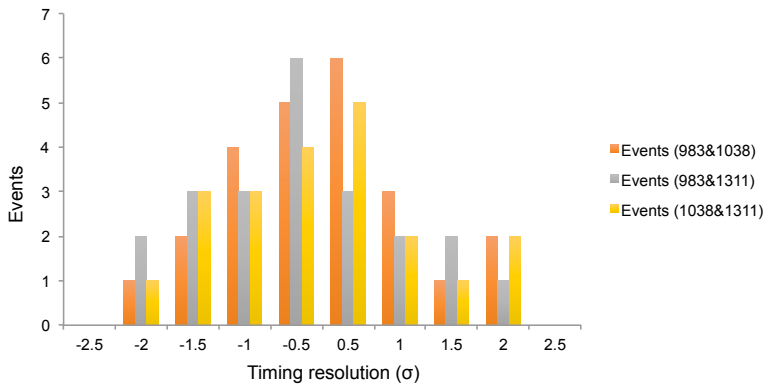

Fig.5.19 Candidate events timing difference distribution for double coincidence

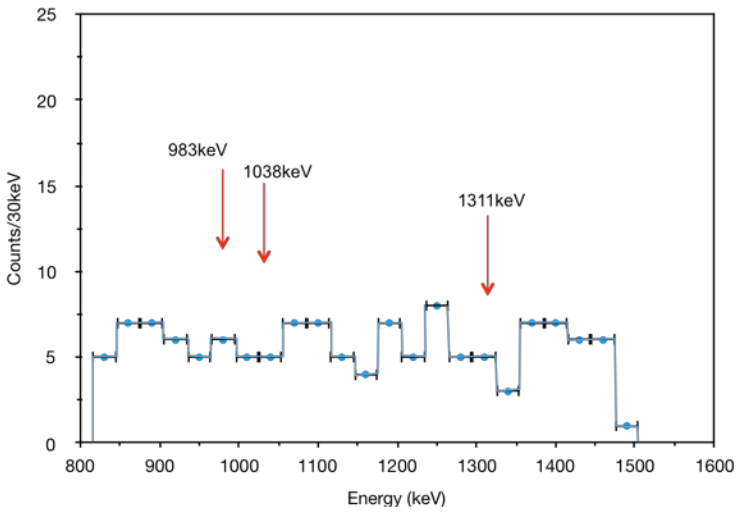

Fig.5.20 Double coincidence energy distribution background events

We showed background events on Fig.5.20. We could clearly found the events that beyond the background level at the 3 interested energy regions of 983keV, 1038keV and 1311keV.

Table.5-9 Double coincidence with ±2σ energy scale

	Measurement time (t: days)	Events (N_b, N_s)	Detection Efficiency	^{48}Ca Atoms (N)
BG	69.8	25		0
Sample	70.7	44	16.5%	2.16×10^{24}
Sideband background	70.7	28		

As listed in Table.5-9 for measurement of ±2σ energy scale, and from the half-life time formula $T_{1/2}=\ln2/\lambda=\ln2\times\varepsilon\times N\times t/N_0$, where the background events were integrated from background measurement and sideband background. We got $T_{1/2} = \ln2\ \varepsilon Nt/N_0=(3.0\pm1.6_{[\text{statistic error}]})\times10^{21}$ yr with 68% C.L.

Table.5-10 Double coincidence with ±4σ energy scale

	Measurement time (t: days)	Events (N_b, N_s)	Detection Efficiency	^{48}Ca Atoms (N)
BG	69.8	43		0
Sample	70.7	67	17.1%	2.16×10^{24}
Sideband background	70.7	50		

As listed in Table.5-10 for measurement of ±4σ energy scale, and from the half-life time formula $T_{1/2}=\ln 2/\lambda=\ln 2\times\varepsilon\times N\times t/N_0$, where the background events were integrated from background measurement and sideband background. We got $T_{1/2} = \ln 2\ \varepsilon Nt/N_0=(3.2\pm1.8_{[\text{statistic error}]})\times10^{21}$ yr with 68% C.L.

From both table.5-9 and table.5-10, we found the sideband background events were higher than the background measurement. We thought there were still some unknown contaminations in the $CaCl_2$ solution that contribute one of the major part of background source.

2.4 Summarize of coincidence analysis

Table.5-11 Half lifetime calculation for triple coincidence and double coincidence with ±4σ energy scale for 68% C.L.

Coincidence Analysis	Half life time (y)
Triple coincidence ±2σ	$(2.2\pm0.8)\times10^{21}$
Triple coincidence ±4σ	$(2.7\pm1.3)\times10^{21}$
Double coincidence ±2σ	$(3.0\pm1.6)\times10^{21}$
Double coincidence ±4σ	$(3.2\pm1.8)\times10^{21}$

We listed all calculation results in table.5-11 for both triple coincidence and double coincidence. We found that those result all consistent with each other. However, the statistic error for double coincidence analysis was much higher than triple coincidence method. For the conclusion, we would believe the calculation based on triple coincidence.

2.5 The effect of plastic scintillator

In order to analyze the background contribution from cosmic rays, we also took the analysis without veto from plastic scintillator. The measurement live time was 74.9 days that became 6.0% longer than the previous veto analysis.

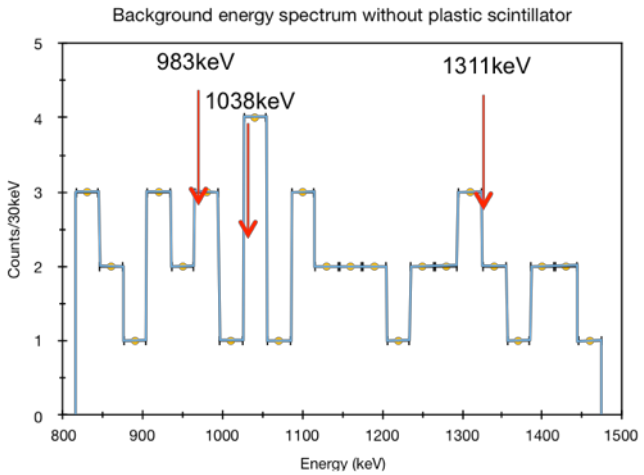

Fig.5.21 The background events distribution for triple coincidence without veto of plastic scintillator

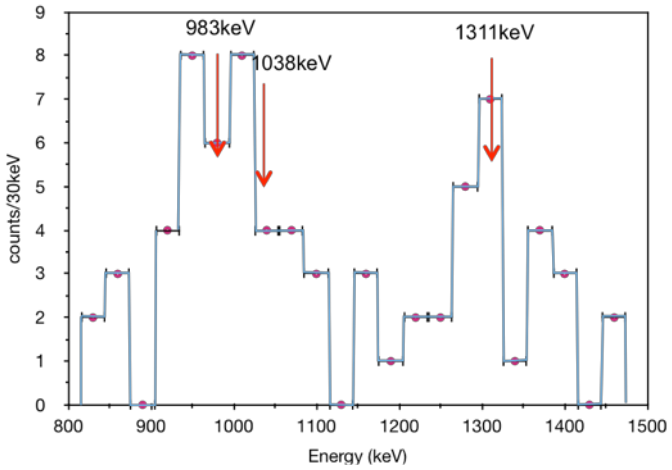

Fig.5.22 The events distribution for triple coincidence without veto of plastic scintillator

Table.5-12 Triple coincidence with ±2σ energy scale without plastic scintillator

	Measurement time (t: days)	Events (N_b, N_s)	Detection Efficiency	^{48}Ca Atoms (N)
Background	73.8	6		0
Sample	74.9	17	8.47%	2.16×10^{24}
Sideband background	74.9	8		

As listed in Table.5-12 for measurement of ±2σ energy scale the events distribution showed in Fig.5.21 and Fig.5.22, and from the half-life time formula $T_{1/2}=\ln2/\lambda=\ln2\times\varepsilon\times N\times t/N_0$, where the background events were integrated from background measurement and sideband background. We got $T_{1/2} = \ln2\ \varepsilon Nt/N_0=(2.9\pm1.6_{[\text{statistic error}]})\times10^{21}$ yr with 68% C.L.

Table.5-13 Triple coincidence with ±4σ energy scale without plastic scintillator

	Measurement time (t: days)	Events (N_b, N_s)	Detection Efficiency	^{48}Ca Atoms (N)
Background	73.8	15		0
Sample	74.9	24	8.82%	2.16×10^{24}
Sideband background	74.9	12		

As listed in Table.5-13 for measurement of ±4σ energy scale, and from the half-life time formula $T_{1/2}=\ln2/\lambda=\ln2\times\varepsilon\times N\times t/N_0$, where the background events were integrated from background measurement and sideband background. We got $T_{1/2} = \ln2\ \varepsilon Nt/N_0=(2.6\pm1.6_{[\text{statistic error}]})\times10^{21}$ yr with 68% C.L.

Table.5-14 Double coincidence with ±2σ energy scale without plastic scintillator

	Measurement time (t: days)	Events (N_b, N_s)	Detection Efficiency	^{48}Ca Atoms (N)
Background	73.8	33		0
Sample	74.9	56	16.5%	2.16×10^{24}
Sideband background	74.9	38		

As listed in Table.5-14 for measurement of ±2σ energy scale, and from the half-life time formula $T_{1/2}=\ln2/\lambda=\ln2\times\varepsilon\times N\times t/N_0$, where the background events were integrated from background measurement and sideband background. We got $T_{1/2} = \ln2\ \varepsilon Nt/N_0=(3.2\pm1.8_{[\text{statistic error}]})\times10^{21}$ yr with 68% C.L.

Table.5-15 Double coincidence with ±4σ energy scale without plastic scintillator

	Measurement time (t: days)	Events (N_b, N_s)	Detection Efficiency	^{48}Ca Atoms (N)
Background	73.8	61		0
Sample	74.9	82	17.1%	2.16×10^{24}
Sideband background	74.9	65		

As listed in Table.5-15 for measurement of ±4σ energy scale, and from the half-life time formula $T_{1/2}=\ln2/\lambda=\ln2\times\varepsilon\times N\times t/N_0$, where the background events were integrated from background measurement and sideband background.

We got $T_{1/2} = \ln 2\ \varepsilon Nt/N_0 = (3.4 \pm 2.2_{[\text{statistic error}]}) \times 10^{21}$ yr with 68% C.L.

Table.5-16 Half lifetime calculation for triple coincidence and double coincidence with ±4σ energy scale for 68% C.L.

Coincidence Analysis	Half life time (y)
Triple coincidence ±2σ	$(2.2\pm0.8)\times10^{21}$
Triple coincidence ±4σ	$(2.7\pm1.3)\times10^{21}$
Triple coincidence without PL ±2σ	$(2.9\pm1.6)\times10^{21}$
Triple coincidence without PL ±4σ	$(2.6\pm1.6)\times10^{21}$
Double coincidence ±2σ	$(3.0\pm1.6)\times10^{21}$
Double coincidence ±4σ	$(3.2\pm1.8)\times10^{21}$
Double coincidence without PL ±2σ	$(3.2\pm1.8)\times10^{21}$
Double coincidence without PL ±4σ	$(3.4\pm2.2)\times10^{21}$

We listed all calculation results in table.5-16 for both triple coincidence and double coincidence with and without plastic scintillator veto. We found that those result all consistent with each other. However, the statistic errors for double coincidence analysis and without plastic scintillator were much higher than triple coincidence method with veto of plastic scintillator. For the final conclusion, we would believe the calculation based on triple coincidence with veto of plastic scintillator.

2.6 The sensitivity of beta decay of ^{48}Ca

From the previous discussion, the sensitivity of this beta decay measurement depended on the triple coincidence analysis. We summarized the sensitivity in table.5-17 for ±2σ and ±4σ, respectively.

Table.5-17 Half lifetime calculation for triple coincidence for 68% C.L.

Coincidence Analysis	Half life time (y)
Triple coincidence ±2σ	$(2.2\pm0.8)\times10^{21}$
Triple coincidence ±4σ	$(2.7\pm1.3)\times10^{21}$

We got the experiment results for beta decay of ^{48}Ca were $T_{1/2(\beta)} = (2.2\pm0.8) \times 10^{21}$ y (68% C.L.). There results were more than 1 order over the previous word record $T_{1/2(\beta)} > 1.1 \times 10^{20}$ y. And they were also partly covered by the theoretical prediction, which was $T_{1/2(\beta)} = (2.3\text{--}12.9) \times 10^{20}$ y.

3. Stability analysis

3.1 Stability of solution circulation

We checked the $CaCl_2$ solution circulation twice everyday to make sure the flow was 2.0L/min.

We also checked the counting rate of ^{214}Bi after we stopped the circulation. Fig.5.23 showed the counting rate of ^{214}Bi before and after the stop of $CaCl_2$ circulation. There was no obvious change in the rate and that implied the ^{214}Bi was not from the $CaCl_2$ solution but environmental background.

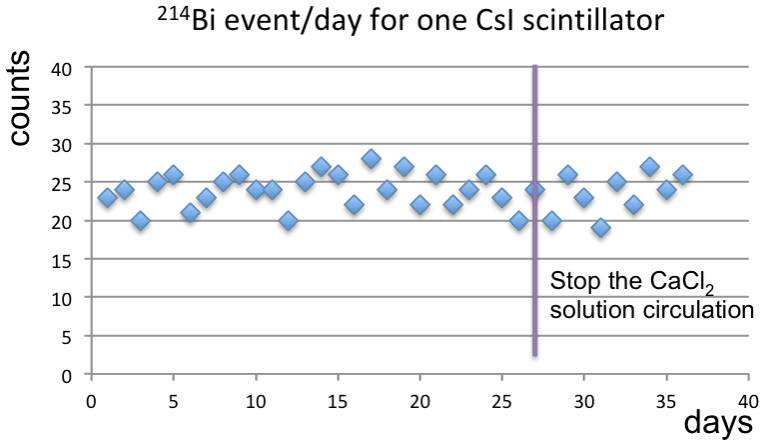

Fig.5.23 ^{214}Bi events before and after $CaCl_2$ solution circulation

We also measured the counting rate for ^{208}Tl before and after stopped the circulation of $CaCl_2$ solution. We measured the ^{208}Tl decay events rate using coincidence of 2.6MeV and 0.58 MeV gamma rays. Fig.5.24 showed the counting rate stability for ^{208}Tl. We didn't found obvious change after stopped the circulation. That implied the resin couldn't capture the ^{208}Tl or there was few ^{208}Tl in the $CaCl_2$ solution. And both assumptions verified that the ^{208}Tl was environmental background.

Both the counting rate from ^{214}Bi and ^{208}Tl showed that the circulation of $CaCl_2$ solution was stable. And the background contribution from ^{214}Bi and ^{208}Tl was not from the circulated $CaCl_2$ solution.

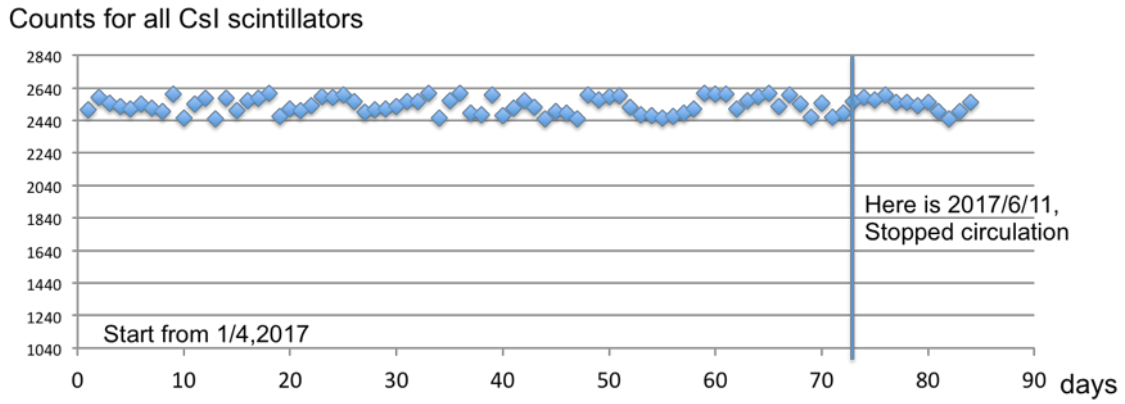

Fig.5.24 ^{208}Tl events stability for beta decay measurement

3.2 Counting rate stability

We checked the counting rate stability for major isotope elements like ^{137}Cs, ^{40}K and ^{208}Tl in the beta decay experiment. The checking started from the beginning of background measurement of 2016/10/18. We measured the rate every 24 hours of live time. Fig.5.25 showed the counting rate for ^{137}Cs. The variation was less than 1.5%. Fig.5.26 showed the counting rate for ^{40}K and the variation was less than 1.8%. Fig.5.27 showed the counting rate for ^{208}Tl and the variation was less than 4.5%.

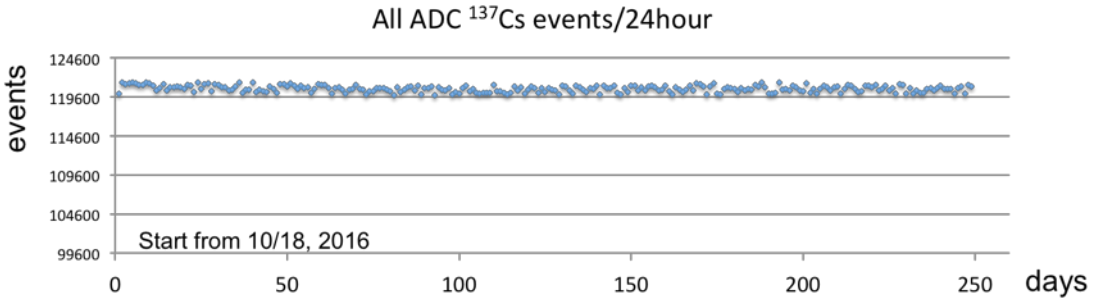

Fig.5.25 ^{137}Cs counting rate stability

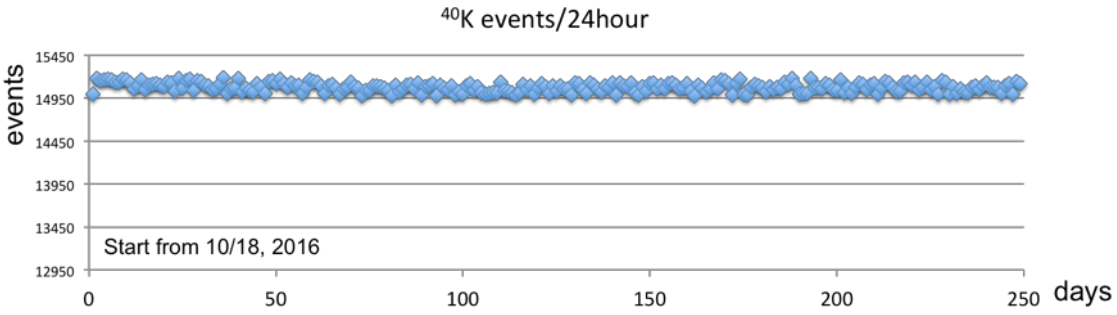

Fig.5.26 ^{40}K counting rate stability

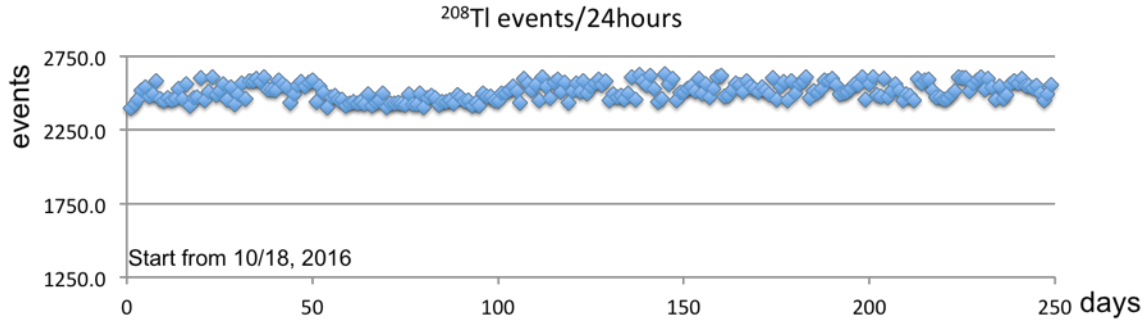

Fig.5.27 ^{208}Tl counting rate stability

3.3 Peak stability

We checked the gain and peak stability for major isotope elements like ^{137}Cs, ^{40}K and ^{208}Tl in the beta decay experiment. The checking started from the beginning of background measurement of 2016/10/18. We measured the peak channel every 12 hours of live time. Fig.5.28 showed the pedestal channel stability and the variation was less than 2.5%. Fig.5.29 showed the peak channel stability for ^{137}Cs. The variation was less than 1.4%. Fig.5.30 showed the peak channel stability for ^{40}K and the variation was less than 1.7%. Fig.5.31 showed the peak channel stability for ^{208}Tl and the variation was less than 2.6%.

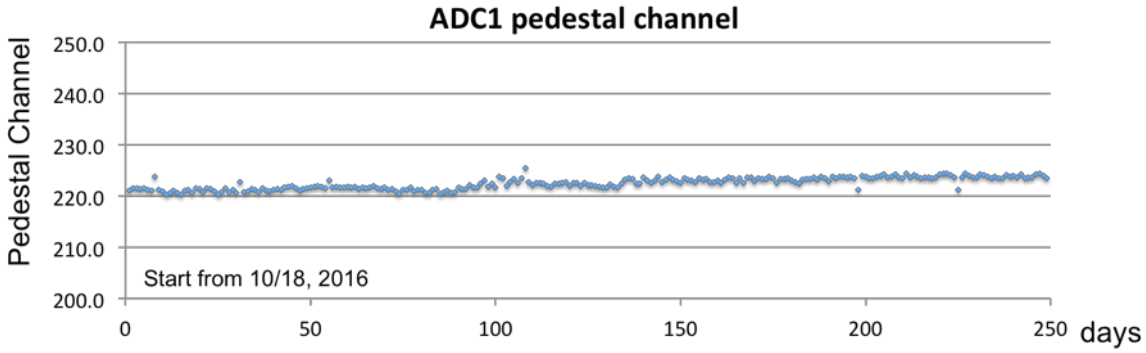

Fig.5.28 ADC pedestal channel stability

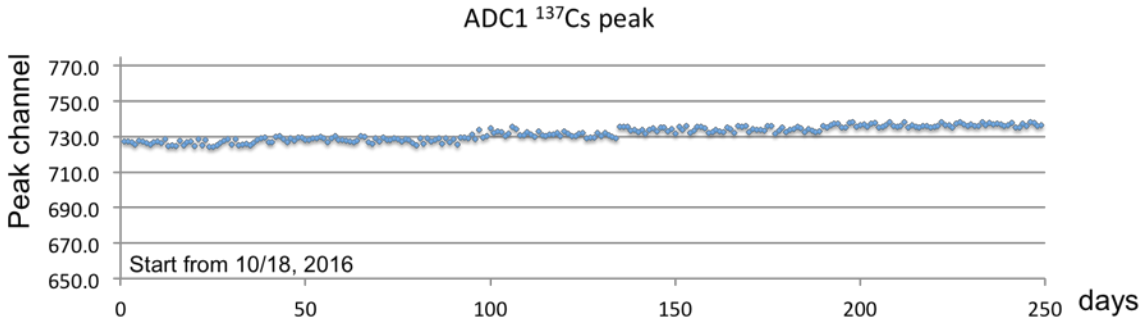

Fig.5.29 ^{137}Cs peak channel stability

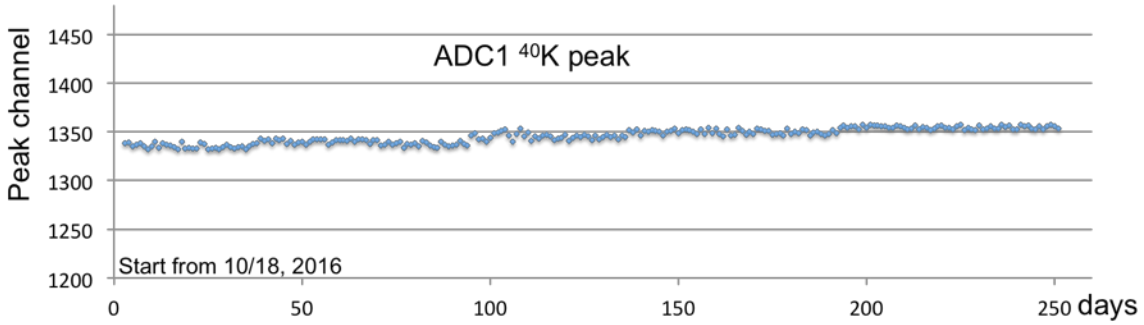

Fig.5.30 ^{40}K peak channel stability

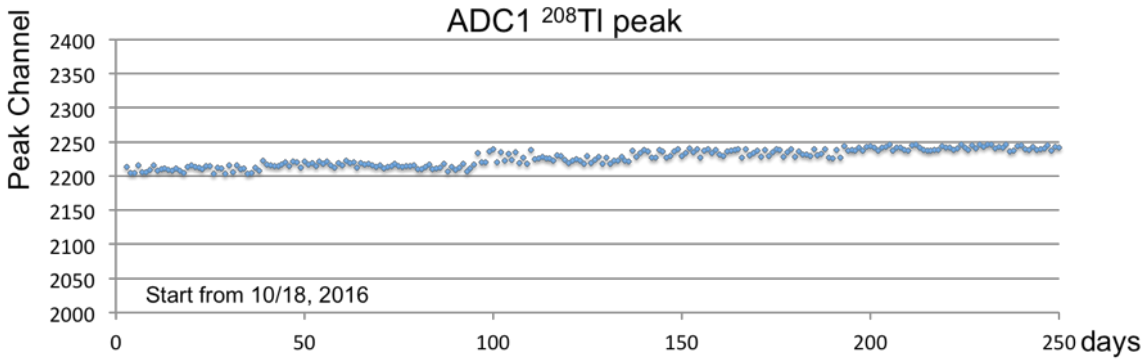

Fig.5.31 ^{208}Tl peak channel stability

We calibrated the CsI scintillators once every two weeks with standard isotope source like ^{137}Cs, ^{60}Co and ^{22}Na. We listed all the ADC peaks for ^{137}Cs in Fig.5.32 and Fig.5.33. From these figures, we found that the variation for ^{137}Cs peak channel for most of CsI scintillators was in 1.5%. ADC23 and ADC24 had higher variation up to 4.0% because of worse energy resolution.

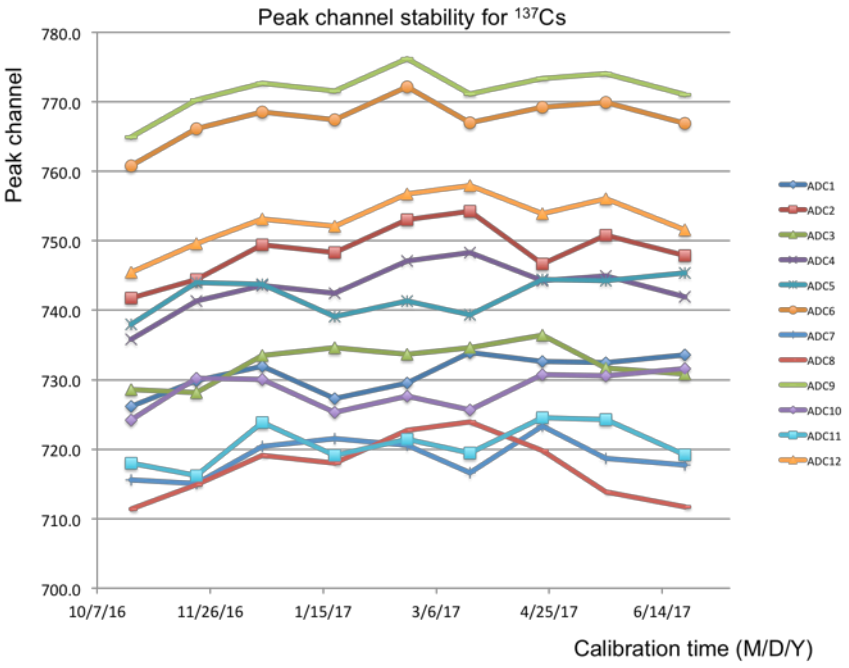

Fig.5.32 ^{137}Cs calibration peak channel stability for ADC 1-12

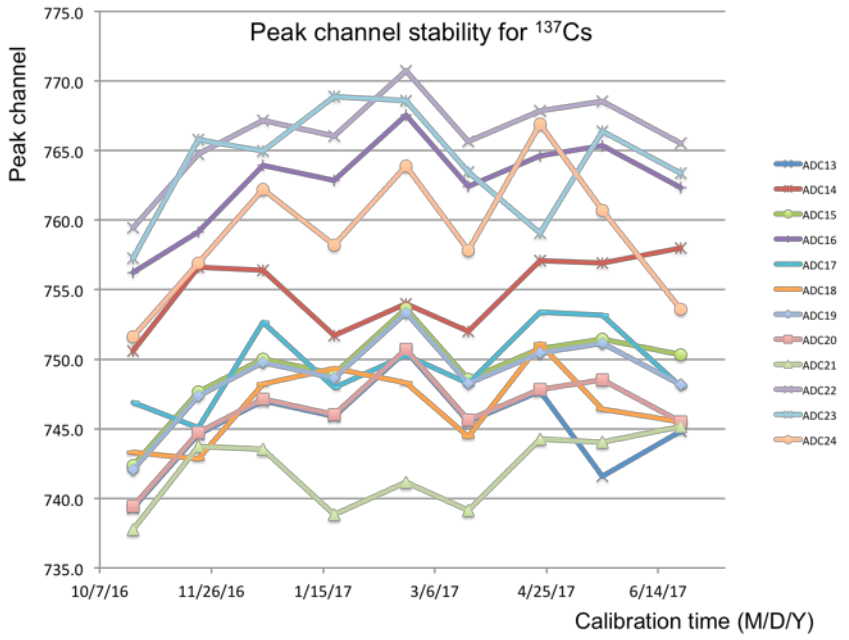

Fig.5.33 ^{137}Cs calibration peak channel stability for ADC 13-24

3.4 Energy resolution stability

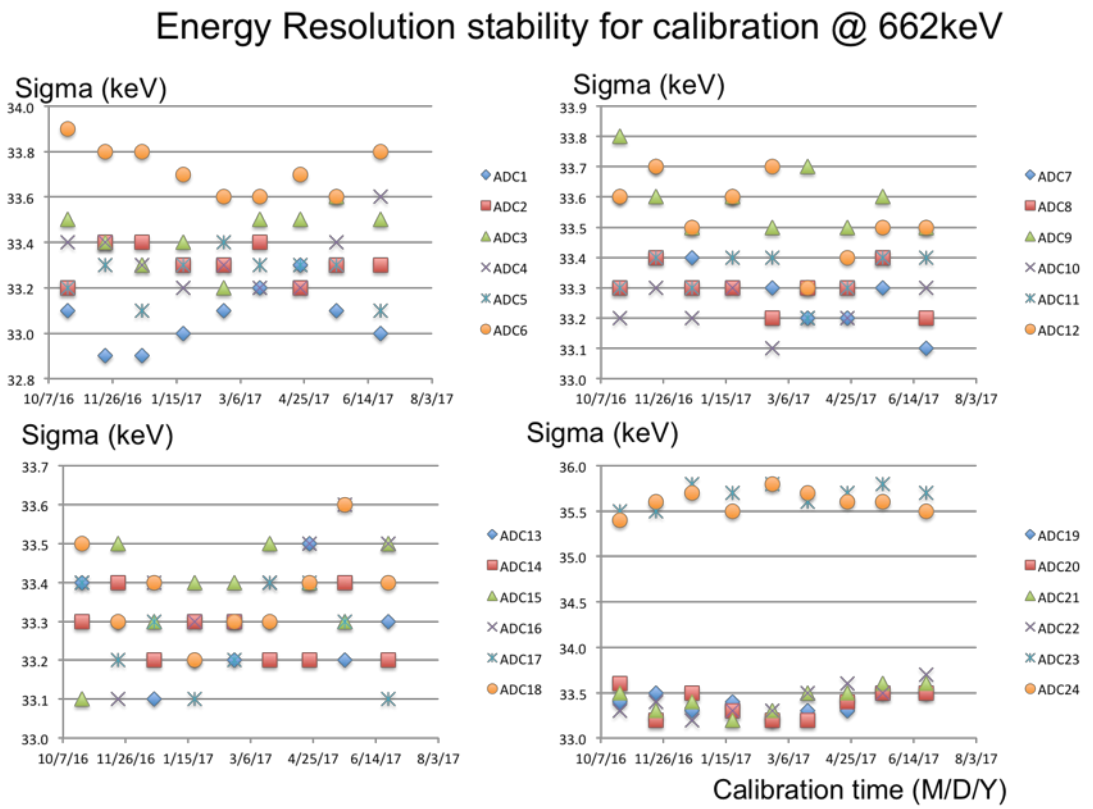

Fig.5.34 Energy resolution stability for ^{137}Cs

We calibrated the CsI scintillators once every two weeks with standard isotope source like ^{137}Cs, ^{60}Co and ^{22}Na. Every time we checked the energy resolution for each ADC channel. We listed all the ADC resolution for ^{137}Cs in Fig.5.34. From the figure, we found that the variation of ^{137}Cs resolution for most of CsI scintillators was in 1.2%. ADC23 and ADC24 had worse energy resolution compare with other ADCs.

4. Error analysis

4.1 Statistic error

The statistic error mostly come from the beta decay events and background events based on Gaussian distribution. And we set the ±2σ for 95% confidence level and ±4σ for 99% confidence level. Meanwhile, we also set the timing difference at ±2σ also for 95% confidence level. Combined all of those statistic error factors, we calculated the total statistic error for this beta decay

measurement was 36% for triple coincidence measurement with ±2σ energy region for 68% C.L. Different analysis methods such as double coincidence with ±4σ energy region had different statistic error. We listed them in the table.5-15.

4.2 Systematic error

The systematic error were much more complicate than the statistic error. Statistic error in this experiment mainly from (1) the stability of the measurement like gain, resolution, timing, rate, and so on. (2) the accuracies of amount of $CaCl_2$ solution volume, ^{48}Ca atoms number, water amount, flow rate of circulation and so on. (3) the uncertainties of detection efficiency, such as validity of simulation, mixture of the liquid during circulation and so on.

4.2.1 Error from stability

Fig.5.22 showed the counting rate for ^{137}Cs. The variation was less than 1.5%. Fig.5.23 showed the counting rate for ^{40}K and the variation was less than 1.8%. Fig.5.24 showed the counting rate for ^{208}Tl and the variation was less than 4.5%.

The timing difference stability error from biweekly calibration was less than 0.5%.

Fig.5.25 showed the pedestal channel stability and the variation was less than 2.5%. Fig.5.26 showed the peak channel stability for ^{137}Cs. The variation was less than 1.4%. Fig.5.27 showed the peak channel stability for ^{40}K and the variation was less than 1.7%. Fig.5.28 showed the peak channel stability for ^{208}Tl and the variation was less than 2.6%.

From the figure Fig.5.31, we found that the variation of ^{137}Cs resolution for most of CsI scintillators was in 1.2%.

4.2.2 Error from measure accuracies

The total amount of ^{48}Ca in $CaCl_2$ powder was 171.0±0.9g. The error was 0.5%;

The total amount of $CaCl_2$ powder was 255.1±0.2kg, so the error was 0.1%;

The total amount of $CaCl_2$ solution was 634.7±0.5L, so the error was 0.1%;

The mass of resin was 138.5±0.3g, so the error was 0.2%;

The $CaCl_2$ solution flow was 2.0±0.2L/min, so the error was less than 10%;

The live time calculation error was less than 1%;

The error for the N_2 gas flow was 2%. The veto time error for Plastic scintillator was less than 1% from Fig.2.6;

The error for timing correction of TDC was less than 1.7% from Fig.2.11 and Fig.2.12.

Those 3 gamma energy peaks and resolutions marched the gamma rays for beta decay of ^{48}Sc with error less than 0.9%.

4.2.3 Error from efficiency uncertainties

From the demonstration experiments, the ^{48}Sc capture efficiency is 94±3%. The lost of efficiency would be 8.9±0.4%, thus we calculated the circulation efficiency was 91.1±0.3% for this beta decay experiment from chapter III, part 2.3.1.

From Monte Carlo simulation and detection efficiency experiment with ^{22}Na and ^{208}Tl, the detection efficiency for triple coincidence was 9.8±0.4% for beta decay measurement with ion exchange resin enrichment of ^{48}Sc.

The final efficiency was the multiply of detector efficiency, ion exchange capture efficiency and circulation efficiency, that was (9.8±0.4%) × (94±3%) × (91.1±0.3%) = 8.4±0.5%.

Combined all of those systematic error factors, we calculated the total systematic error for this beta decay measurement was 17.0%.

4.3 Total error in conclusion

In conclusion, the total error for triple coincidence measurement of beta decay for ^{48}Ca was 36% for statistic error and 17.0% for systematic error.

5. Measurement result

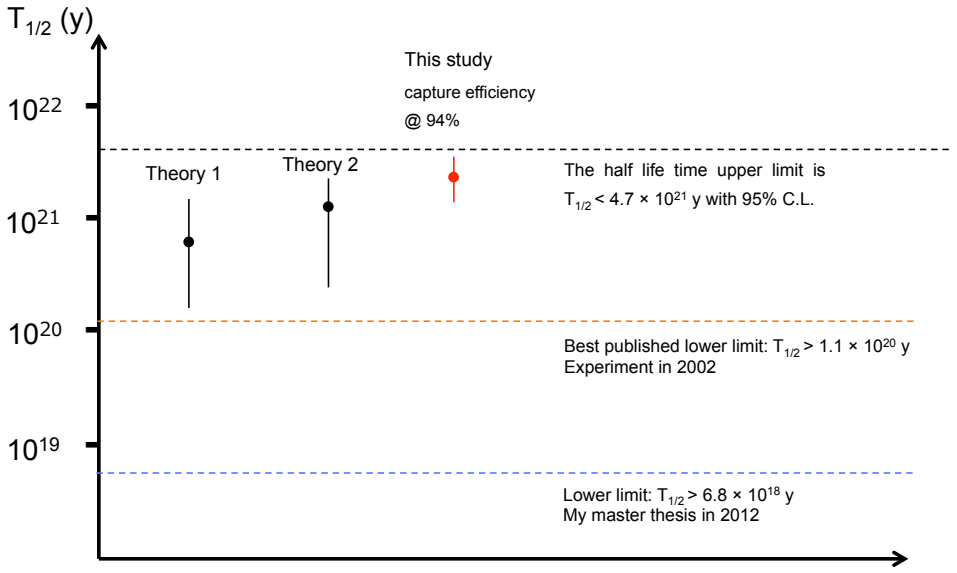

Fig.5.35 Summarize of beta decay half life time studies

We did experiment for Sc capture efficiency in ppm level and Bi capture efficiency in atoms level. The capture efficiency was around 94% for both experiments. Since we didn't measure the capture efficiency in atoms level with Sc directly. There was uncertainty from 5% (according to the published lower limit) to 100%. Thus we could estimate the experimental upper limit of beta decay half life time 4.7×10^{21} y with 95% C.L. for 100% capture efficiency as showed in Fig.5.35.

We measured the half-life time of beta decay of ^{48}Ca is $T_{1/2(\beta)} = (2.2 \pm 0.8_{[\text{statistic}]} \pm 0.4_{[\text{systematics}]}) \times 10^{21}$ y with 68% C.L. by 94% Sc capture efficiency. The half lifetime measurement result for β decay of ^{48}Ca is partly covered by the theoretical prediction upper limit of 1.29×10^{21} y. Corresponding to the new measured have lifetime is the limit log*ft* = 26.7(3) for the β^- transition. This is greater than that for any observed β^- transition.

Chapter VI: Conclusion and Discussion

1. Conclusion

Observation of $0\nu\beta\beta$ is the evidence for neutrinos are massive Majorana particles. The $0\nu\beta\beta$ decay rate is extremely low with lifetime over 10^{25} years, thus any of its background should be clearly understood. $2\nu\beta\beta$ decay is the intrinsic background for $0\nu\beta\beta$ research. That means precisely measure half-life time of $2\nu\beta\beta$ is necessary.

For CANDLES experiment with ^{48}Ca as target, use 10cm cubic pure CaF_2 crystals, single ß decay is the intrinsic background for the $2\nu\beta\beta$ spectrum. In order to precisely measure the $2\nu\beta\beta$, precisely measure the half-life time of single β is necessary.

We made 634.7L $CaCl_2$ solution with 255.1kg $CaCl_2$ powder (^{48}Ca natural abundance). The $CaCl_2$ solution passed though 138.5g Chelate resin with circulation rate of 2.0L/min. We measured the gamma rays with energy of 983keV, 1038keV and 1311keV from beta decay of ^{48}Sc that is the beta decay product of ^{48}Ca with 30 CsI scintillators. The total detection efficiency for this experiment was 8.47% for triple coincidence measurement. We measured the background for live-time of 69.8 days and measured the ^{48}Sc enriched sample for live-time of 70.7 days. The half-life time of beta decay of ^{48}Ca was estimated at $T_{1/2(\beta)} = (2.2 \pm 0.8_{[statistic]} \pm 0.4_{[systematics]}) \times 10^{21}$ y with 68% C. L., about 2.5σ excess was observed from this measurement. The half lifetime measurement result for β decay of ^{48}Ca was partly covered by the theoretical prediction upper limit of 1.29×10^{21} y. We also got the experimental upper limit of beta decay half life time $T_{1/2(\beta)} < 3.9 \times 10^{21}$ y with 95% C.L.

The half-life time we measured in this experiment is the longest for all known β^- transition. Corresponding to the new measured have lifetime is the log*ft* = 26.7(3) for the $ß^-$ transition. This is greater than that for any observed $ß^-$ transition.

From this measurement, the background contribution from β decay for 2νββ above 3MeV spectrum is less than (3±1)%. There will be no background contribution for 0νββ of ^{48}Ca.

2. Discussion

Single beta decay of ^{48}Ca is the intrinsic background for 2νββ in CANDLES experiment. Since 2νββ is the intrinsic background for 0νββ, the precisely single beta decay measurement is every important for double beta research in order to understand the background clearly. The half-life time of β decay is strongly depending on the atoms level Sc capture efficiency at atoms level. The half-life time of β decay of ^{48}Ca is $T_{1/2(\beta)} = (2.2 \pm 0.8_{[statistic]} \pm 0.4_{[systematics]}) \times 10^{21}$ y with 68% C. L if Sc capture efficiency is the same as ppm level @94%. The background contribution to 2νββ spectrum is (3 ± 1)%.

If we want to get more precise result for the half-life measurement, we need reduce the statistics error by increasing the measurement time and reduce the background. We believe that the origin background source is the cosmic rays. So one effective way is set the experiment in underground laboratory. We assume the Sc capture efficiency is 94%, then 1 year measurement sensitivity is $(2.2\pm0.7)\times10^{21}$ with 95% C.L.; 2 year measurement sensitivity is $(2.2\pm0.5)\times10^{21}$ with 95% C.L. By reducing background in underground lab, we assume to reduce 70% of background, then 1 year measurement sensitivity is $(2.2\pm0.5)\times10^{21}$ with 95% C.L.

Meanwhile we can work on the double coincidence method because of its higher detection efficiency if we could reduce most of the background. With higher precision of half-life time, we can estimate the background contribution for 2νββ more precisely. Meanwhile, since part of the result is beyond the theoretical prediction, we can also verify if any improvement for the theoretic calculation is needed, which is very important for the matrix elements calculation for 0νββ research.

Although we measured the half-life time of ^{48}Ca, we don't know it decay though 4+, 5+ or 6+. People need measure ^{48}Ca directly in order to check the single beta decay model of ^{48}Ca.

In this measurement, we didn't check the capture ability of atoms level with Sc (we used ^{214}Bi), demonstration with ^{46}Sc is very important to get more precise capture efficiency for the Chelate resin since the measurement accuracy for CsI scintillators is better than chemistry method (ICP-MS).

Reference

[1] Avignone, Elliott, and Engel,2008. Rev. Mod. Phys., 80, No. 2.

[2] Fukuda S et al., 2000, Phys. Rev. Lett. 85 3999

[3] Ahmad Q.R. et al, 2002, Phys. Rev. Lett. 89 011301

[4] Eguchi K. et al., 2003, Phys. Rev. Lett. 90 021802

[5] Iwata I et al. 2016 Phys. Rev. Lett. 116 112502.

[6] Rodriguez T R and Martinez-Pinedo G 2010 Phys. Rev. Lett. 105 252503

[7] Klapdor-Kleingrothaus et al. 2001 Mod. Phys. Lett. A. 16 (37): 2409.

[8] Arnold R et al. 2015 Phys. Rev. D 92 072011.

[9] Alduino C et al. 2016 Phys. Rev. C 93 045503.

[10] Gomez H 2016 Nucl. Part. Phys. Proc. 273-275 1765.

[11] Agostini M 2016 Presentation at NEUTRINO-2016 (July, London UK).

[12] Gando Y 2016 Nucl. Part. Phys. Proc. 273-275 1842.

[13] Agostini M et al. 2015 Eur. Phys. J. C 75 416.

[14] N. Abgrall, et al. 2014 Adv. High Energy Phys., p. 365432

[15] Gando A et al. 2016 Phys. Rev. Lett. 117 082503; 109903

[16] Pocer A et al. 2015 Nucl. Part. Phys. Proc. 265-266 42.

[17] Umehara S et al. 2008 Phys. Rev. C 78 058501.

[18] Iida T et al. 2016 J. Phys. Conf. Ser. 718 062026.

[19] R.A. Sen'kov, M. Horoi 2013 Phys. Rev. C 88, 064312

[20] E.K. Warburton, 1985 Phys. Rev. C 31 (1985) 1896.

[21] M. Aunola et al. 1999 Europhys. Lett., 46 (5), pp. 577-582

[22] D.E. Alburger, J.B. Cumming, 1985 Phys. Rev. C 32 (1985) 1358.

[23] R. Bernabei, et al. 2002 Nuclear Physics A 705 (2002) 29-39

[24] A. Bakalyarov et al., 2002 Nuclear Physics A 700 (2002) 17–24

Acknowledgement

There are so many people helped and encouraged me to finish this thesis. The very special appreciation goes out to my supervisor, Prof. Tadafumi Kishimoto for giving me the many chances to make life decisions. He accepted me as his graduated students in 2010 and helped me on both research and lives in Osaka University from then. In 2014, he accepted my decision to leave of absence from university to startup and gave lots of encouragements for it. In 2016, he accepted my decision to go back to university to continue the research after my failure on startup, still with full of encouragement. In 2017, he accepted again for my decision to work at industry and leave the university before finish the PhD defense. I feel that I am the luckiest student to have such good supervisor.

My forever love, Aimee Huo married with me at my most difficult time in 2015. She is the lighthouse for my life sailing and always the harbor to start and stop. I couldn't imagine how my life would be without her accompany. My lovely son, Ziang Wang was born in April 2017. I was so happy and also so busy from that time. I had to work for the company, work on PhD research and take care of him. Many times I felt extremely tired, but with his lovely smile I recovered with full of energy again.

I am grateful to my father and mother Chuguo Wang and Mingqiong Chen, who have provided me through moral and emotional support in my life. I am also grateful to my other family members and friends who have supported me along the way, especially uncle Wang and uncle Peng.

Specially thanks for Prof. Sei Yoshida for supporting me on experiment and thesis writing. It was so difficult for me to finish this experiment. I couldn't continue the research without his carefully guide, help and encouragement especially for the data analysis after April 2017 when I left the university.

And finally, last but by no means least; also to everyone in the Kishimoto Lab, Prof. Sakguchi, Prof. Umehara, Matsuda-san, Chan-san, Trang-san, Lee Xiaolong, Lee Ken Keong… it was great laboratory with all of you during last seven years. Also the reviewers of this thesis, Prof. Kuno, Prof. Nomachi, Prof. Shima, Prof. Hosaka and Prof. Iida, I am appreciating for all your comments and suggestions.

Thanks for all your encouragement!